ABOUT THE AUTHOR

Venu R. Vangala was born in Hanamkonda, a town in the Warangal district of Andhra Pradesh, India, in 1975. He received his elementary and secondary school education in Hanamkonda. After the completion of B.Sc. and M.Sc. (Medicinal Chemistry-Organic division) from Kakatiya University, he joined the School of Chemistry, University of Hyderabad for the Ph.D. degree in 1998.

LIST OF PUBLICATIONS

1 Interplay of phenyl-perfluorophenyl stacking, C–H···F, C–F···π and F···F interactions in some crystalline aromatic azines.
V.R. Vangala, A. Nangia and V.M. Lynch
Chem Commun., **2002**, 1304–1305.

2. 1:1 Molecular complex of bis(4-aminophenyl)disulfide and 4-aminothiophenol.
V.R. Vangala, G.R. Desiraju, R.K.R. Jetti, D. Bläser and R. Boese
Acta Crystallogr., *Section C*, **2002**, *58*, o635–o636.

3. Correspondence between molecular functionality and crystal structures. Supramolecular chemistry of a family of homologated aminophenols.
V.R. Vangala, B.R. Bhogala, A. Dey, G.R. Desiraju, C.K. Broder, P.S. Smith, R. Mondal, J.A.K. Howard and C.C. Wilson
J. Am. Chem. Soc., **2003**, *125*, 14495–14509.

4. Dianiline–diphenol molecular complexes based on supraminol recognition.
V.R. Vangala, R. Mondal, C.K. Broder , J.A. K. Howard and G.R. Desiraju (communicated).

5. A novel saturated hydrogen bond architecture in supraminols.
B.R. Bhogala, **V.R. Vangala**, P.S. Smith, J.A.K. Howard and G.R. Desiraju (communicated).

To
Amma and Bapu

STATEMENT

I hereby declare that the matter embodied in this thesis entitled "**From Molecular to Crystal Structure: Crystal Engineering of Some Supraminols**" is the result of investigations carried out by me in the School of Chemistry, University of Hyderabad under the supervision of **Prof. Gautam R. Desiraju**.

In keeping with the general practice of reporting scientific observations due acknowledgements have been made wherever the work described is based on the findings of other investigators.

Hyderabad
March 2004

Venugopal Rao Vangala

UNIVERSITY OF HYDERABAD
सा विद्या या विमुक्तये

CERTIFICATE

Certified that the work **"From Molecular to Crystal Structure: Crystal Engineering of Some Supraminols"** has been carried out by **Venugopal Rao Vangala** under my supervision and that the same has not been submitted elsewhere for a degree.

Dean
School of Chemistry

Prof. Gautam R. Desiraju
Thesis Supervisor

UNIVERSITY OF HYDERABAD
सा विद्या या विमुक्तये

ACKNOWLEDGEMENT

It gives me immense pleasure to express my profound gratitude and deep respect to my guide, **Prof. Gautam R. Desiraju** for teaching me research methodology and introducing me to this fascinating field of research. He has been inspiring with thought provoking discussions and invaluable lectures.

My indebtedness and sincere respects are due to Prof. Ashwini Nangia for his helpful guidance and encouragement. I have been fortunate to have his obliging discussions.

It is my pleasure to thank Prof. Judith A.K. Howard, University of Durham, U.K., for collecting all the X-ray diffraction data discussed in the thesis. My heartfelt thanks for her precious help. I thank Dr. C.C. Wilson, ISIS, Rutherford Appleton, U.K. for the neutron diffraction. Special thanks are due to Dr. C.K. Broder. I also thank R. Mondal and P.S. Smith for friendly and helpful discussions.

I would like to acknowledge the assistance of Prof. R. Boese, University of Essen, Germany, Dr. V.M. Lynch, University of Texas, Austin, U.S.A. and Dr. H.L. Carrell, Fox Chase Cancer Center, Philadelphia, U.S.A., for X-ray data collection on the various other crystals. I thank Dr. J.S. Yadav, Dr. S. Chandrashekar and their group members at IICT, Hyderabad for timely help.

I thank the Dean, School of Chemistry and all the faculty members of the School for their cooperation.

I also thank Mr. V.M. Shetty, all the staff of the School of Chemistry, COSIST building and the Computer Centre for their assistance on various occasions.

I wish to record my thanks to CSIR, New Delhi for fellowship support.

I am thankful to Prof. A. Krishna Murthy, Dr. M.S.S. Shankar and all my other M.Sc. teachers at C.K.M. P.G. Centre, Kakatiya University, Warangal.

I wish to thank alumni group members Drs. J.A.R.P. Sarma, R. Kishan, V.R. Pedireddi, C.V.K. Sharma, D.S. Reddy and K. Biradha for their encouragement.

A special note of thanks to Praveen, Senthil, Vishu, Sumod and Sairam for their support and pleasant company during my research tenure.

I wish to thank my friendly and cooperative labmates Drs. V.R. Thalladi, A. Anthony, N.N.L. Madhavi, T. Ram, S.S. Kuduva, R.K.R. Jetti, A.K. Varma, S. Sarkhel, M.T. Kirchner, Messrs. Balakrishna, Basavoju, Vasulu, Rahul, Dinu, Malla Reddy, Sreenivas Reddy, Binoy, Aparna, Archan, Sunil, Saikat, Prashant, Tejender, Jagadeesh, Sreekanth, Ravi and Jeevan for creating a cheerful work atmosphere. My stay on this campus has been pleasant with the association of all the scholars at the School of Chemistry. I am thankful to Messrs. Vamsee, Srivardhan, Jayapal, Raghu, Kommana, Sampath, Phani, Sastry, Chandu, Alchemie-99 batch, Gupta, Pavan, Sharath, Pradeep, Pratap, Mahidhar, Kishore, Banala, Jagan, all Life Sciences friends, Raghavaiah, Manoj, Naga Srinu, Jayaprakash, Rajender, Mrs. Vani, Subbalakshmi, Rajitha, Rama, Sunita, Messrs. Aruna, Kavitha, Pooja, Sandhya and Prashanthi.

I thank my M.Sc. friends Chandu, Gopal, Venkat, Srimanth, Veeresh, Prasad, Swarna, Bhanu, Ram and Srinivas Reddy for their company. I also thank S Raju, Prasad, Mallik, Madhu, Ramesh, Vishnu, Srikanth, Hari, Naga, Gopi and Shyam.

It would be too formal to thank my bosom friends Vijender, Vasu and Kiran for their unreserved encouragement. Special note of thanks to Kiran. I also thank Murali, Damu, Kishore, Yogi, Seshu, Kireeti, Varma, Sreedhar, Babu, Srinivas, Srikanth, Chisty, Chintu, Mendu, Vijay and Koshy for their cheerful troupe.

Special thanks are due to my brother, Mohan, for his constant encouragement and care. I fall short of words to express my feelings and gratitude towards him.

The blessings and best wishes of **my parents**, brothers, sister, brother-in-law and sisters-in-law have made me what I am and I owe everything to them. Last, but certainly not the least, all the children in my family deserve a word of thanks for their smiles.

Venu R. Vangala

PREFACE

Crystal engineering, the design of organic solids with predictable structures and/or properties, has emerged as an important cross-disciplinary field of basic and applied endeavour. The continuing growth of this subject is revealed by the appearance of three journals particular to the area—*Crystal Engineering* was launched by Elsevier in 1998, *CrystEngComm* by the Royal Society of Chemistry in 1999 and *Crystal Growth & Design*, by the American Chemical Society in 2001. To date, the most fundamental problem in crystal engineering is to establish rigorous connections between molecular and crystal structure. This thesis is an attempt to understand such relationships by utilizing amino-hydroxy (supraminol or aminophenol) recognition.

Rationalization, analysis and design are the key elements in crystal engineering. An organic crystal is the ultimate supermolecule and therefore crystal engineering is a supramolecular equivalent of organic synthesis. Crystal engineering as complementary molecular recognition has been used in the work reported in this thesis and an overview of it is provided in Chapter 1. The strategy used is to identify the robust *supramolecular synthons,* that are associated with the complex convolutions of molecular functionality *i.e.* respectively the hydroxy group (phenolic), the amino group (anilino), phenyl rings, and a linker group–classically the polymethylene chain, and exchange of CH_2 by S or O-atom in some cases, which links the phenyl rings.

Chapter 2 deals with the systematic studies of possible structure types and their properties have been described for the homologous aminophenols. A family of supraminols **1**–**5** of the general type HO–C_6H_4–$(CH_2)_n$–C_6H_4–NH_2 (n = 1 to 5) and both OH and NH_2 in a *para* position have been synthesized, analyzed and correlated. These supraminols can be described in terms of three major supramolecular synthons

based on hydrogen bonding between OH and NH_2 groups: the tetrameric loop or square motif, the infinite N(H)O chain and the β-As sheet. Compounds **1** through **5** show an alternation in melting points and compounds with *n* = even exhibit systematically higher melting points compared to those with *n* = odd. The alternating melting points are reflected in and explained by the alternation in the crystal structures.

The phenomenon of isosteric group replacement and the isostructurality of some supraminols is demonstrated in Chapter 3. Substitution of a methylene group by an isosteric S-atom in a supraminol may causes a change in the crystal structure. These observations are rationalized in terms of geometrical and chemical effects of the functional groups.

In Chapter 4, the self-assembly between molecular complexes of some diphenols and dianilines is delineated. Studies of the molecular complexes of organic substances are paramount for studying intermolecular interactions. Molecular recognition among alcohol and amine has a noted propensity towards the formation of 1:1 molecular complexes.

Reliable connections between the molecular and the structural paradigm are examined in Chapter 5. This chapter also discusses a novel O–H···N and N–H···O saturated hydrogen bridge (SHB) tube architecture and its topological similarity with the anion framework in the rare zeolite narsarsukite $Na_2TiOSi_4O_{10}$.

Salient crystallographic details of the crystal structures discussed in this thesis are listed in Appendix-II. A full list of atomic coordinates has been deposited with University of Hyderabad and can be obtained from Prof. Gautam R. Desiraju (desiraju@uohyd.ernet.in).

Hyderabad *Venu R. Vangala*

March 2004

CONTENTS

CHAPTER ONE

CRYSTAL ENGINEERING – COMPLEMENTARY MOLECULAR RECOGNITION

1.1 Overview

The subject of crystal engineering was developed by Schmidt during 1950–1971 in the context of organic solid state photodimerizations of cinnamic acids and their derivatives [1.1]. A broad definition of crystal engineering was provided by Desiraju in 1989 as "*the understanding of intermolecular interactions in the context of crystal packing and in the utilization of such understanding in the design of new solids with desired physical and chemical properties*" [1.2]. Crystal engineering [1.3] is intimately linked to supramolecular chemistry. According to Lehn [1.4] supramolecular chemistry is chemistry beyond the molecule [1.5]. According to this paradigm, crystal engineering is a form of supramolecular synthesis in the solid state. Crystals can be considered as the supramolecular equivalents of molecules and thus crystal engineering is a supramolecular equivalent of organic synthesis. Salient features of this molecular to supramolecular paradigm are summarized in Table 1.

The most fundamental problem in crystal engineering is the prediction of crystal structure from the molecular structure of a compound [1.6]. Difficulties in this regard stem from the complementary nature of the recognition phenomenon [1.7]. In any kind of molecular recognition including the recognition between identical molecules it is the dissimilar rather than the similar functionalities that come into closest contact. This complementarity is characteristic of both geometrical and chemical recognition and renders a functional group or modular approach to be of limited applicability. That means that crystal structures of many simple compounds need not be simple at all.

Table 1. Characteristics of molecular and supramolecular synthesis.

	Organic synthesis	**Crystal engineering**
Target	Molecule	Supermolecule (crystal)[b]
Molecular weight	1–1000 Da	1–100 kDa
Connectivity	Covalent	Non-covalent: hydrogen bond, ionic, hydrophobic, metal coordination[c]
Reaction path	Reactant → Transition state → Product	Molecule → Crystal nucleus → Crystal
Bond energy	50–135 kcal/mol	2–20 kcal/mol
Kinetic stability	High	Low
ΔG components	ΔH » TΔS	ΔH ≈ TΔS
Solvent effects	Secondary	Primary
Phenomena	Isomers (geometrical and stereo-) are common	Polymorphism[d] could be common. Formerly called the Nemesis of crystal engineering, it is now of significance to the subject.
Motivations	Pharmaceuticals, agrochemicals, fine chemicals	Nanostructures, materials and functional solids,[e] NLO, molecular electronics, molecular modeling.[f]
Challenging tasks	Vitamin B_{12}, gingkolide, taxol, epothilone, palytoxin, brevetoxin.[a]	*Ab initio* prediction of crystal structure from molecular structure.

[a]Total synthesis of very complex molecules [1.8]. [b]An organic crystal recognized as a supermolecule *par excellence* [1.9]. [c]Nonorganic crystal engineering [1.10]. [d]The ability of a molecule to crystallize in different lattices or conformations [1.11]. [e]References for functionalized solids and NLO materials [1.12]. [f]For molecular modeling and drug design see [1.13].

The first well documented attempt to correlate molecular and crystal structure was the work of Robertson in 1951. He examined planar fused-ring aromatic hydrocarbons and showed that the packing is revealed by the value of the crystallographic short axis [1.14]. Hydrocarbon crystal structures can be predicted with relative ease using Kitaigorodskii's close packing model [1.15] because they are

of the van der Waals type. Desiraju and Gavezzotti reexamined Robertson's correlation and further improved it [1.16]. In heteroatom containing structures, however, direct correspondences between molecular and crystal structures are difficult to establish and the work presented in this thesis is an attempt to establish such relationships in a particular set of compounds, the aminophenols.

1.2 Non-covalent interactions and supramolecular synthons

Rationalization, analysis and design are the key elements in crystal engineering. In this context, the *supramolecular synthon* [1.17] concept simplifies the rationalization and non-covalent synthesis of crystal structures [1.18]. Analysis is mainly carried out with the aid of Cambridge Structural Database (CSD) [1.19] and through computational methods. Intermolecular interactions have been used as design elements in a great many crystal structures. The complementary recognition of molecules in the crystal is governed by non-covalent interactions. Therefore, an understanding of these interactions is essential for crystal engineering studies. In organic compounds the interactions are of two types: medium range isotropic forces and long range anisotropic forces. Isotropic forces include C···C, C···H and H···H interactions and define molecular shape, size and close packing [1.15]. Heteroatom interactions such as strong hydrogen bonds (O–H···O, O–H···N and N–H···O) [1.20], weak hydrogen bonds (C–H···O, C–H···N, C–H···halogen, N–H···S, C–H···S, O–H···π, N–H···π and C–H···π) [1.21] and also interactions between X···X (X = O, N, S, P and halogen) [1.22] represent the anisotropic forces. Hydrogen bonds can be more appropriately termed as hydrogen bridges [1.23]. Among all these, the hydrogen bridges are versatile design elements. The observed crystal structure is a free energy minimum resulting from the optimization of attractive and repulsive intermolecular interactions with varying strengths, directional preferences and distance-dependence properties.

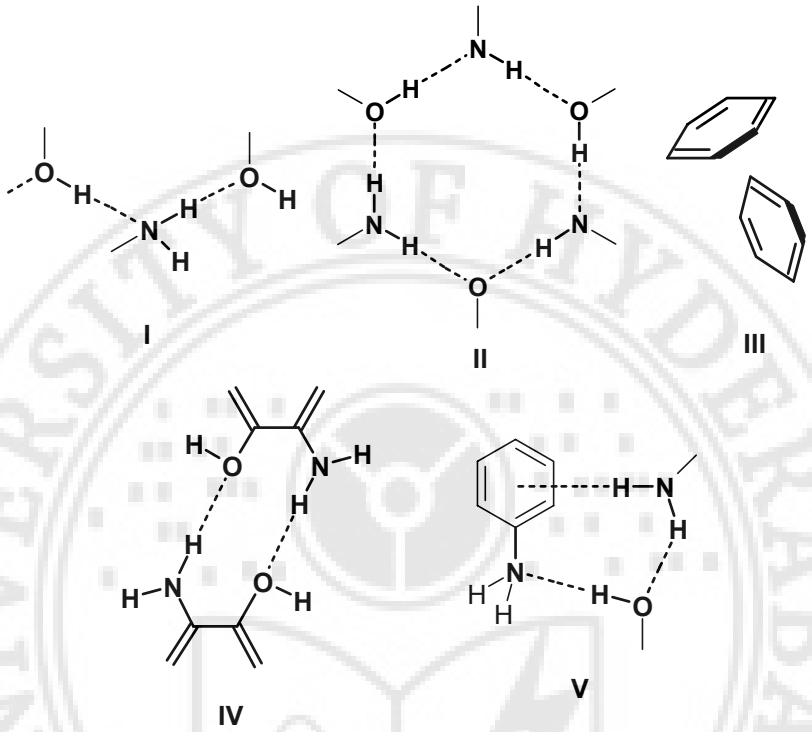

Scheme 1. Some supramolecular synthons discussed in this thesis.

The CSD facilitates the analysis of a large number of crystal structures. The geometrical attributes of intermolecular interactions and their chemical characteristics can be studied reliably by statistical analysis. These interactions can be combined by the designed placement of functional groups in the molecular skeleton to generate supramolecular synthons. The supramolecular synthon was defined by Desiraju as *"a structural unit within supermolecules which can be formed and/or assembled by known or conceivable synthetic operations involving intermolecular interactions"* [1.17]. It is noteworthy that supramolecular synthons are designed combinations of interactions and are not identical to the interactions. Knowledge about the supramolecular synthon is clearly as important to crystal engineering as is an

understanding of reaction mechanisms and reagents in conventional covalent synthesis. The supramolecular synthon approach is flexible and permits classification over a wide range of structures. In some crystal structures a single interaction may be considered as a synthon while in other structures many interactions may be embedded in a particular synthon. Accordingly, much chemical and geometrical information is contained in useful supramolecular synthons. Scheme 1 shows various supramolecular synthons. This concept is utilized extensively in this thesis.

1.3 Amine and hydroxy (Supraminols or Aminophenols) recognition and their patterns

The primary amino group has two hydrogen bridge donors and one acceptor whereas the hydroxy group has one donor and two acceptors. Therefore these molecular functionalities have been considered to be complementary hydrogen bond functionalities both stoichiometrically and geometrically (Scheme 2). Crystal engineering of hydroxy and primary amino recognition in the design of predictable structures has been recently highlighted. In 1994, Ermer and Eling elaborated for the first time the general principles for molecular recognition among amine and hydroxy groups utilizing aromatic systems [1.24]. Independently and simultaneously, Hanessian and co-workers [1.25] showed the first examples of metal-free three-dimensional triple-stranded helicates through spontaneous self-assembly of chiral C_2-symmetrical diamines and diols. Compounds or molecular complexes containing equal stoichiometries of $-NH_2$ and –OH groups are benefited by a 50% increase in the number of hydrogen bridges when compared to either pure alcohols or primary amines. This permits the formation of one O–H···N and two N–H···O hydrogen bridges (for one NH_2 and one OH group) resulting in a tetrahedral configuration at both hetero-atoms with a complete saturation of hydrogen bonding potential. In the supraminols there is a general tendency to avoid N–H···N bridges, because they are

weaker than O–H···N and N–H···O interactions. The combination of O–H···N and N–H···O interactions is referred to in this thesis as N(H)O.

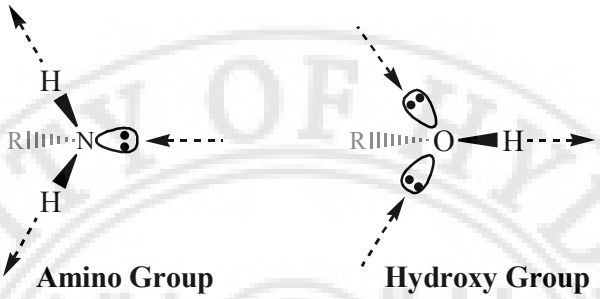

Scheme 2. H-bridge donor:acceptor complementarity of amino and hydroxy groups.

According to Ermer and Eling [1.24], the reasonable structural possibility in amino-hydroxy recognition is a zigzag chain of hydrogen bridges joined together exclusively by N(H)O bridges to generate sheets of *trans*-fused super-cyclohexane rings with chair-like conformations. From a topological viewpoint, these superstructures resemble the sheet structure of the stable allotrope of (grey) arsenic and are therefore referred to as β-As sheets or super-arsenic sheets. These sheets in turn may be dissected out of both the cubic diamond (zinc blende, cristobalite) lattice or the hexagonal diamond (wurtzite, tridymite) lattice. As shown below the sheets are held together solely by O–H···N and N–H···O interactions (Scheme 3).

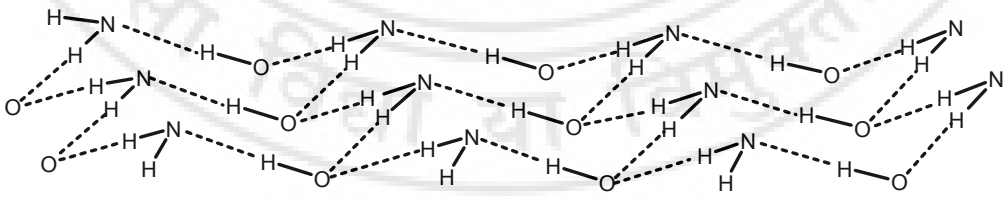

Scheme 3. Hydrogen bridge pattern of 1:1 amino-hydroxy recognition. Notice the β-As (super arsenic) type H-bonded sheet with exclusively N(H)O interactions.

Alternatively, the usual zigzag chains of hydrogen bridges are joined together alternately by N–H···O interactions to furnish sheets of *trans*-fused super-cyclohexane rings. These sheets are constituted with one third each of interactions of the type O–H···O, N–H···O and N–H···N (Scheme 4).

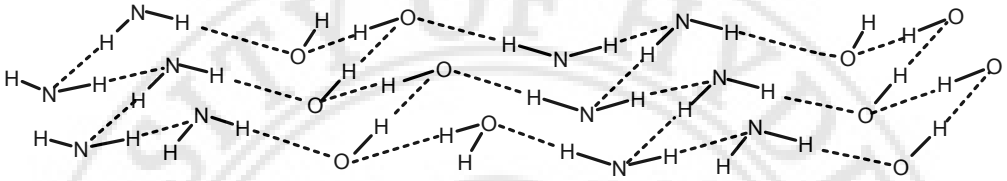

Scheme 4. Alternative hydrogen bridge pattern of 1:1 amino-hydroxy recognition. Notice the super arsenic type H-bonded sheet with 1/3 O–H···O, N–H···O and N–H···N interactions.

H-bonded sheets analogous to those of black phosphorous (black-P) are possible when two thirds of the *trans*-fusions between the super-cyclohexane chairs are replaced by *cis*-fusions. Such a super black-P type sheet structure may be obtained by cutting through a cubic diamond lattice rather than a hexagonal diamond lattice (Scheme 5).

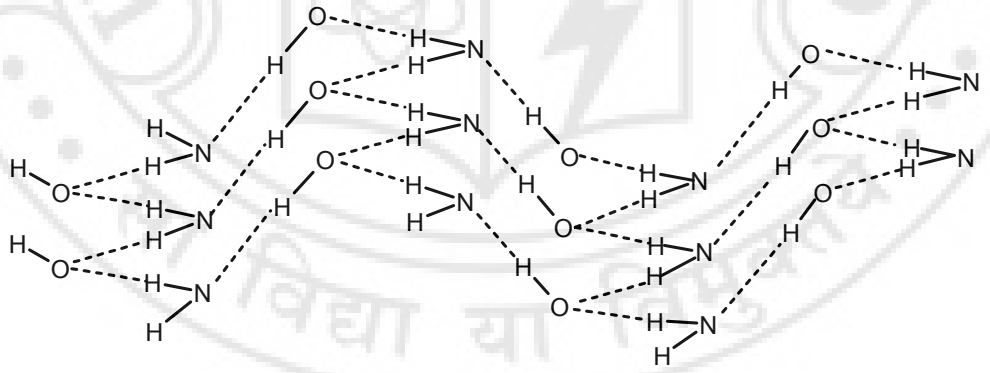

Scheme 5. Alternative hydrogen bridge pattern of 1:1 amino-hydroxy recognition. Notice the super black-P type H-bonded sheet with exclusively N(H)O interactions.

In systems where the amino and hydroxy groups occur on the same molecule linked by a linear linker, the whole structure can be considered analogous to structures such as diamond and wurtzite. Instead of a structure built up of tetrahedral units joined by covalent bonds, the hydroxy and amino groups act as the tetrahedral units, three of the covalent bonds are replaced by three hydrogen bonds, and the last covalent bond is replaced by the rest of the molecule.

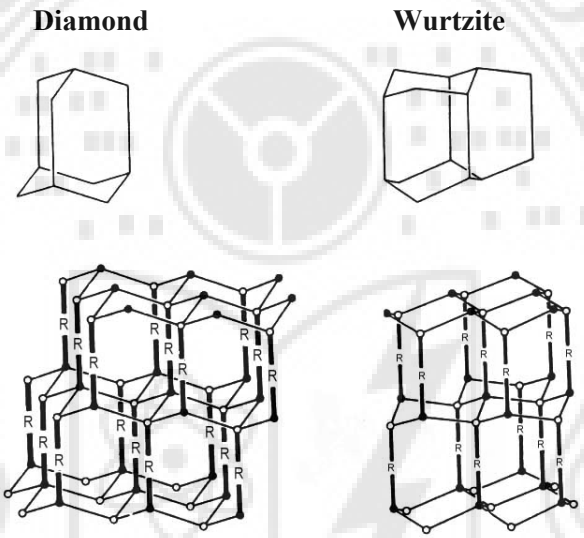

Scheme 6. The diamond and wurtzite based structures built up from layers of β-As sheets. R=Linear linking unit between amino and hydroxy groups (represented by thick and open circles respectively).

The first structure of an H-bonded super network between amines and alcohols is that of 4-aminophenol (4AP) described by Brown (1951), but in this study the positions of the H-atoms were not determined [1.26]. Ermer and Eling (1994) redetermined the crystal structure of 4AP, located H-atom positions and formulated principles for such complementary molecular recognitions [1.24]. Supraminol

recognition was first identified by Liminga (1967) in the crystal structure of the hydrazine–bis(ethanol) adduct [1.27].

1.4 Archetypal aminophenols (4AP and 4APP)

A compound that exemplifies the Ermer-Eling model is 4AP [1.24]. It forms the expected tetrahedral network exclusively of the N(H)O synthon, **I**, (Scheme 1) and is characterised by a complete saturation of the hydrogen bonding potential of both amine and hydroxy molecular functionalities (Figure 1). Notably in the case where –OH and $–NH_2$ groups are disposed linearly, synthon **II** (Scheme 1) is always observed. The β-As sheet pattern of 4AP (Scheme 3) is topologically similar to the wurtzite network (Figure 2).

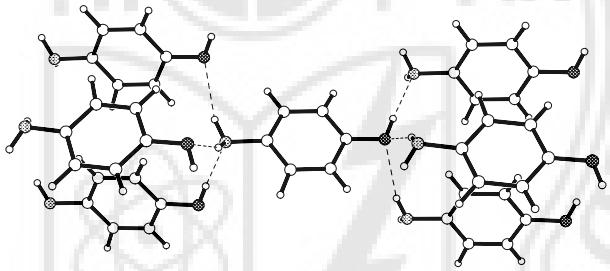

Figure 1. Tetrahedral hydrogen bridge network around NH_2 and OH functionalities in 4AP. Notice the herringbone interactions (synthon **II**) between aromatic rings.

4-(4-Aminophenyl)phenol (4APP) forms a structure that is directly analogous to 4AP, consisting of parallel β-As sheets linked by a biphenyl spacer group. The phenyl group in 4AP is in effect replaced by the biphenyl group in 4APP (Figure 2). Accordingly, 4AP and 4APP are identifiable as archetypal examples of this family. Both molecules take the same space group ($Pna2_1$) with similar dimensions for the *a* and *b* axes [8.184(1) and 5.262(1)Å for 4AP and 8.096(1) and 5.396(1)Å for 4APP respectively] and this is the plane in which the β-As sheets form. The change in

spacer is reflected in the length of the *c* axis, which at 12.951(2)Å for 4AP, and 21.217(2)Å for 4APP, is approximately equal to the molecular length. Thus, in 4AP and 4APP, the crystal structure retains the robust amino-hydroxy synthons **I** and **II**. In these two crystal structures the competing herringbone [1.28] and hydrogen bonding interactions are effectively insulated.

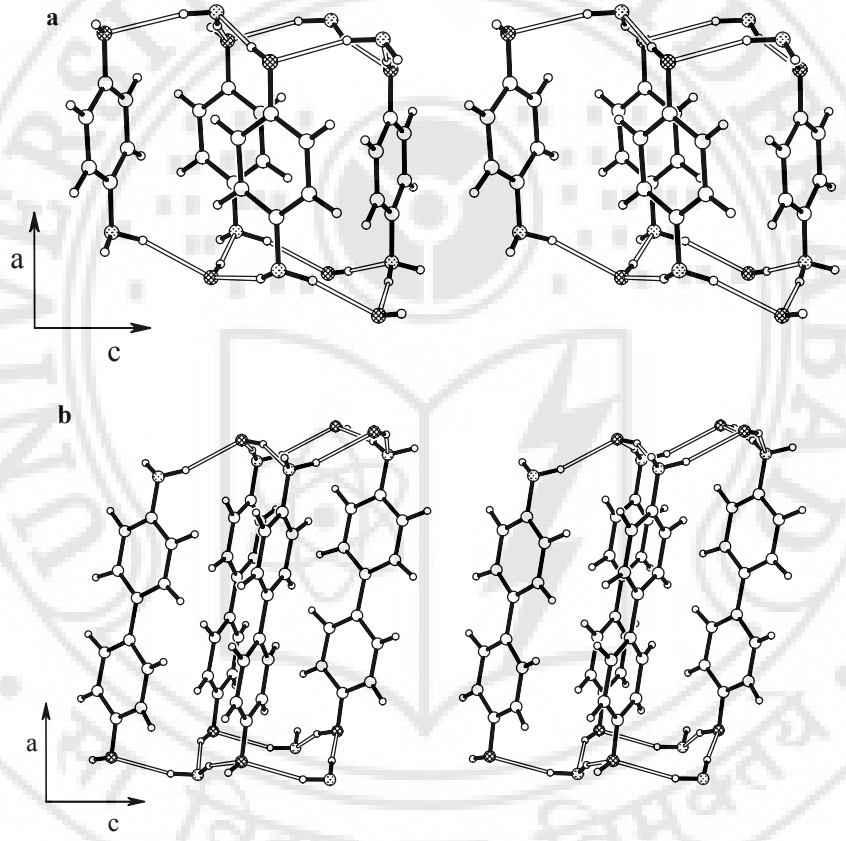

Figure 2. Stereoview of the β-As sheet structure in (a) 4AP and (b) 4APP [1.24].

Ermer and Eling [1.24] also noted that various linear aromatic based 1:1 amino-hydroxy complexes take the cubic diamond architecture, whereas 4AP and 4APP prefer the super-wurtzite network. A plausible reason for this observation could

be that aromatic ring tilting preferences at oxygen and nitrogen determine whether a super-wurtzite (1.5 kcal mol^{-1} less favoured) or a cubic diamond network is built up.

1.5 Helical structures: Supramolecular chirons

Hanessian and co-workers [1.25] recognized the spontaneous self-assembly between C_2-symmetrical chiral 1,2-diols and 1,2-diamines. The molecular recognition between these groups is robust and predictable because of the complementary hydrogen bridge donor:acceptor ratios.

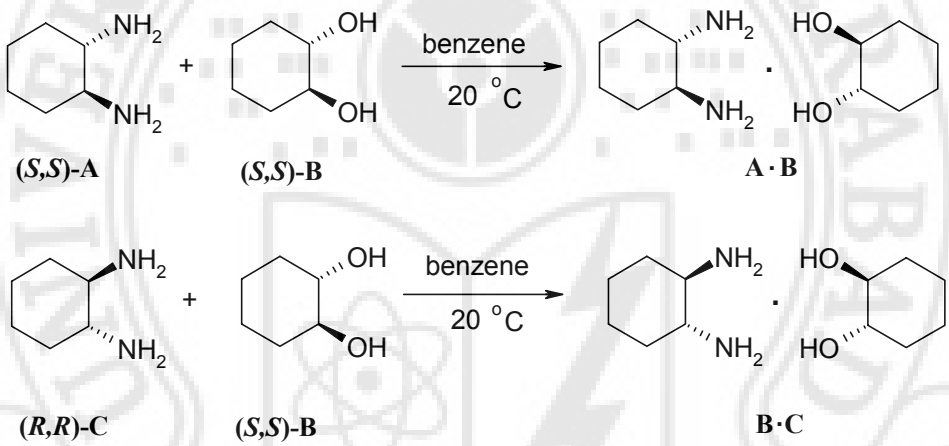

Scheme 7. Supraminol complexes **A**·**B** and **B**·**C** obtained from equimolar amounts of enantiomerically pure *trans*-1,2-diaminocyclohexanes (**A** and **C**) and *trans*-1,2-cyclohexanediol (**B**).

In the crystal structure of the 1:1 adduct **A**·**B** of (1*S*,2*S*)-1,2-diaminocyclohexane **A** and (1*S*,2*S*)-1,2-cyclohexanediol **B** (Scheme 7), the cyclohexane rings align into four vertical columns and the polar hydrogen bonding groups face inward. The structure is a pleated sheet-like array of eight-membered, square planar, hydrogen bonded units in which the O- and N-atoms are tetracoordinated (Figure 3) [1.3d]. The remaining hydroxy and amino functional

groups are engaged in two symmetrical side rows of tricoordinated zigzag hydrogen bridge patterns which flank opposite sides of the central octagonal staircase core.

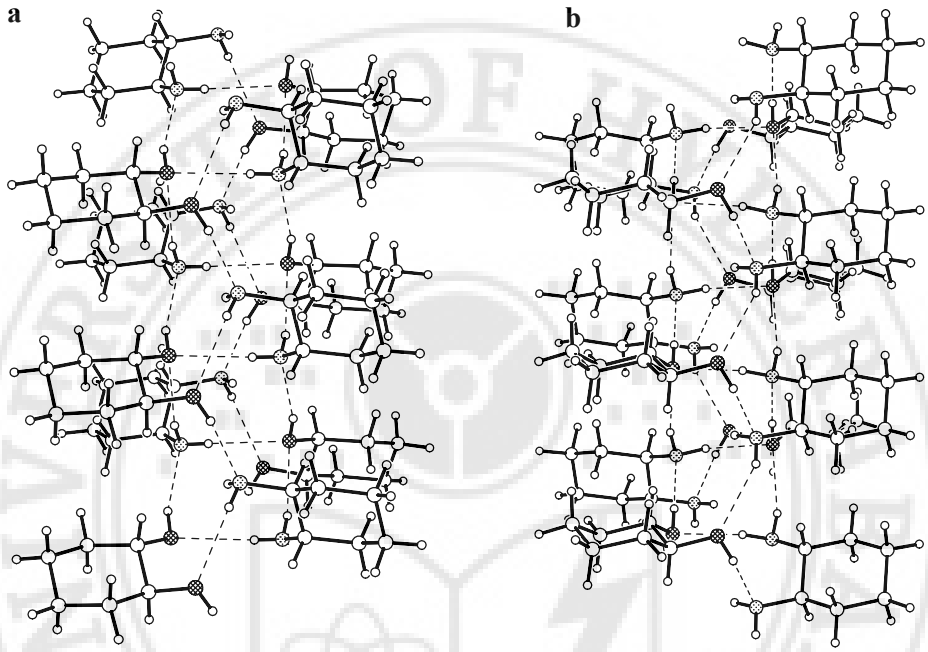

Figure 3. Pleated sheet hydrogen bond network in (a) 1:1 homochiral complex **A**·**B** and (b) 1:1 heterochiral complex **B**·**C**. Notice the left-handed (**A**·**B**) and right-handed (**B.C**) helicity of the assembly.

The crystal structure of the 1:1 complex **B**·**C** of enantiomerically pure (1*R*,2*R*)-1,2-diaminocyclohexane **C** and (1*S*,2*S*)-diol **B** is also predictable and similar to that of the homochiral complex **A**·**B**. The relative sense of H-donation in the core is opposed to that in the side rows in both **A**·**B** and **B**·**C** (Figure 3). Interestingly, the chirality of the diol and diamine components controls the tertiary structure of the complex, in other words the sense of chirality with which the cyclochexane rings wrap around the central core in the triple-stranded helicate. Thus, whereas the (*S*,*S*)-diamine **A** gives a left-handed helicate **A**·**B** with the (*S*,*S*)-diol **B**, the (*R*,*R*)-diamine **C**

gives a right-handed helicate **B·C** with the same diol. This example highlights that the handedness of the crystal structure is related to the chirality of the molecular components and this in turn also shows relationships between molecular and crystal structures.

From an analysis of various supraminols, Hanessian and co-workers are able to predict structures of the best-matched pairs of diamines and diols in terms of supramolecular chirons. The concept of the *supramolecular synthon* is that it is a small substructural unit that contain the logical code for self-assembly by noncovalent interactions. A chiral counter part of the supramolecular synthon is termed as *supramolecular chiron* [1.25]. Thus, supramolecular chiron is the minimal homo- or heterochiral molecular unit or ensemble capable of generating ordered superstructures by self-assembly through H-bonding or other noncovalent forces, and leading to topologically distinct enantio- or diastereopure architectures.

1.6 Anomalous Aminophenols (2AP and 3AP)

Desiraju and co-workers [1.29] determined the structures of the isomeric 2-aminophenol (2AP) and 3-aminophenol (3AP) [1.30] with neutron diffraction to seek further insight into molecule-to-crystal extrapolation. These structures show unusual N–H···π hydrogen bridges (Figure 4) [1.31]. In 2AP, each –OH group donates a hydrogen bridge to an $–NH_2$ group (O–H···N) and accepts one (N–H···O) from another. The fourth coordination site is occupied by a C–H···O hydrogen bridge [1.21]. Each $–NH_2$ group similarly donates and accepts a strong hydrogen bridge with different molecules. The second H atom participates in the N–H···π bridge. The hydrogen bonding interactions in 3AP is similar to that in 2AP. In both these structures the tetrahedral environment around the O- and N-atoms is maintained but the hydrogen bridges are not completely of the strong type.

It may be noted that the structures of 2AP and 3AP are distinctly different from the isomeric 4AP. The reason for the anomalous structures of 2AP and 3AP compared with the normal structure of 4AP is understood in terms of the need to attain herringbone or T-shaped geometry of the phenyl rings in the two structures (Figure 5). The preference for two weak (N–H···π and C–H···O) instead of one strong hydrogen bridge (N–H···O) is caused by the optimisation of the herringbone interactions and this is identified as the primary structural effect in these compounds. However, in 4AP the herringbone packing is able to co-exist with the hydrogen bonded wurtzite network and the interference between these two sets of interactions is minimal.

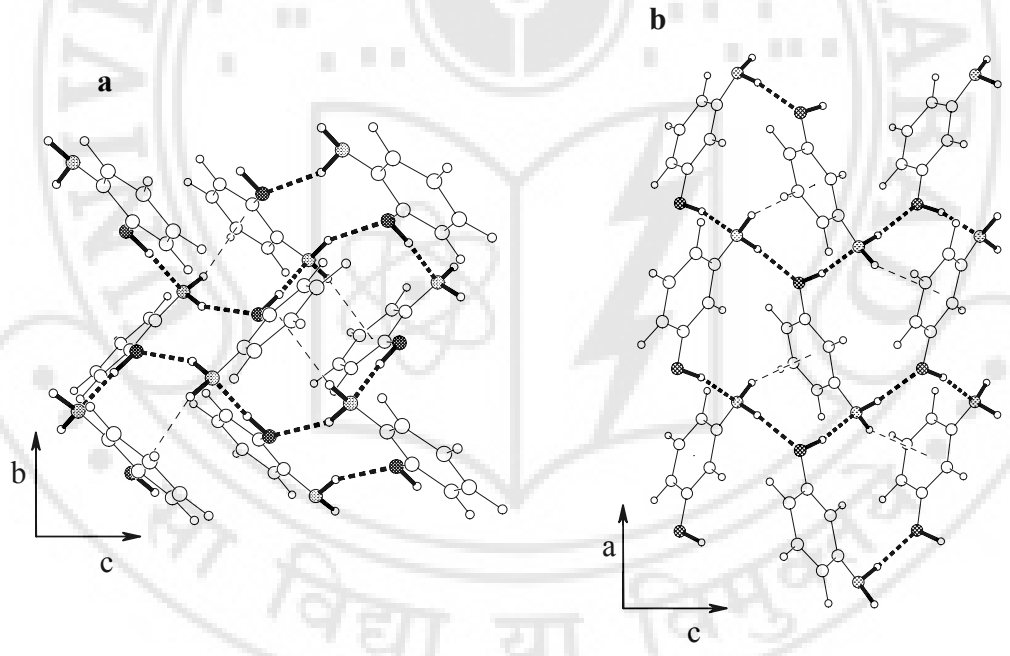

Figure 4. Hydrogen bridges in (a) 2AP and (b) 3AP.

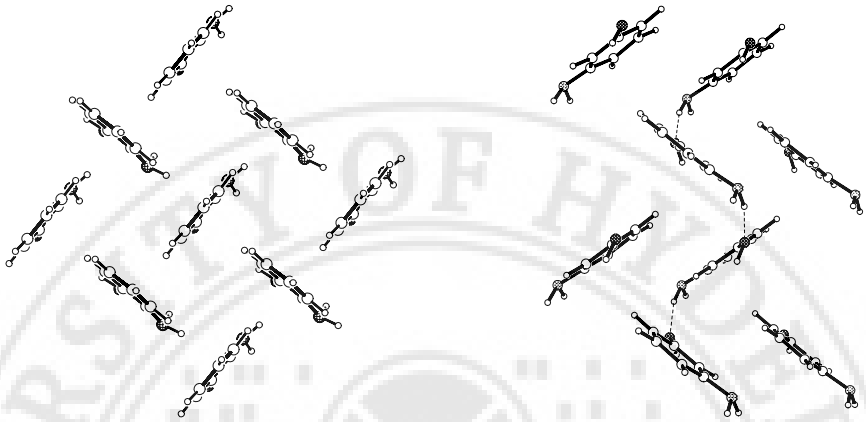

Figure 5. Herringbone interactions in (a) 2AP and (b) 3AP. Notice that the arrangement of aromatic rings is similar to that in the structure of benzene.

The crystal structures of 2AP and 3AP are very different from that of 4AP. However, structures of all these three isomeric aminophenols contain the infinite chain of N(H)O synthon **I** (Scheme 1). It is possible then that the infinite chain synthon **I** is the prototype structure element and that it has the encoding information for molecular recognition. Herringbone synthon **III** plays an equally significant role and if it has minimal interference with synthon **I** then it may lead to the most stable synthon **II** found in 4AP and all the β-As sheet structures. When interaction interference is more pronounced a better alternative synthon is **V** found in the crystal structures of 2AP and 3AP and absent in the crystal structure of the 4AP isomer. In 2AP additionally there is the presence of synthon **IV**. In effect, the most useful supramolecular synthons combine form with compactness. It is further mentioned that the number of supramolecular synthons in a supermolecule may be very large but that only some of these are useful. The generality of these prototype structures may be appreciated from the fact that 4-methyl-2-aminophenol [1.32] and 4-chloro-2-

aminophenol [1.33] have structures very similar to that of 2AP. It is a useful exercise to establish generalisations from the 3AP structure. Hanessian's compound are somewhat less problematic because they do not contain aromatic groups [1.25].

1.7 Some prior study on amino-hydroxy recognition

The hydroxy-amino recognition has also been implicit in some other studies [1.34]. Mootz and co-workers reported the crystal structure of ethanolamine in which the hydroxy and amino groups are separated by a two-carbon ethano spacer. This structure reveals a distorted super-tetrahedral architecture formed by N(H)O bridges and generate a super-black phosphorus sheet connected in a three dimensional network [1.35]. Mootz and co-workers also studied the crystal structure of diethanolamine. In this case, O–H···O dimers are formed and these dimers are further connected by O–H···N bridges in a one dimensional tubular super architecture in which NH groups point to the inner side.

Meyers and Lipscomb [1.36] and Donohue [1.37] reported the crystal structure of hydroxylamine. It is a single and characteristic 3D connected network formed by undulating H-bonded sheets with a repetitive covalent O–N bond. The H-bridge sheets generate distorted super-cyclohexane boats (and not chairs) that are neither zincblende-nor wurtzite-like structures (Figure 6).

Toda and co-workers [1.38] studied the 1:1 amine-hydroxy complex between hydrazine and hydroquinone. This adduct forms a fully saturated super-tetrahedral architecture. In this molecular complex a super-black phosphorus sheet-like structure can be seen with alternating hydrophobic (benzene rings) and hydrophilic (OH and NH_2) regions. It is interesting that the introduction of an aromatic spacer in the hydrazine molecule affords the cubic diamond hydrogen bridge network. Toda and co-workers have noted amino-hydroxy recognition in various other molecular complexes [1.39]. Loehlin and co-workers [1.40] reported some molecular complexes

between 1:2 diamines–monoalcohols and 1:1 diamines–diols and classified these saturated hydrogen bridges into hexagonal-like (chicken wire) and ladder patterns.

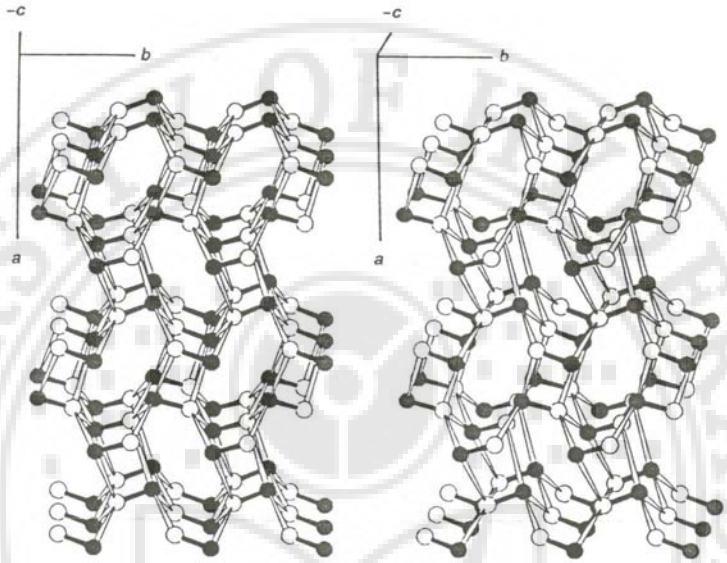

Figure 6. Stereoview of the super-tetrahedral H-bonded 3D network of hydroxylamine. O, white, N, black spheres; N(H)O bridges drawn as open white, covalent O–N bonds as filled black sticks. Notice the H-bridge sheets consisting of fused distorted super-cyclohexane boats.

In summary, simple molecules can have complex crystal structures and the relationship between molecular and crystal structures can accordingly be difficult to delineate. Considering the molecular basis of organic chemistry seeking such connections is only natural. Therefore any rational approach that associates functional groups with crystal structure attributes is considered to be important and the hydroxy-amino recognition falls into this category.

This thesis begins with a description of some methylene linked supraminols. The following compound numbering is followed throughout the thesis (Scheme 8).

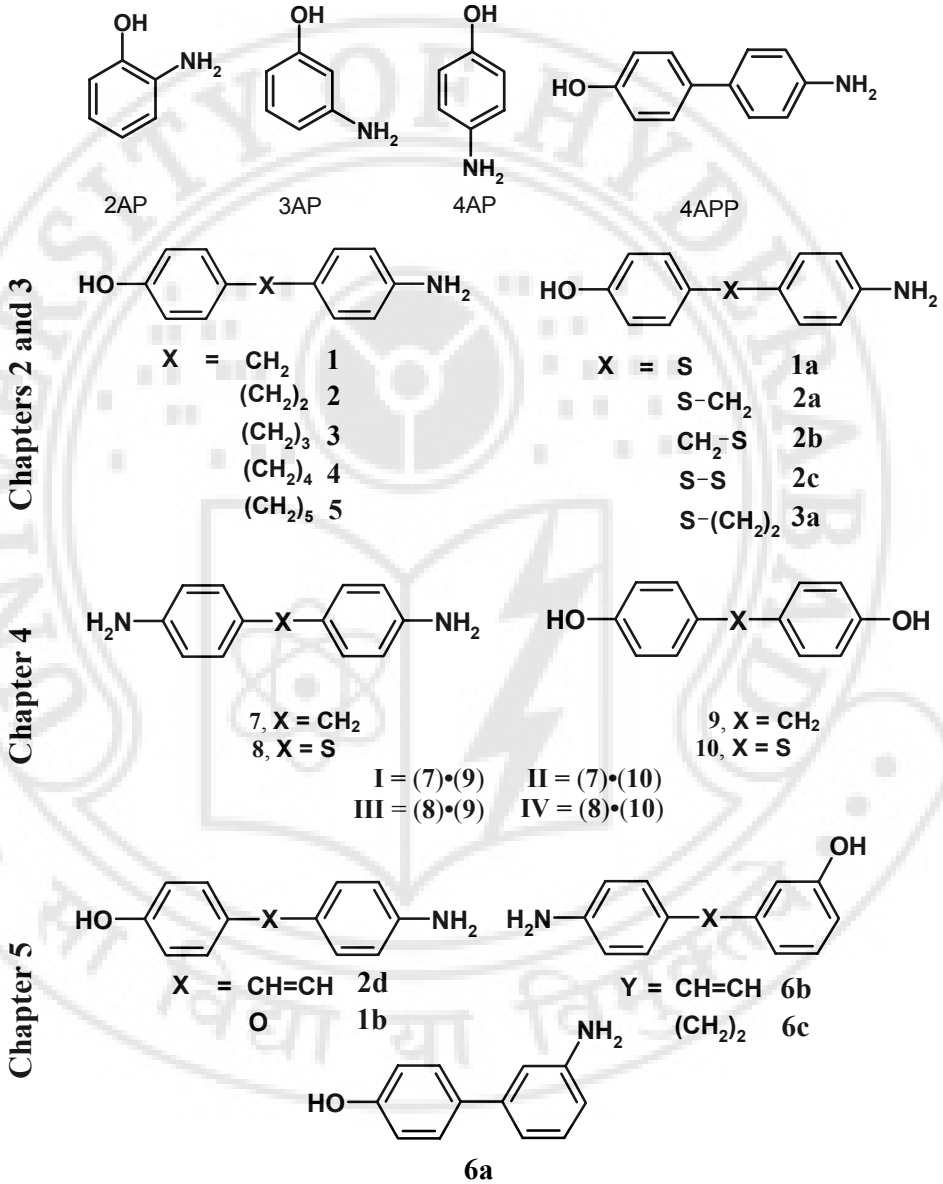

Scheme 8

CHAPTER TWO

CRYSTAL CHEMISTRY OF HOMOLOGATED AMINOPHENOLS

2.1 Introduction

Crystal engineering, the design of organic solids with specified architecture and properties continues to fascinate chemists [2.1]. The prediction of crystal structure based solely on the structure of molecular components remains one of the foremost challenges in crystal engineering [1.6]. In order to establish correspondences from molecular functionality into the supramolecular realm, a precise understanding of noncovalent intermolecular interactions that control crystal packing is essential. A molecule is made up of functional groups but the supramolecular behaviour of any particular functional group in a molecule depends on the position and location of all the other functionalities, with the further condition that all portions of a molecule including the hydrocarbon residues have supramolecular functionality. This renders the functional group or modular approach to be of limited applicability. Complementarity is characteristic of both geometrical and chemical recognition [1.7] and leads to structural complexity. To simplify and understand this complexity, the structural chemist identifies recurring structural units, known as *supramolecular synthons* [1.17]. When *robust* synthons are recognized, crystal design may become straightforward. Any organic crystal structure can be simplified to a network wherein the molecules are the nodes and the supramolecular synthons are the node connections. The strength and directionality of strong intermolecular interactions of the O–H···O, O–H···N and N–H···O types had provided enormous predictability in many studies of crystal engineering [1.20].

The family of aminophenols or supraminols offers sufficient structural consistency with adequate supramolecular diversity to explore the interactions between molecular functionality in crystal packing. Ermer and Eling [1.24], and

Hanessian *et al*. [1.25] elaborated elegant principles of recognition for such molecules. The β-As sheet and its alternative structures have been implicated in a number of N(H)O structures of supraminols [1.24-1.40]. It is interesting to note that in a number of aromatic compounds or molecular complexes where amino and hydroxy groups are disposed linearly, β-As sheets in other words N(H)O saturation are observed (archetypal 4AP and 4APP). However, prediction of crystal structures are formidable task. Desiraju, Howard and co-workers [1.29] recognized that factors other than N(H)O saturation may need to be considered in supraminol recognition. For example in 2AP and 3AP the potential for the formation of strong O–H···N and N–H···O bridges is not completely fulfilled. Instead, there is the formation of weak N–H···π and C–H···O hydrogen bridges at the expense of strong N–H···O bridge. That means that a change from the 4AP to the 2AP and 3AP structures is effectively a change from a more *hierarchical arrangement* [2.2] to one where there is more *structural interference* [2.3] between molecular functionality. It is important to investigate whether 2AP and 3AP structures can be reproduced. Even with just three molecular functionalities, hydroxy, amino and phenyl, there are two quite distinct structural possibilities.

2.2 *n*-Even and *n*-odd structures

By examining two β-As structures 4AP and 4APP, the question arises as to when and why the β-As sheet structures are formed. Would this structure type be reproduced with more extended linking units between the aniline and phenol moieties? Systematic studies of possible structure types have not been numerous. In order to study these questions and to establish the requirements for β-As sheet formation in homologous supraminols, a series of aminophenols **1** through **5** with methylene spacers of the general type $HO–C_6H_4–(CH_2)_n–C_6H_4–NH_2$ (n = 1 to 5) and both OH and NH_2 in a *para* position were prepared (Scheme 1). Accordingly, 4APP

can be considered as the n = 0 aminol. These aminols also provided an interesting synthetic exercise, with each compound requiring a different multi-step route. Details are given in the experimental section.

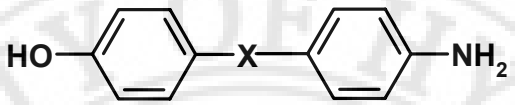

X = CH_2 **1**
$(CH_2)_2$ **2**
$(CH_2)_3$ **3**
$(CH_2)_4$ **4**
$(CH_2)_5$ **5**

Scheme 1

All the five supraminols above can be described in terms of three major supramolecular synthons based on hydrogen bonding between OH and NH_2 groups: the tetramer loop or square motif, the infinite N(H)O chain and the β-As sheet. These three synthons are not completely independent of each other but are interrelated with the structures tending towards the more stable β-As sheet in some cases. This series of homologated aminols also provides an opportunity for investigation into the even-odd effect in the alternation of melting points and other physical properties of *n*-alkanes and substituted *n*-alkanes [2.4, 2.5]. The n = even (**2** and **4**) exhibit systematically higher melting points compared to those with n = odd (**1**, **3** and **5**). The alternating melting points are reflected in and explained by the alternation in the crystal structures.

This chapter explores these ideas further and provides an analysis of the crystal structures of five supraminols that contain *four* molecular functionalities. These are the hydroxy group, the amino group, the phenyl rings and a linker group,

classically a polymethylene chain which links phenyl rings respectively. It is an attempt to find the correspondence between molecular structure and crystal structure for these compounds.

2.3 β-As sheet structures in aminols 2 and 4

The crystal structure of 4-(4-aminophenethyl)phenol, **2**, shows the expected tetrahedral hydrogen bonded network of one O–H···N and two N–H···O hydrogen bridges (Figure 1). The packing is directly analogous to that of 4AP and 4APP in which the N(H)O sheet is arranged in a hexagonal manner like the chair form of cyclohexane. This is the β-As sheet or super arsenic sheet structure. The parallel β-As sheets are linked by the rest of the molecule (Figure 2).

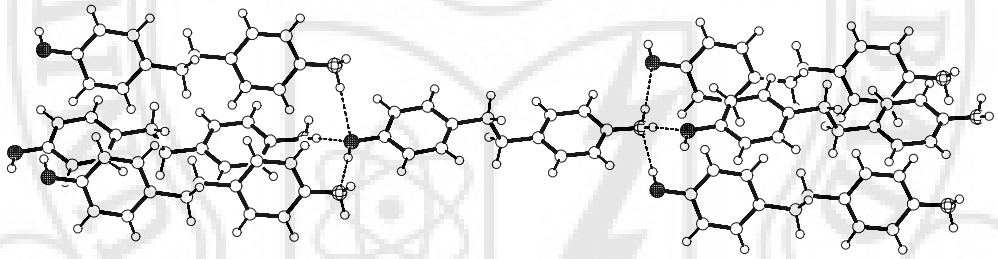

Figure 1. Tetrahedral hydrogen bridge network around NH_2 and OH functionalities in **2**.

There are subtle differences between this structure and those of 4AP and 4APP. Firstly, there is a change in space group from $Pna2_1$ to *Pc*; secondly, while 4AP and 4APP take a wurtzite-like structure, supraminol **2** is analogous to cubic diamond and to super adamantane (Figure 3). The structure is further stabilized by herringbone interactions [1.28] with an angle of 67° between adjacent phenol rings and of 70° between adjacent aniline rings. The structure is comparable to the arrangement of aromatic rings in 4APP, simple aminophenols and crystalline benzene. The structural and geometrical parameters are given in tables 1 and 2.

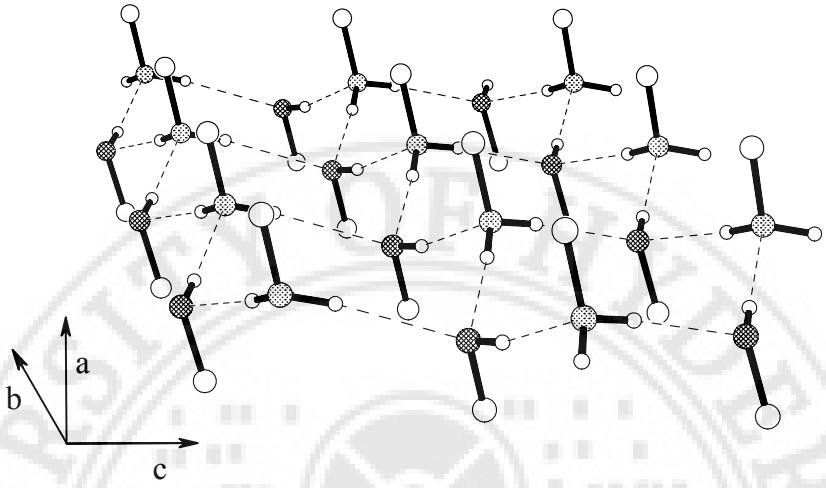

Figure 2. β-As sheet. Note that N(H)O synthons exclusively are involved.

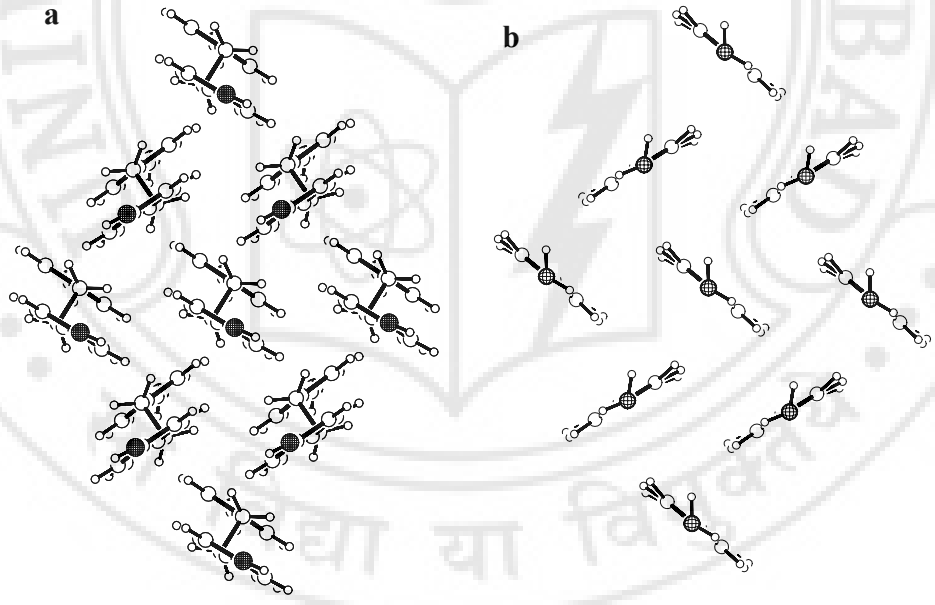

Figure 3. Herringbone interactions in (a) aminol **2** and (b) 4APP (adapted from ref [1.24]). Notice that in **2** the arrangement of aromatic rings is similar to that in 4APP.

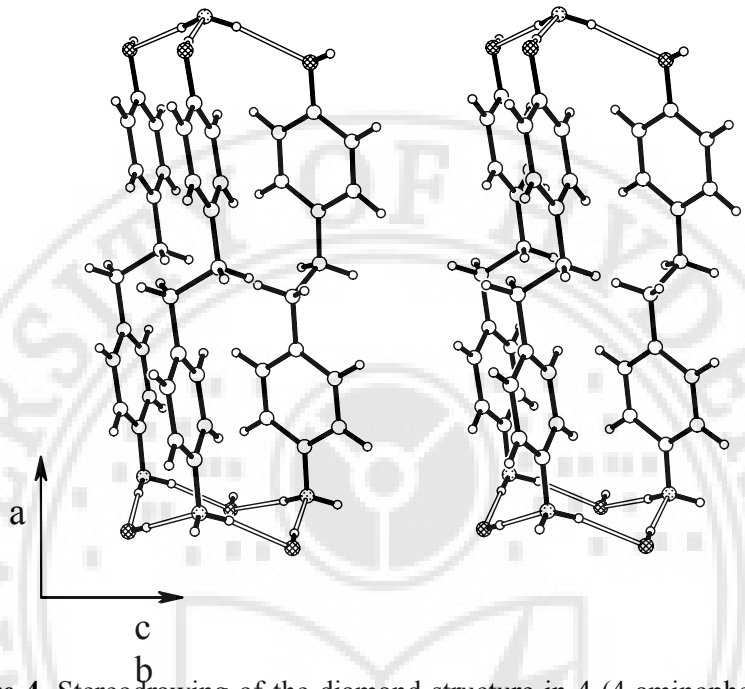

Figure 4. Stereodrawing of the diamond structure in 4-(4-aminophenethyl)-phenol **2**.

The structure of 4-[4-(4-aminophenyl)butyl]phenol, **4**, is isostructural to that of **2,** and β-As sheets are observed. The space group is *Pc* and the structure is diamond-like rather than wurtzite-like (Figure 4). The structure is further stabilized by herringbone interactions with ring plane–ring plane angles of 69° and 72° respectively for the phenol and aniline ring pairs. The relevant structural and geometrical parameters are given in tables 1 and 2.

Thus in the β-As sheet (*n*-even) structures **2** and **4** the crystal structure is consistent with those of other hydroxy-amino compounds and the molecular complexes described by Ermer [1.24] because the competing herringbone and hydrogen bonding interactions are effectively insulated. This implies that the

molecule-to-crystal extrapolation is of good fidelity and is taking place when there are 'even' methylene chains as linkers between the aniline and phenol rings.

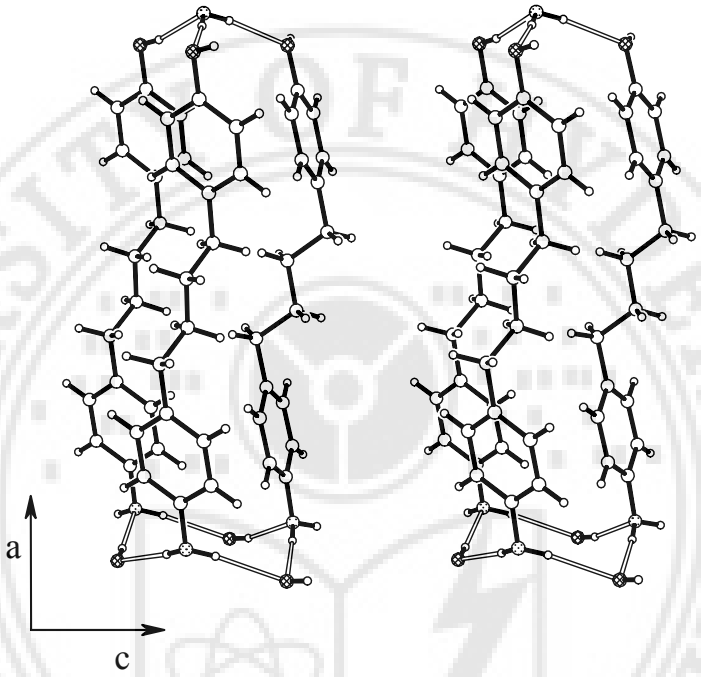

Figure 5. Stereopacking of the cubic diamond in 4-[4-(4-aminophenyl) butyl]phenol **4**.

2.4 Tetramer loop synthon in 1

Suitable crystals of **1** were obtained in Hyderabad for neutron diffraction studies and neutron data were collected (in collaboration with Prof. J.A.K. Howard, University of Durham at ISIS, Oxford, U.K.). For comparison with the other compounds in this series, the low temperature single crystal X-ray data were also collected. The X-ray data are in good agreement with the neutron data and in the following discussion of molecular interactions, the geometries derived from both the X-ray (**X**) and neutron (**N**) data sets are quoted.

Table 1. Geometrical parameters of hydrogen bridges in aminols **1-5**.

Aminol	H-bridge	*d* (Å)[a]	*D* (Å)	*θ* (deg)
1-Neutron	O–H···N	1.76	2.723(7)	167.8
	N–H···O	1.99	2.908(5)	150.2
	N–H···π	2.39	3.334	155.5
	C–H···π	2.57	3.536	147.6
	C–H···π	2.66	3.727	173.1
1-X-ray	O–H···N	1.77	2.7485(18)	170.5
	N–H···O	1.99	2.9281(17)	152.2
	N–H···π	2.43	3.377	156.0
	C–H···π	2.63	3.582	145.9
	C–H···π	2.72	3.797	172.1
2	O–H···N	1.84	2.815(2)	173.3
	N–H···O	2.13	3.130(2)	169.7
	N–H···O	2.30	3.312(2)	177.3
3	O–H···N	1.79	2.776(2)	172.5
	N–H···O	2.26	3.205(2)	154.3
	N–H···π	2.38	3.354	161.2
	C–H···O	2.53	3.268(2)	124.5
	C–H···O	2.59	3.564(2)	149.3
4	O–H···N	1.88	2.818(3)	159.0
	N–H···O	2.15	3.155(3)	172.3
	N–H···O	2.29	3.307(3)	174.5
5	O–H···N	1.80	2.758(2)	163.1
	O–H···N	1.82	2.788(2)	169.0
	N–H···O	2.09	3.067(2)	162.7
	N–H···O	2.28	3.181(2)	146.9
	N–H···O	2.57	3.461(2)	146.4
	N–H···π	2.60	3.542	154.2
	C–H···O	2.47	3.305(2)	132.9
	C–H···O	2.60	3.298(2)	121.0
	C–H···O	2.62	3.312(2)	120.5
	C–H···O	2.67	3.510(2)	133.8

[a] O–H, N–H and C–H distances are neutron normalized to 0.983, 1.009 and 1.083 Å.

Table 2. Details of some structural parameters for the supraminols in this study.

compound	**1N**	**1X**	**2**	**3**	**4**	**5**
structure	square motif		β-As	infinite chain	β-As	infinite chain
C–O, C–N angle [°][a]	117		174	124	174	129 (A) 125 (B)
herringbone angle [°][b]	88		67 and 70	41	69 and 72	25 and 20
mp [°C]	147.6		222.5	141.9	185.9	106.6
D_{calc} [mg/m^3]	1.230	1.194	1.258	1.208	1.190	1.162
C_k* [%][c]	0.69	0.66	0.71	0.68	0.69	0.67
pyramidal factor[d]	0.305	0.278	0.320	0.284	0.304	A=0.308 B=0.347
latt. energies [kcal mol^{-1}][e]:						
van der Waals	–15.5103	–16.9782	–22.6960	–23.9593	–25.8799	–26.5133
electrostatic	–12.6148	–10.5619	–14.9624	–13.3021	–15.2413	–12.8726
hydrogen bridge	–5.8331	–6.4404	–9.0674	–5.2543	–8.8910	–6.2596
total energy	–33.9582	–33.9805	–46.7258	–42.5157	–50.0122	–45.6455

a) The angle between the C–O and C–N vectors in the aminol have been calculated using *RPluto*. This gives a measure of the linearity of the molecule. b) Details are given in the Experimental Section. c) C_k*, packing co-efficient calculated with *PLATON*. d) The perpendicular distance from the basal plane to the apex of the pyramid. e) Lattice energies calculated using *Cerius*^{2} from Accelrys.

The crystal structure of **1** does not make use of complementary recognition of NH_2 and OH moieties to give a saturated N(H)O packing. Instead, an unsaturated arrangement of N(H)O hydrogen bridges is seen. In this structure only two of the three possible N(H)O hydrogen bridges are formed. The structure is based on a fourfold arrangement of N(H)O hydrogen bridges, a tetramer loop synthon, henceforth referred to as a square motif (Figure 6). These square motifs are built up to form chains: Sets of two molecules bend towards each other and are linked to another set of two molecules by a square motif to form chains. The aniline hydrogen that is not involved in a hydrogen bridge to the hydroxy group interacts with an adjacent phenol ring to form a N–H···π interaction (2.43Å, 156° (**X**); 2.39Å, 155.5° (**N**))

[1.31]. A C–H···π interaction is formed at the other face of the same phenol ring and another C–H···π interaction with the anilino ring completes the packing [1.21].

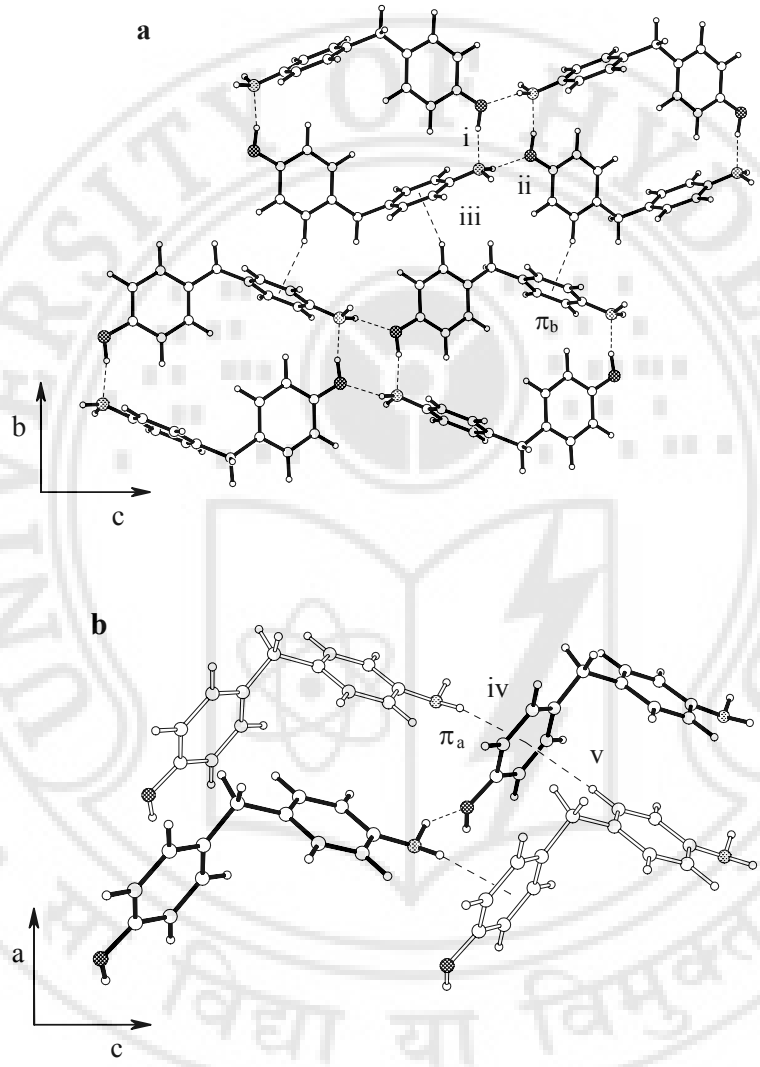

Figure 6. (a) Square motif synthon formed by O–H···N (i) N–H···O (ii) hydrogen bridges and C_5–H_5···π_B (iii) interactions in the crystal structure of aminol **1**. (b) N_1–H_{1b}···π_a (iv) and C_9–H_9···π_a (v) interactions to the same phenyl ring in **1**.

With all π-bases there is some question as to where exactly the hydrogen bridge accepting site is located. Such questions can be answered satisfactorily with neutron diffraction analysis. In X–H···π interactions the X–H bond vector can be directed either towards the ring centroid or towards an individual C–C bond within the ring. In the N_1–H_{1b}···π_A interaction (interaction iv in Figure 6b), the N–H vector is directed towards one of the C–C bonds of the phenol ring (Table 3) but the C_9–H_9···π_A bridge to the other face of the same ring (v in Figure 6b) is directed towards the ring centroid. In contrast, the C–H vector in the C_5–H_5···π_B interaction (iii in Figure 6a) is directed towards one of the C–C bonds. In all cases, the direction of the X–H vector with the closest approach is to the ring centroid and not to a specific C–C bond. Using the X–H···π categories defined by Malone et al [1.31e]. N_1–H_{1b}···π_A and C_9–H_9···π_A are type I whereas C_5–H_5···π_B is a type III interaction.

It can be seen from the tables below that in every case the hydrogen atom is closer to the aromatic ring centroid (π) than to any of the ring atoms or bonds. However, the C_9–H_9 vector points directly towards the ring centre.

Table 3. Geometry of N_1–H_{1b}···π hydrogen bridges in aminol **1** (X and N)

		X-ray			Neutron	
H-bridge	***d* (Å)**	***D* (Å)**	**θ (deg)**	***d* (Å)**	***D* (Å)**	**θ (deg)**
N_1–H_{1b}···π	2.43	3.377	156.0	2.39	3.334	155.5
H_{1b}···C_1	2.59	3.401	136.4	2.56	3.359	136.5
H_{1b}···C_2	2.84	3.546	127.3	2.81	3.507	126.8
H_{1b}···C_3	3.02	3.776	132.8	2.98	3.726	131.8
H_{1b}···C_4	2.99	3.889	148.3	2.97	3.852	147.1
H_{1b}···C_5	2.76	3.764	170.0	2.74	3.724	168.9
H_{1b}···C_6	2.56	3.523	159.0	2.53	3.486	159.9
N_1–H_{1b}···π (C_5–C_6)	2.57	3.578	173.7	2.54	3.539	174.7

Table 4. Geometry of C_9–H_9···π interactions in aminol **1** (X and N)

	X-ray			Neutron		
H-bridge	***d* (Å)**	***D* (Å)**	**θ (deg)**	***d* (Å)**	***D* (Å)**	**θ (deg)**
C_9–H_9···π	2.72	3.797	172.1	2.65	3.727	173.1
H_9···C_1	3.10	4.056	147.6	3.04	3.995	148.1
H_9···C_2	3.00	4.003	154.0	2.94	3.939	153.9
H_9···C_3	2.96	4.001	160.0	2.92	3.943	158.8
H_9···C_4	3.04	4.057	156.6	2.98	3.985	155.2
H_9···C_5	3.09	4.073	150.0	3.03	4.003	149.5
H_9···C_6	3.13	4.080	146.0	3.06	4.008	146.3

Table 5. Geometry of C_5–H_5···π interactions in aminol **1**(X and N)

	X-ray			Neutron		
H-bridge	***d* (Å)**	***D* (Å)**	**θ (deg)**	***d* (Å)**	***D* (Å)**	**θ (deg)**
C_5–H_5···π	2.63	3.582	145.9	2.57	3.536	147.6
H_5···C_8	3.01	3.739	125.2	2.94	3.698	127.1
H_5···C_9	2.89	3.842	146.6	2.83	3.798	148.8
H_5···C_{10}	2.87	3.951	174.0	2.82	3.901	176.6
H_5···C_{11}	2.95	3.950	152.3	2.91	3.903	151.6
H_5···C_{12}	3.06	3.844	129.5	3.01	3.795	129.7
H_5···C_{13}	3.07	3.732	119.5	3.02	3.693	120.7
C_5–H_5···π (C_9–C_{10})	2.79	3.834	160.5	2.74	3.786	162.9

2.5 Infinite chain synthon in aminol 3

The most notable supramolecular synthon in 4-[3-(4-aminophenyl)-propyl]phenol, **3**, is a chain of N(H)O hydrogen bridges. This motif (previously observed in 2AP and 3AP) is of major significance in this structural series and is henceforth referred to as the infinite chain. The fragments at both ends of a given molecule are involved in different chains, so that the molecule acts as a linker between chains, thus creating sheets. Once again, the amino hydrogen atom that is not involved in the chain forms an N–H···π hydrogen bridge (Table 1). The infinite chain, and the accompanying N–H···π hydrogen bridges that strengthen the chain, are

directly comparable to 3AP (Figure 7), but not to 2AP [1.29]. Both **3** and 3AP adopt the same space group $Pca2_1$ and the axial lengths along *b* and *c* are nearly equal.

However, there are two differences between 3AP and aminol **3**. One is the spacer length and the other is that while 3AP is stabilized by herringbone interactions **3** is not. The angle between the ring planes in the herringbone interaction [1.28] of 3AP is 60° whereas in **3** the angle between the planes of aromatic rings in adjacent molecules is only 41°. So the herringbone interaction cannot be the only driving force for the formation of this motif.

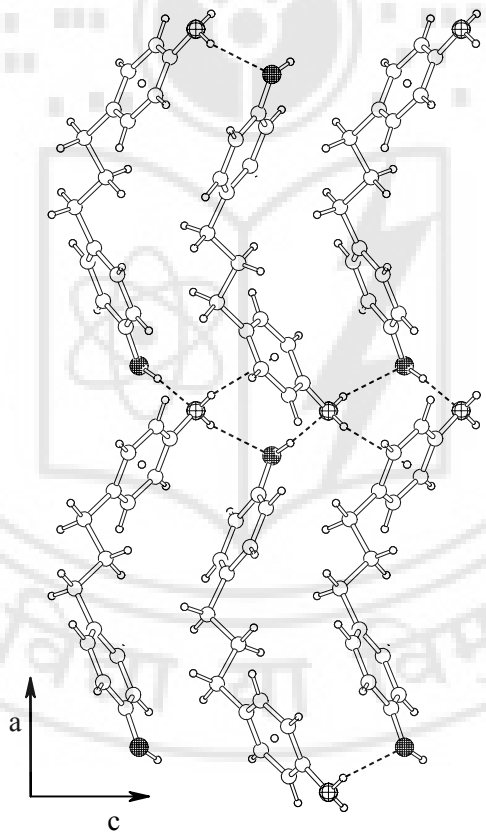

Figure 7. Infinite chain motif in 4-[3-(4-aminophenyl)propyl]phenol **3**.

2.6 A structure tending towards the β-As sheet, aminol 5

There are two independent molecules in the asymmetric unit of 4-[5-(4-aminophenyl) pentyl]phenol, **5**, and these molecules have different geometries (Figure 8). One is similar to **3** while the other is more twisted. The latter (**A** = $N_{(1)}O_{(1)}C_{(1\text{-}15)}$) is saturated in terms of N(H)O hydrogen bridges (forming 3 N(H)O hydrogen bridges at each oxygen and nitrogen), while the former (**B** = $N_{(21)}O_{(21)}C_{(21\text{-}35)}$) is unsaturated forming only two hydrogen bridges at each O- and N-atom and requiring N–H···π and C–H···O interactions to complete the supramolecular valence.

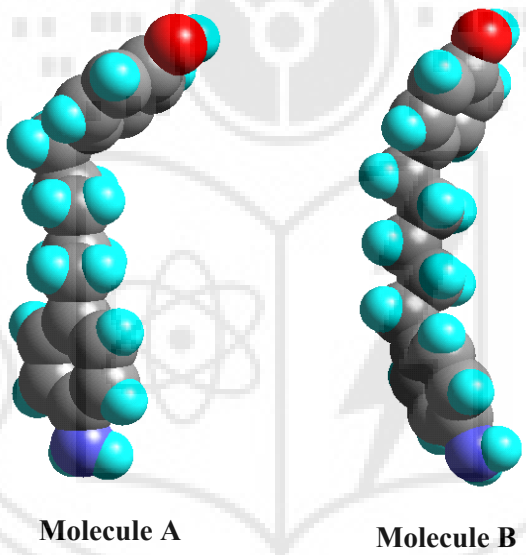

Figure 8. Space-filling model of **5** showing the two symmetry independent molecules.

The structures of aminols **5** and **3** appear to be very similar, and in both cases the major structural synthon is the infinite chain of N(H)O hydrogen bridges (compare Figures 7 and 9). However, in **5** the infinite chains are partially cross-linked by additional N(H)O interactions so that they can be considered as running in two

directions (Figure 10). For comparison, β-As sheets can be considered as fully cross-linked infinite chains. So, **5** can be considered as bridging the β-As sheet (aminols **2** and **4**) and infinite chain structures (aminol **3)**, with molecules **A** and **B** taking the β-As structure and the (single) infinite chain structure, respectively. As in **3** there is no evidence of stabilization by herringbone interactions; the ring plane (**A**)—ring plane (**B**) angle between adjacent molecules is 25° and 20°. One could say that **5** has the same basic structure type as **3** but strives towards the β-As sheet.

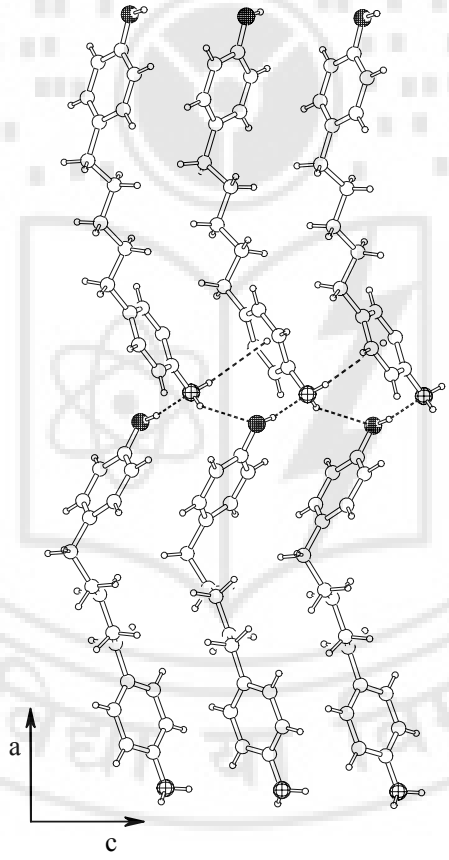

Figure 9. Infinite chain in 4-[4-(4-aminophenyl)pentyl]phenol **5**. Compare this with Figure 7.

2.7 Fixed and variable series

The *n* = odd structures tend towards the β-As sheet as *n* increases and can be considered as a *variable series* whereas for *n* = even, the β-As sheet is invariably formed constituting a *fixed series*. The structures with *n* = odd as the value of *n* increases are as follows: **1** takes a structure that is far from the β-As structure without any infinite chains just square motifs. **3** is closer to the β-As sheet with infinite chains, while **5** is still closer with cross–linked infinite chains. The fact that **5** has two molecules in the asymmetric unit suggests that the structure tends towards the β-As structure preferring to take a more intricate structure, involving two symmetry independent molecules, that is more closely related to the β-As sheet rather than a simpler structure like **3** [2.6]. An overlay of the sheets of the N(H)O interactions in **5** on the β-As sheet shows just how closely these two structures are related (Figure 10).

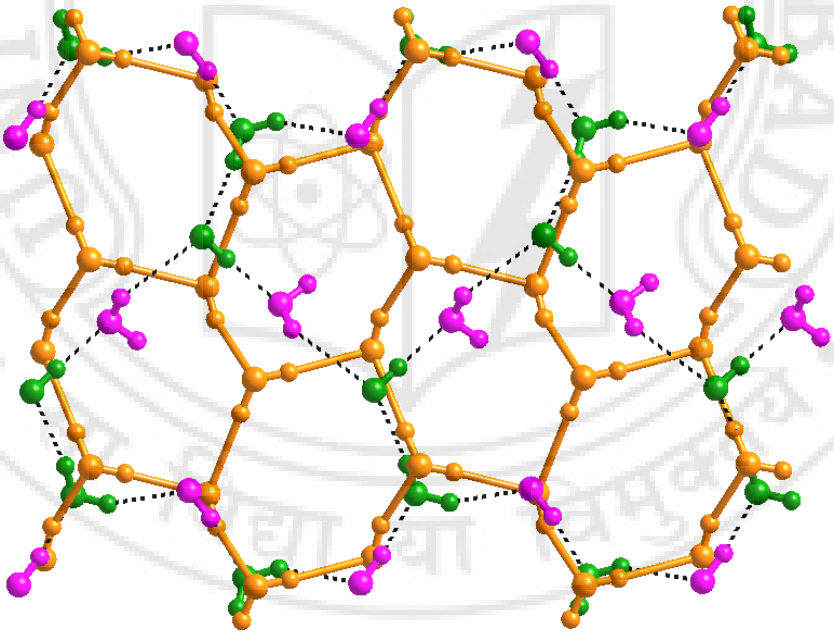

Figure 10. Showing how the cross-linked infinite chains in supraminol **5** relate to the β-As sheet in **4** (overlaid in orange). Symmetry independent molecules **A** (green) and **B** (magenta) are colour coded.

In summary, the *n* = odd series can be considered as a variable series, with the structure moving towards a β-As sheet structure as the length of the linker unit increases:

1 → **3** → **5** → → β-As

In comparison the *n* = even series is a fixed series:

0 = **2** = **4** = β-As

2.8 Melting point alternation

Determination of melting-points is used to establish purity but the melting phenomenon itself is an enigmatic property to structural chemists. Melting points are difficult to correlate with molecular structure because their understanding requires a thorough understanding not only of the strength and nature of the various intermolecular interactions in the crystal but also of other factors such as the size, shape and symmetry of the molecule. The melting event is associated with both enthalpic (ΔH_f) and entropic (ΔS_f) changes. At the fusion temperature, we note that $\Delta H_f = T_f \cdot \Delta S_f$. The melting point of a substance is high not only when the enthalpy change is large but also when the entropy of phase transition is small.

The aminol series provides a good example of the even–odd effect in substituted *n*-alkanes. This effect was first studied by Baeyer in 1877 who noted that *n*-alkane dicarboxylic acids where *n* = even melt at higher temperatures than where *n* = odd [2.4]. This phenomenon has since been observed in many other *n*-alkanes and end-substituted *n*-alkanes. In particular, detailed studies of homologous *n*-alkanes, α,ω-alkanediols, α,ω-alkanediamines, α,ω-alkanedithiols and α,ω-alkanedicarboxylic acids have been carried out by Boese and co-workers [2.5]. The phenomenon of alternation in solid state properties has been attributed to crystal packing factors so that even *n*-alkanes pack more efficiently than odd *n*-alkanes. Apart from normal alkanes, the melting points of the *meta*- and *para*-isomers of anisylpinacolone,

cyclopropane and benzene [2.7] have been rationalized using molecular dynamics simulations.

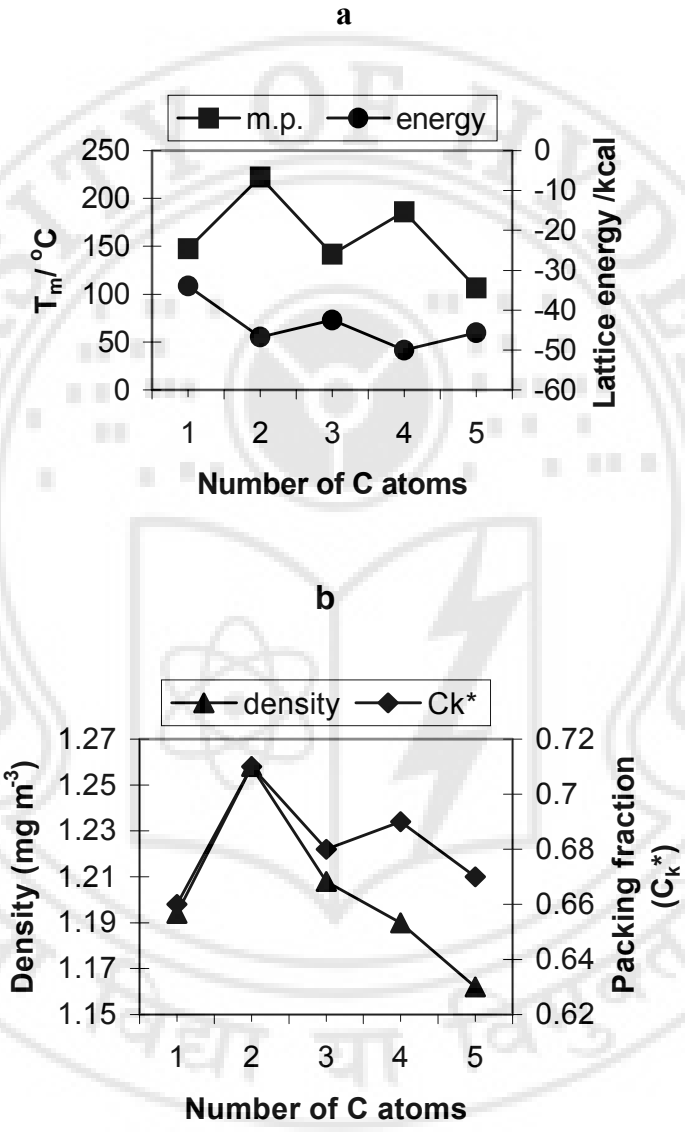

Figure 11. (a) Even–odd effect in aminols **1-5** of melting points and lattice energy. (b) alternation in density and packing fraction.

In our series the even–odd effect is apparent from the alternation of melting points and also from the marked alternation of the crystal structure types. Aminols **1** through **5** show an alternation in melting points, and compounds with *n* = even exhibit systematically higher melting points compared to those with *n* = odd. The alternating melting points are reflected in, and explained by, the alternation in the crystal structures.

The even structures take the β-As sheet structures, while the odd ones take infinite chain structures (or a square motif structure in **1**). This sort of structural variation where the types of interactions and indeed the entire packing arrangements alternate based on whether the member is even or odd is very dramatic. Lattice energy calculations [2.8] confirm that the β-As structures are more stable. The decrease of melting points with an increase in chain length show the importance of entropic factors (Figure 11). Correlation of melting point with crystal density (D_{calc}) and/or packing fraction (C_k^*) is reasonable because these parameters are a measure of how closely molecules can pack in the solid state (Table 2 and Figure 11).

2.9 Similarities and differences between aminols 3AP, **3** and **5**

Three examples of the infinite chain motif have now been observed: (i) 3AP, **3**; (ii) the partially cross–linked infinite chains of **5**, and; (iii) the fully cross-linked chains of the β-As sheet structures. The differences between these structures may be rationalised by analysing the geometries and relative positions of the N(H)O infinite chains. In the following discussion a 2D schematic (Figure 12) of the infinite chains of N(H)O hydrogen bridges is drawn from two different perspectives: from side on (the infinite chain projected on to the *ac* plane of the crystal lattice) and from above (projected on to the *bc* plane). When considered in projection from either direction, the infinite chain takes the form of a zigzag chain of N(H)O bridges. The zigzag of

the chain in 3AP and **3** contains twice the repeat unit of **5**, with peaks and troughs of the zigzag occurring only at the O-atom rather than peaks at O and troughs at N as in **5**. This affects the relative orientation of the N–H···π interactions. In 3AP and **3** they form on both sides of the chain whereas in **5** they form only on one side. In the *bc* plane the situation is different. In both 3AP and **3** the zigzag runs parallel with a peak coinciding with a peak of the chain below. In the β-As sheet one zigzag chain is offset with relation to the next allowing a close approach between the O- and N-atoms of adjacent layers and so to the formation of additional cross-linking hydrogen bridges.

Analysis of **5** is complicated by the presence of two molecules in the asymmetric unit. In the *bc* plane two different infinite chains, running in the *c* direction, can be distinguished. Each chain is formed with both **A** and **B** molecules. One of the infinite chains on average consists of weaker hydrogen bridges while the other has a saw-tooth geometry and can be almost be directly mapped onto a section of the β-As sheet.

The length of the *b* axis is directly related to the distance between adjacent chains. The closest approach between two adjacent chains occurs in the β-As sheet where the adjacent chains are cross-linked by additional hydrogen bridges creating a saturated system. The distance between two adjacent chains of the β-As sheet is approximately 5.2Å. In **3** the separation between chains is greater at 6.2Å while in **5** where there is some cross-linking between chains with the average separation being 5.6Å. With two molecule in the asymmetric unit the length of axis *b* is double the average separation ($2 \times 5.6 = 11.2$).

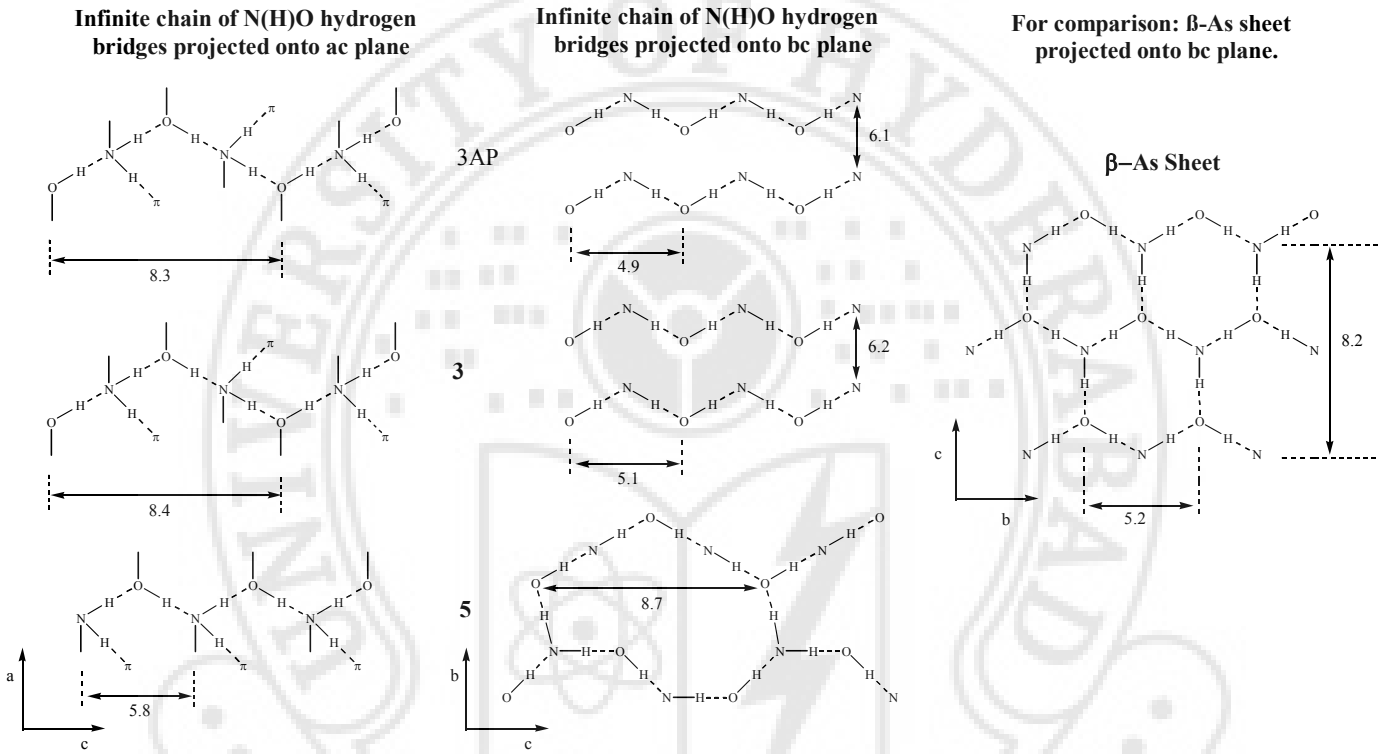

Figure 12. Schematic of the N(H)O infinite chains, showing the similarities and differences of chains in 3AP, **3** and **5**. The β-As sheet is shown for comparison.

2.10 Interaction interference and supramolecular synthons

Crystallization is a complex convolution of recognition events and complementary molecular recognition is a key phenomenon during this process. Therefore various intermolecular interactions interfere with one another during crystallization. In this context, the supramolecular synthon approach depicts the various ways in which complementary portions of molecules approach each other. Accordingly, supramolecular synthons consist of chemical and geometrical information necessary for molecular recognition. In the case of aminophenols this information corresponds to hydrogen bonding and herringbone interactions. The aminophenols are a very interesting series of compounds and unusual in both the extent of the structural repetition and the degree to which the structural changes within the series can be understood and explained. The structures observed can be described by just three major synthons: the square motif, the infinite chain, and the β-As sheet (Scheme 2). The best way to understand the relationship between these five structures is in terms of the infinite chain of N(H)O synthons. The β-As sheet {4APP (or **0**), **2** and **4**} can be considered as a very special case of the infinite chain wherein the chains run in two directions. In **3** only single or one-dimensional chains are found. In **5**, each symmetry independent molecule has one of the above characteristics. The underlying reason for taking the infinite chain as the basic structure motif can be seen from the unit cell dimensions: In all the cases where there is an infinite chain (**2** through **5**), the chain runs parallel to the *c* axis and the dimensions of the *c* axis are approximately equal (8.2-8.7 Å). In the β-As sheet structures, the *b* axis (in the plane of the β-As sheet) is also equal and the *a* axis reflects the overall length of the molecule.

In order to further determine the significance of these structures, *ab initio* structure predictions were attempted with the Polymorph Predictor (PP) module in the *Cerius*^{2} program [2.8, 2.9]. The prediction was carried out for compounds **0**

through **5**, in each of the observed space groups. In case of **1** and **4**, a structure was obtained that closely matched the experimental structure. This simulation demonstrates the potential application and limitations of available crystal structure modelling techniques as part of a strategy.

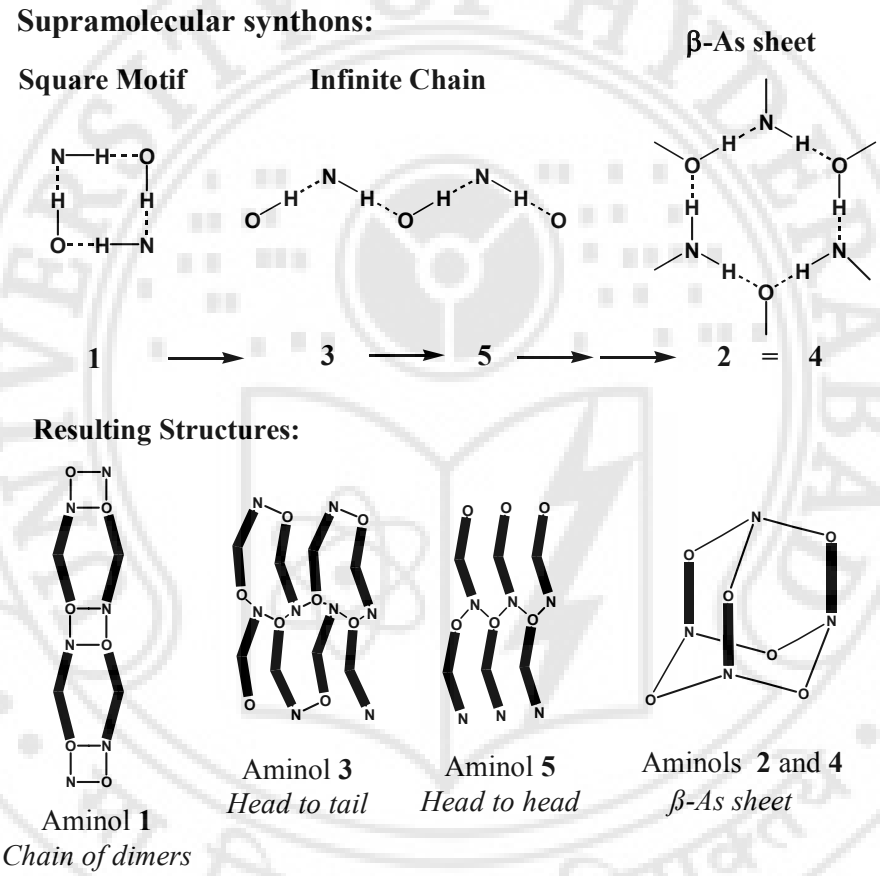

Scheme 2. Supramolecular synthons for the supraminols **1** through **5**. N—O represents the N(H)O hydrogen bridge *i.e.,* either an O–H···N or an N–H···O interaction. Thick lines represent the hydrocarbon fragment of the molecule.

From this series it would appear that the driving force for the formation of β-As structures, over the (single) infinite chains, is the molecular geometry. While

4AP, 4APP, **2** and **4** are approximately linear; 2AP, 3AP, **1**, **3** and **5** are much more bent. A measure of molecular linearity can be obtained from the angle between the C–O (phenolic) and the C–N (anilino) vectors (Table 2). This angle is nearly 180° for the β-As structures, and close to 120° for the other structures. The pyramidality factor shows that the N atoms are distinctly pyramidal in all the five supraminols [2.10] (Table 2 and experimental section).

2.11 Conclusions

Scheme 2 summarises the structural features in this family of compounds.

1) Neutron diffraction analysis of **1** has led to the unequivocal structural characterisation of N–H···π and C–H···π as to where exactly the hydrogen bridge accepting site is located.

2) Molecule-to-crystal extrapolation is possible in β-As sheet (*n*-even) structures **2** and **4** wherein the competing herringbone and hydrogen bonding interactions are effectively insultaed.

3) Supraminol **3** shows that 2AP and 3AP are not anomalous structures and that **5** is close to the more stable β-As sheet structure.

4) The infinite chain is the key synthon in this family. The way in which the fixed and the variable series relate to each other is also clearly understood:

1 → **3** → **5** →→ **0** = **2** = **4** = β-As sheet

Variable → Fixed

5) It is noteworthy that the synthons discussed here are all constructed from a combination of O–H···N and N–H···O hydrogen bridges and that nowhere in these structures do O–H···O or N–H···N interactions occur. In many cases the observed crystal structures result from a fine balance between several factors leading to both hierarchic packing and to structures wherein interaction interference is more pronounced.

From the present work, it would be interesting to extend the 4-amino-4'-hydroxybiphenyl-*n*-alkanes series to include the hexane and heptane derivatives (*n* = 6 and 7). The *n* = 6 compound would surely take the β-As structure, since it is the next compound in the fixed series. However, is the *n* = 7 compound flexible enough to obtain the β-As sheet structure, or will it form another bridging structure like compound **5**?

2.12 Experimental section

Synthetic procedures for the compounds in this study

General Methods. Melting points of compounds **1**–**5** were measured on a Perkin-Elmer model DSC-4. IR spectra were recorded on a Jasco-FT-IR model 5300 or a Perkin-Elmer model 1310 spectrometer. ^{1}H NMR (200 MHz) was recorded in DMSO-d_6 on a Bruker-AC-200 spectrometer. All reactions were carried out using standard techniques and general literature procedures. Work up means drying of the combined organic extracts with $MgSO_4$, filtration, and concentration of the crude residue in vacuo. All compounds were purified by column chromatography using silica gel (100-200 mesh) with EtOAc–hexane. Yields reported here are for column separated products. All reagents and solvents were dried and distilled prior to use. Details of the synthetic procedures for compounds **1** through **5**.

4-(4-Aminobenzyl)phenol, 1

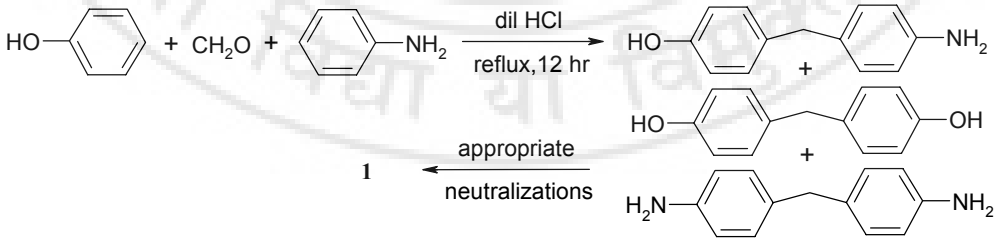

Aminol **1** [2.11a] was prepared in 20% yield according to the published procedure, mp 147 °C. IR (cm^{-1}): 3381, 3310, 3015. ^1H NMR : δ 3.61 (s, 2H), 4.81 (s, 2H), 6.46 (d, J 8, 2H), 6.66 (d, J 8, 2H), 6.80 (d, J 8, 2H), 6.96 (d, J 8, 2H) and 9.12 (s, 1H).

4-(4-Aminophenethyl)phenol, 2

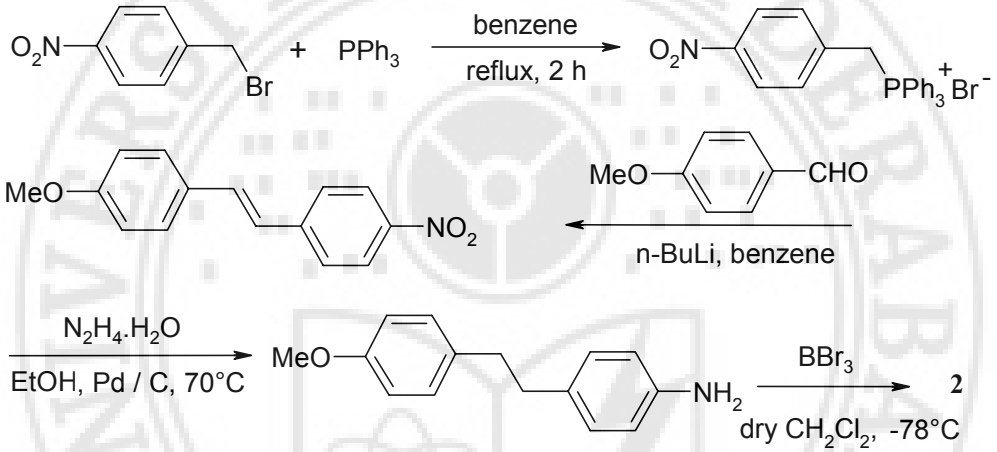

trans-4-Nitro-4'-methoxystilbene was prepared according to the Wittig reaction [2.11b]. To this compound (510 mg, 2 mmol) 15 mL of EtOH and $N_2H_4.H_2O$ (0.38 mL, 8 mmol) were added and stirred. Pd/C was slowly added and the reaction mixture refluxed at 70 °C for 3 h. The reaction mixture was filtered off to remove Pd/C, then the filtrate evaporated to yield 320 mg (71%) of 4-amino-4'-methoxydiphenylethane [2.11c]. To a degassed solution of this compound (227 mg, 1 mmol) in dry CH_2Cl_2 (15 mL), a solution of BBr_3 in CH_2Cl_2 was added dropwise and the mixture was stirred under N_2 at –78 °C for 3 h and stirring was continued overnight. The mixture was diluted with CH_2Cl_2 (10 mL), and washed with H_2O. Workup afforded 100 mg (42%) of **2** [2.11d] with mp 222 °C. IR (cm^{-1}): 3370,

3310, ^{1}H NMR: δ 2.70 (s, 4H), 4.8 (s, 2H), 6.57 (d, J 8, 2H), 6.67 (d, J 8, 2H), 6.90 (d, J 8, 2H), 7.00 (d, J 8, 2H), 9.15 (s, 1H).

4-[3-(4-Aminophenyl)propyl]phenol, 3

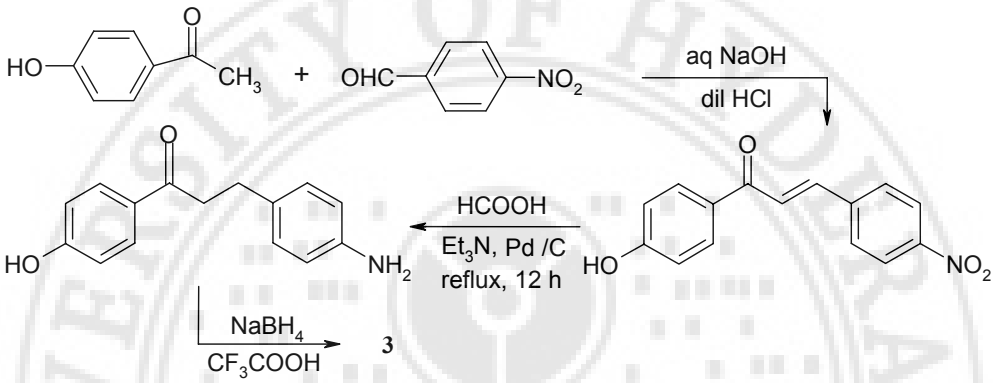

4'-Hydroxy-4-nitrochalcone was prepared in 78% yield by the Claisen-Schmidt condensation [2.11e] of 4-hydroxyacetophenone (1.49 g, 11 mmol) and 4-nitrobenzaldehyde (1.51 g, 10 mmol) in aqueous NaOH (1.14 g, 28 mmol) by stirring at room temperature. This chalcone (1.85 g, 7 mmol) was reduced to furnish 1.25 g (67%) of 4'-hydroxy-4-hydroxylamino-1,3-diphenyl propane-1-one by refluxing overnight with Et_3N (15 mL), HCO_2H (1.7 mL, 45 mmol) and Pd/C (144 mg, 0.14 mmol) [2.11f]. This product (1.2 g, 4.7 mmol) was further reduced using CF_3COOH (25 mL) and $NaBH_4$ (1.02 g, 27.5 mmol) at 0-5 °C for 30 min under N_2 and then for an additional 30 h at room temperature [2.11g], to yield 180 mg (17%) of compound **3** with mp 142 °C, IR (cm^{-1}): 3372, 3308, ^{1}H NMR: δ 1.75 (m, 2H), 2.43 (m, 4H), 4.84 (s, 2H), 6.05 (d, J 8, 2H), 6.70 (d, J 8, 2H), 6.85 (d, J 8, 2H), 7.00 (d, J 8, 2H), 9.10 (s, 1H).

4-[4-(4-Aminophenyl)butyl]phenol, 4

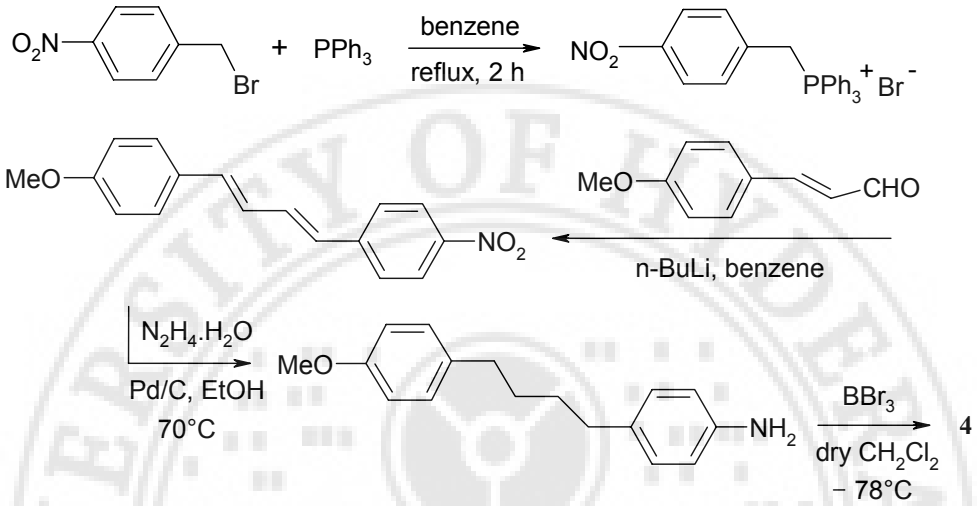

Wittig reaction [2.11b] between *p*-nitrobenzyltriphenylphosphonium bromide and 4-methoxycinnamaldehyde gave 1-(4-methoxyphenyl)-4-(4'-nitrophenyl)-1,3-butadiene in 51% yield. As described in **2**, this compound was reduced to give 1-(4-methoxyphenyl)-4-(4'-aminophenyl)butane in 70% yield. Methoxy deprotection afforded **4** in 40% yield, mp 185 °C. IR (cm^{-1}): 3366, 3290.^{1}H NMR: δ 1.4 (s, 4H), 2.4 (m, 4H), 4.8 (s, 2H), 6.42 (d, J 8, 2H), 6.64 (d, J 8, 2H), 6.82 (d, J 8, 2H), 6.92 (d, J 8, 2H), 9.07 (s, 1H).

4-[5-(4-Aminophenyl)pentyl]phenol, 5

4-Hydroxybenzylideneacetone was prepared in 62% yield by the condensation of 4-hydroxybenzaldehyde and acetone [2.11h]. Pure 4-hydroxybenzylideneacetone was further condensed with 4-nitrobenzaldehyde to give (81%) 4-hydroxy-4'-nitrodibenzylideneacetone. This compound (885 mg, 3 mmol) was subjected to hydrogenation with PtO_2 (56.25 mg, 3 mmol)/H_2 in MeOH/THF (1:1) solution for 15 h [2.11i] to give 150 mg (18%) of 1-(4-

hydroxyphenyl)-5(4'-aminophenyl)pentane-3-one. This was further reduced with Zn–Hg, HCl (g), conc. HCl as described [2.11j] (Na_2CO_3 was used for the neutralisation) to get 62% of 5, mp 106 °C. IR (cm^{-1}): 3375, 3304, 2924,1616, ^1H NMR: δ 1.22 (m, 2H), 1.47 (m, 4H), 2.4 (m, 4H), 4.75 (m, 4H), 6.45 (d, J 8, 2H), 6.65 (d, J 8, 2H), 6.80 (d, J 8, 2H), 6.92 (d, J 8, 2H), 9.1 (s, 1H).

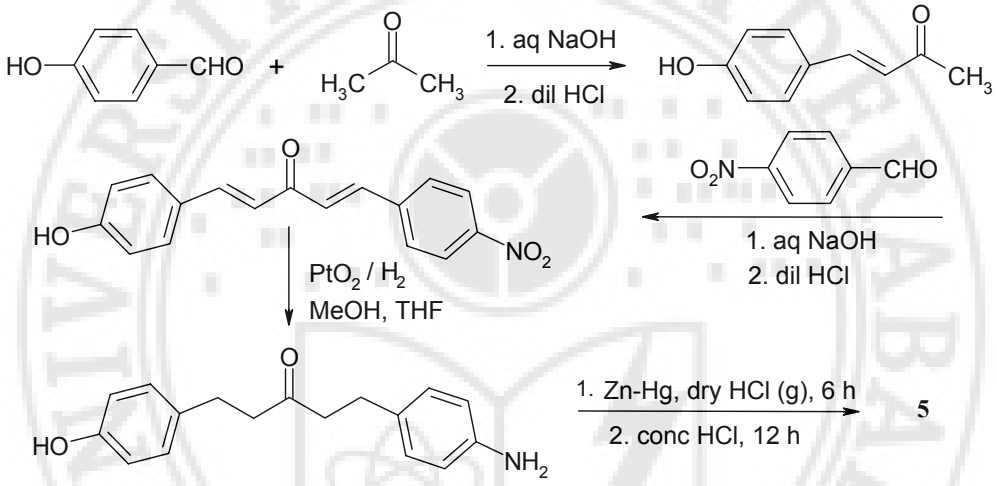

Crystallization

Diffraction quality single crystals were obtained by recrystallizing the aminol **1** from 1:1 CH_3OH/benzene. Crystals of **2**, **3** and **4** were obtained from 1:1 EtOH/benzene and **5** was recrystallized from 1:1 CH_3CN/EtOH.

X-ray crystallography

The X-ray data were collected at the University of Durham, U.K. by Dr. C.K. Broder and Mr. R. Mondal under the supervision of Prof. J.A.K. Howard. All the X-ray experiments were carried out on a Bruker SMART CCD 1K area detector, using Mo K_α radiation (λ = 0.71073 Å). The structure solutions and refinements were achieved using the SHELXS-97 and SHELXL-97 programs built-

in with the Siemens SHELXTL-98 (Version 5.1) package [2.12]. In all cases the hydroxy and amine hydrogen atoms were located in difference Fourier maps and refined isotropically. The other hydrogen atoms were either fixed in geometrically sensible positions (compounds **1**, **2** and **3**), or located in difference Fourier maps and refined isotropically (**4** and **5**). All interatomic distance and related calculations were carried out with PLATON 2002 [2.13] on Silicon Graphics Octane2 workstation (Table 2). Further crystallographic details are summarised in appendix.

Neutron crystallography

Prism-like crystals of 4-(4-aminobenzyl)phenol **1** for neutron diffraction analysis were grown in Hyderabad. Colourless prism shaped crystals were obtained after one week upon slow evaporation of EtOH. The neutron diffraction study was performed by Drs. C.K. Broder and C.C. Wilson at the ISIS, Rutherford laboratories, Oxford, under the supervision of Prof. J.A.K. Howard. The neutron structure determination of **1** was conducted at the ISIS pulsed neutron source on the Laue time–of–flight diffractometer, SXD [2.14]. Since the crystals (1.5x1.5x1.3 mm) were smaller than is usually required for a neutron single crystal experiment, the new technique of a multi–crystal experiment [2.14c] was used. An array of four small crystals was mounted in the SXD ω–CCR and data collected at 12K in a series of 10 frames with 25°ω steps. Intensities from all four crystals were extracted, resulting in 2403 unique, merged reflections. The structure solution and refinements were carried out using SHELXTL (Version 5.1) programs [2.12]. The pertinent crystallographic information is given in the appendix.

Analysis of herringbone interactions

The angle between two adjacent aromatic ring planes have been calculated using RPluto [2.10] (phenol-phenol rings and aniline-aniline rings (2 values) or

phenol-aniline rings (one value) depending on the relative orientation of the adjacent molecules head to head or head to tail. Throughout this thesis work the herringbone interaction has been described in terms of the angle between adjacent aromatic rings. This is not the only factor influencing the nature of this interaction, and the separation and the degree to which the rings are offset is also important; however the relative ring plane angle gives a single value by which the interactions may be conveniently compared.

Lattice energy calculations

The lattice energy calculations were carried out for all the supraminols studied in this thesis on Indigo Solid Impact and Octane workstations from Silicon Graphics using the Dreiding 2.21 force field in the *Cerius*^{2} suit of programs (Version 4.2) [2.8]. The experimental crystal structure is given as input and the charges were determined by charge-equilibration method. The van der Waals, electrostatic and hydrogen bridge energies per molecule were measured (Table 2).

Polymorph prediction

Polymorph predictions on aminols **1** through **5** were carried out using the Polymorph Predictor (PP) module in the *Cerius*^{2} program [2.8, 2.9]. Initial molecular minimisation was carried out with the AM1 Hamiltonian in Mopac 6.0. ESP charges, geometry optimization were assigned using Mopac 6.0. Dreiding 2.21 force field was used for all PP calculations. The Ewald long-range summation method was used for electrostatic interactions. The number of molecules in the asymmetric unit was specified. The package works by using a Monte Carlo simulated annealing approach to generate possible crystal packing alternatives for a given molecule. Each unique crystal structure found by this method is subjected to a lattice energy minimization with respect to all inter- and intramolecular degrees

of freedom to obtain the relative stability ranking of the various packing possibilities. Large numbers of structures were produced for each space group. The resulting 10 lowest-energy and highest density structures were considered for further analysis.

CHAPTER THREE

SHAPE AND SIZE EFFECTS IN THE CRYSTAL STRUCTURES OF SOME CH_2/S EXCHANGED SUPRAMINOLS

3.1 Introduction

A ubiquitous exercise in crystal engineering is to investigate the changes in crystal packing that are obtained when molecular structural features are altered. In general, if the molecular structure is varied gradually, the changes in the crystal structure are smooth and predictable. The more the abundance of a synthon within a family of compounds, the more reliable and useful it is in developing molecular to crystal relationships. One can use the CSD [1.19] as a retrosynthetic tool for the analysis of common synthons and intramolecular geometry of large number of compounds. The results of this examination leads to the reasonable identification of the starting materials and conditions that will produce the target structure.

Chapter 2 shows good trends that can be clearly explained in terms of odd and even structures. The method of exchanging one functionality with another of similar shape and size is a technique that has greatly furthered the field of crystal engineering. Whether the new structure is geometrically isostructural [3.1] with the original, or not, can reveal a great deal about the ability and role of the exchanged group in determining the crystal structure. To confirm the trends observed in Chapter 2 structural analyses of more related compounds are desirable. This is especially true at the lower end of the *n* = odd compounds where the square motif of **1** becomes the infinite chain synthon in **3**. With this aim a selection of S-substituted supraminols of the general type 4-amino-4'-hydroxybiphenyl-*n*-alkanes and both OH and NH_2 in a *para* position was synthesised and analyzed. Such replacement gives aminophenols **1a** (4-amino-4'-hydroxydiphenylsulfide), **2a** (4-amino-4'-hydroxydiphenylmethyl-sulfide), **2b** (4-amino-4'-hydroxydiphenylsulfide methane), **2c** (4-amino-4'-hydroxy-

diphenyldisulfide) and **3a** (4-amino-4'-hydroxydiphenylethylsulfide). It is noteworthy that all these compounds required a different synthetic route for the preparation to that used to obtain the parent compound. Details of the synthetic procedures are given in the experimental section.

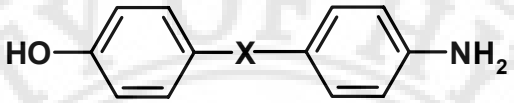

X =		
	S	**1a**
	S-CH_2	**2a**
	CH_2-S	**2b**
	S-S	**2c**
	S-$(CH_2)_2$	**3a**

Scheme 1

All the five aminols can be explained in terms of three supramolecular synthons based on complementary molecular recognition between OH and NH_2 groups. They are respectively the tetramer loop or square motif, the infinite N(H)O chain and the β-As sheet. These aminols can be classified into isostructural S-spacer supraminols and non-isostructural S-spacer supraminols. If the substitution of a methylene group by an isosteric S-atom causes no change in the crystal structure then this can be termed as isostructural S-spacer supraminols (**2a**, **2b** and **3a**). In non-isostructural S-spacer supraminols (**1a**, **2c**) CH_2/S exchange is not possible. These observations are rationalised in terms of geometrical and chemical effects of the molecular functionalities. These structures are compared with supraminols **1**, **2**, **3** and **5** discussed in Chapter 2.

3.2 Isosteric group replacement and isostructurality

Kitaigorodskii [1.15] proposed that under appropriate circumstances interchanging a single functional group with another of comparable volume in a molecule such as the S–atom and the $–CH_2–$ group, benzene–thiophene exchange [3.2], or chloro–methyl exchange [3.3] are isosteric and that substitution of one for another need not alter the crystal structure. A CSD search was carried out for Ar–S–Ar / Ar–CH_2–Ar sets of compounds [1.19]. A total of 21 pairs were found of which 8 are similar. The S-atom is approximately the same size as the CH_2 group (22.8 $Å^3$ and 19.1$Å^3$ respectively) and the idealized C–S–C angle is 100° compared to a C–C–C angle of 109°. However the geometry of Ar–S–S–Ar (torsion angle ~ 90°) is very different to that of Ar–C–C–Ar or Ar–S–C–Ar (torsion angle ~ 0°). Disulfide compounds are comparatively rare with only a total of 51 CSD occurrences. The relevant CSD details are given in the experimental section.

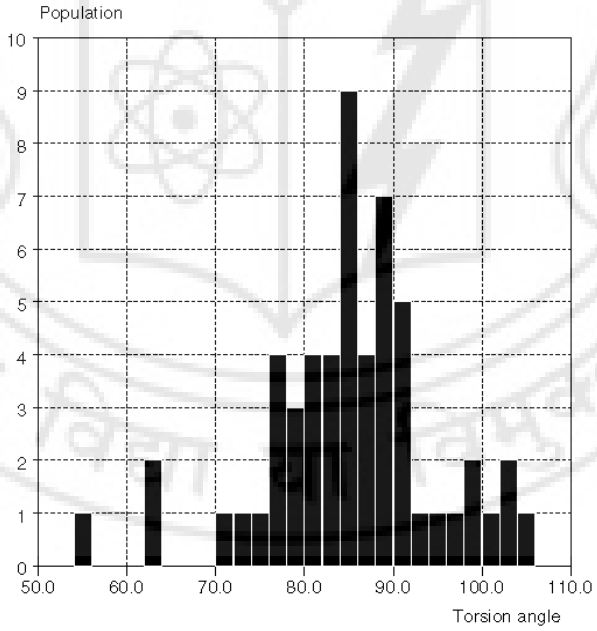

Figure 1. **C-S-S-C torsion angle**.

Kitaigorodskii was the first to summarise isostructurality behaviour in *organic* compounds [1.15]. Kálmán *et al*. have reported pairs of isostructural cardenolides and bufadienolides and termed the 'main-part' isostructuralism in related molecules [3.4]. Nevertheless, there are pairs termed homostructural that do display some sort of packing similarity even if replacement takes place that involves more than one group on the molecule [1.15]. A homostructural crystal pair was described by Desiraju *et al*. in the molecular complexes of *sym*-trinitrobenzene with some trigonal donors where two substituents (Me, phenyl→Cl, thienyl) can be interchanged without changing the crystal packing. There are only a few substituent pairs whose members can replace each other without altering the existing packing of the crystals. This is one reason why shape/size isostructurality is generally rare. Apart from the Cl→Br→I series [3.5], CH_3 can almost equally be replaced with H, Cl and occasionally with an ethyl moiety and the –OH group can be replaced with =O and H in some cases [3.6].

Kálmán has suggested two parameters, which estimate the extent of isostructurality or likeness between two similar structures. These are the unit cell similarity index (Π) and the isostructurality idex ($I_i(n)$). In the equation for the unit cell similarity index (Π), a, b, c, and a', b', c' are the orthogonalised lattice parameters of the related crystals. Ideally, for a pair of completely isostructural crystals, Π should be zero.

$$\Pi = \left| \frac{a+b+c}{a'+b'+c'} \right| - 1 \cong 0$$

The isostructurality index, ($I_i(n)$) is a measure of the degree of internal isostructuralism where n is the number of distance differences (ΔR_i) between the absolute coordinates of identical non-hydrogen atoms within the same section of

asymmetric units of related (A and B) structures. Ideally, $I_i(n)$ should be close to 100% for isostructural crystals.

$$I_i(n) = \left[1 - \left(\frac{\sum \triangle R_i^2}{n} \right)^{1/2} \right]$$

3.3 Isostructural S-spacer supraminols

3.3.1 4-(4-Aminobenzylsulfamyl)phenol, 2a and 4-(4-aminophenylsulfamyl-methyl)phenol, 2b

The substitution of one CH_2 group for a sulfur atom in aminol **2** to give compound **2a** has very little effect on the crystal structure (Figure 2). The same β-As sheet structure is found with an identical herringbone interaction between adjacent molecules of 68° and 71° for the phenol ring pair and the aniline ring pair respectively, compared to 67° and 70° in **2** (Figure 3) [1.28]. In **2a** additional stability is conferred by a C–H···S interaction between adjacent molecules. This C–H···S hydrogen bridge can form without requiring any structural change. Aminol **2b** is isostructural with **2a** (Figure 4). A comparison of the unit cell dimensions (Table 1) gives an isostructurality parameter [3.7] (Π) of 0.00031 (where zero indicates an exact match). For comparison the value of Π for **2** in relation to **2b** is 0.0047. There is a notable change between the structures of compounds **2a** and **2b**. In compound **2a** a C–H···S interaction [1.21] has been found whereas in **2b** the equivalent interaction is much longer (Figure 4).

Table 1. Lattice parameters of **2a**, **2b** and **2** in the space group *Pc*.

compound	*a* /Å	*b* /Å	*c* /Å	*α* /°	*β* /°	*γ* /°
2	13.682(3)	5.2619(11)	8.1916(2)	90	107.28(3)	90
2a	13.844(3)	5.1626(10)	8.2485(16)	90	107.22(3)	90
2b	13.7422(12)	5.1725(4)	8.3055(7)	90	105.548(4)	90

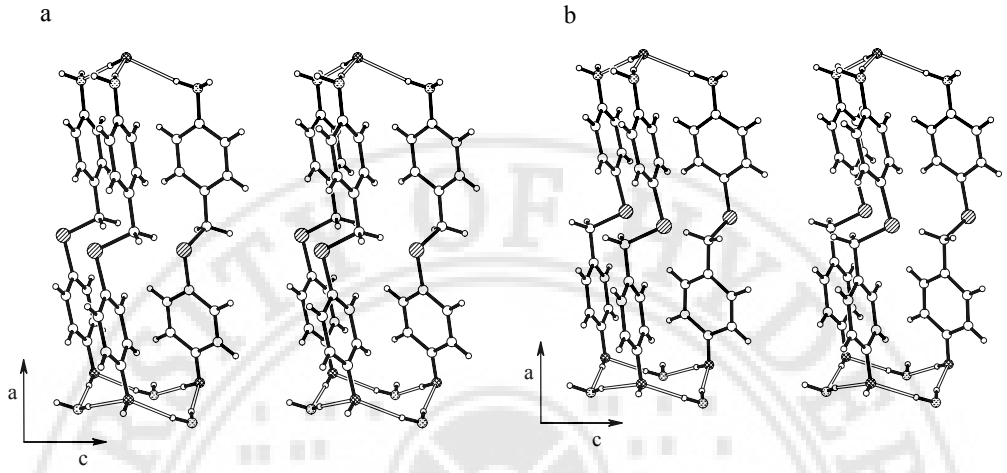

Figure 2. (a) Stereoview of the β-As sheet in 4-(4-aminobenzyl sulfamyl)phenol **2a** and (b) in 4-(4-aminophenylsulfamylmethyl)phenol **2b**.

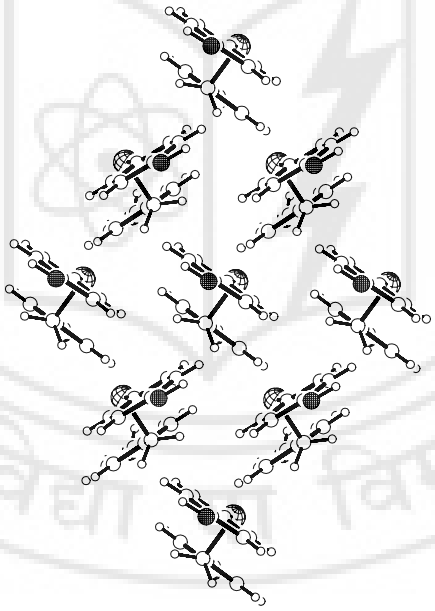

Figure 3. Herringbone interactions in **2a**. Notice that in **2b** the arrangement of aromatic rings is similar to that of **2a** and **2**.

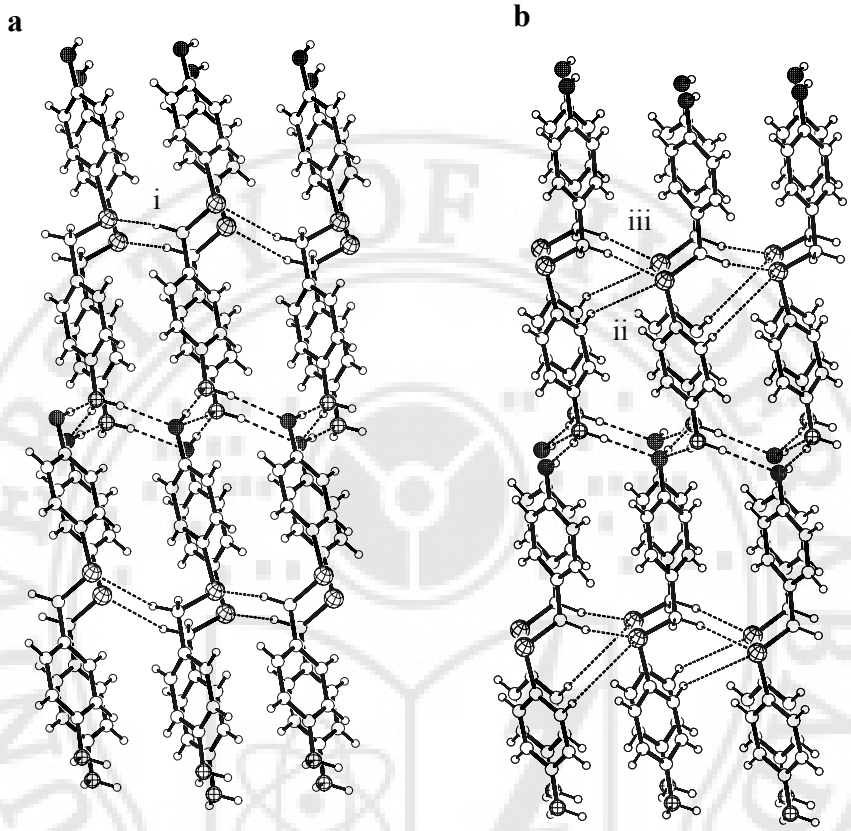

Figure 4. (a) Crystal packing in **2a**. C–H···S (i) (2.86Å, 152.3°) interaction, (b) in **2b**. C–H···S (ii) (2.97Å, 132.8°), (iii) (3.03Å, 146.5°).

3.3.2 4-[2-(4-Aminophenylsulfamyl)ethyl]phenol, 3a

Aminol **3a** has a very similar geometry and also a similar crystal packing to that of aminols **3** and **5**. Again the dominant hydrogen bonding motif is the infinite chain. The arrangement of the molecules is similar in each structure but not identical. In **3** the molecules align head to tail (as discussed in structural description of **2c**). This allows the chains to be linked into sheets with the molecule acting as a cross-links between adjacent chains. In **3a** and **5** the molecules align head to head preventing the

formation of sheets (Figure 5). There is a good herringbone interaction between adjacent phenol rings (74°) that is promoted by a phenolic C–H···S hydrogen bridge (Table 2). However, the formation of herringbone interactions at the phenol end of the molecule prevents the aniline end obtaining the correct geometry for a good N–H···π interaction [1.21]. As in **1** there is a C–H···π interaction to the other face of the same aniline ring.

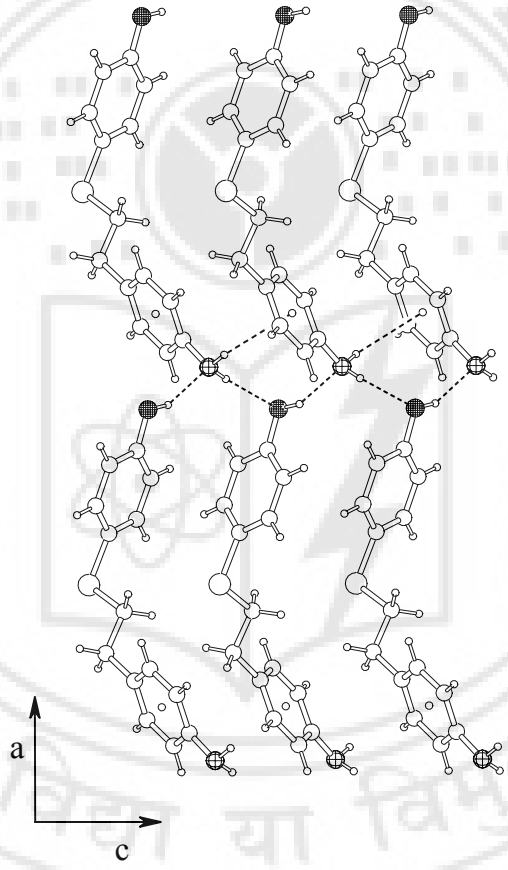

Figure 5. Infinite chain in 4-[2-(4-aminophenylsulfamyl)ethyl]phenol **3a**. Note the head to head arrangement of the molecules within a row. This differs from the head-to-tail arrangement in aminol **3** (Figure 7, Chapter 2).

3.3.3 Structural comparison between aminols 3a, 3, 5 and the β-As sheet

The infinite chain of aminol **3a** is projected on to both the *ac* and *bc* planes of the crystal lattice. The infinite chain in **3a** takes the form of a zigzag chain of N(H)O hydrogen bridges in both the projected planes (Figure 6). This zigzag of the chain in **3a**, similar to aminol **5**, has half the repeat unit of aminol **3** with peaks of the zigzag occurring at the O- and troughs at N-atom rather than peaks and troughs occurring only at the O- as in **3**. Therefore the relative orientation of N–H···π in **3a** and **5** is only on one side whereas in **3** they form on both sides of the chain.

In the *bc* plane the repeat unit of the **3a** zigzag is twice that of **3**. This zigzag chain is analogous to one of the infinite chains of **5** (on average consisting of weaker hydrogen bridges). In both **3a** and **3** the zigzag runs parallel with a peak coinciding with a peak of the chain below. However, in the β-As sheet one zigzag chain is offset with the next allowing a close approach between the O- and N-atoms of adjacent layers and thus to the formation of additional cross-linking that leads exclusively to the saturated N(H)O hydrogen bridges.

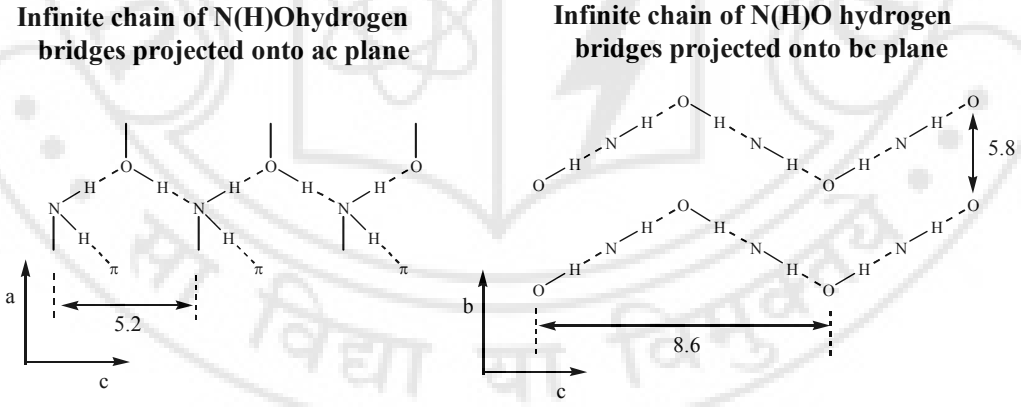

Figure 6. Schematic of the N(H)O infinite chain in **3a**.

Table 2. Structural parameters for the supraminols in this study.

compound	1a	2a	2b	2c	3a
structure	square motif	β-As	β-As	infinite chain	infinite chain
mp [°C]	147–148	211–212	205–207	113–115	116–118
C–O, C–N angle [°][a]	106.93 (A) 100.16 (B)	171.9	174.7	91.184	115.6
herringbone angle [°][b]	75 (A) 71(B)	68 and 71	69 and 72	86	74 and 49
C_k* [%][c]	0.70	0.713	0.706	0.69	0.685
pyramidal factor[d]	0.262 (A) 0.315 (B)	0.328	0.300	0.290	0.318
latt. energies [kcal mol^{-1}][e]:					
van der Waals	–21.2104	–22.8127	–24.1992	–23.6826	–24.0041
electrostatic	–13.4020	–18.4422	–18.9782	–14.8522	–12.7148
hydrogen bridge	–5.4285	–8.4105	–8.8847	–7.4514	–5.9412
total energy	–40.0409	–49.6654	–52.0621	–45.9862	–42.6601

a) The angle between the C–O and C–N vectors have been calculated using *RPluto*. b) The angle between two adjacent aromatic ring planes calculated using *RPluto*. c) C_k*, percentage of filled space calculated with *PLATON*. d) The perpendicular distance from the basal plane to the apex of the pyramid. e) Lattice energies calculated using *Cerius*^{2} from Accelrys.

Table 3. Geometrical parameters for various interactions for the aminols in the study.

Aminol	H-bridge	*d* (Å)[a]	*D* (Å)	θ (deg)
1a	O–H···N	1.77	2.745(2)	171.5
	O–H···N	1.91	2.871(2)	164.6
	N–H···O	2.06	3.001(2)	153.7
	N–H···O	2.31	3.261(2)	156.9
	N–H···S	2.91	3.875(2)	158.9
	N–H···S	3.15	4.016(2)	150.2
	C–H···S	2.78	3.833(2)	163.7
	C–H···S	2.83	3.646(2)	131.9
	C–H···S	2.90	3.7428(19)	134.4
	C–H···S	2.96	3.9422(19)	150.6
	C–H···π	2.56	3.329	126.5
	C–H···O	2.77	3.634(2)	136.4

2a	O–H···N	1.80	2.786(4)	178.1
	N–H···O	2.15	3.148(5)	172.1
	N–H···O	2.30	3.299(4)	169.6
	C–H···S	2.86	3.849(4)	152.3
	C–H···S	3.02	3.774(4)	127.2
2b	O–H···N	1.84	2.822(4)	173.3
	N–H···O	2.11	3.119(4)	177.1
	N–H···O	2.28	3.268(4)	166.9
	C–H···S	2.97	3.787(3)	132.8
	C–H···S	3.03	3.984(3)	146.5
	C–H···S	3.06	4.045(3)	151.8
2c	O–H···N	1.78	2.7623(19)	176.6
	N–H···O	2.04	3.031(2)	166.7
	N–H···π	2.58	3.530	156.4
	C–H···O	2.64	3.449(2)	130.4
	C–H···S	2.88	3.6853(17)	131.3
	C–H···S	2.93	3.1300	169.4
	C–H···π	2.56	3.629	167.5
3a	O–H···N	1.86	2.754(2)	149.7
	N–H···O	2.11	3.114(2)	174.1
	N–H···π	2.51	3.382	143.7
	C–H···O	2.51	3.199(2)	120.7
	C–H···O	2.51	3.192(2)	120.3
	C–H···S	2.91	3.9167(17)	154.9
	C–H···S	2.92	3.8520(18)	144.1
	C–H···π	2.67	3.426	126.5

[a] O–H, N–H and C–H distances are neutron normalized to 0.983, 1.009 and 1.083 Å.

3.4 Non-isostructural S-spacer supraminols

3.4.1 4-(4-Aminophenylsulfamyl)phenol, 1a

Aminol **1a** crystallizes in the space group $P2_1/n$ (Z=4). There are two independent molecules in the asymmetric unit of compound **1a** (molecule **A** = $N_{(1)}O_{(1)}S_{(1)}C_{(1\text{-}12)}$ and **B** = $N_{(2)}O_{(2)}S_{(2)}C_{(21\text{-}22)}$) but the geometry of both molecules and the way in which they interact within the crystal are similar. The crystal structure consists of alternate sheets of molecules of **A** and molecules **B**. Both sheets are built

up of square motifs of N(H)O hydrogen bridges (Figure 7). The difference between this structure and that of **1** is that the four molecules spiral out from the square motif in a windmill type arrangement to form chains (Figure 8). The driving force for this difference appears to be the exchange of an N–H···π bridge by an N–H···S bridge [1.21]. The sheets consisting of molecules of **A** and those consisting of molecules of type **B** are similar in appearance but on average the interactions of **A** are stronger than **B** especially when considering the N–H···S interactions. Molecules **B**, however, have an additional C–H···S interactions that counterbalance the weakeness of the N–H···S bridge. Sheets of molecules **A** and **B** stack alternately with herringbone interactions between the layers (ring plane angle 75°). There are C–H···O and C–H···π interactions which hold the sheets together.

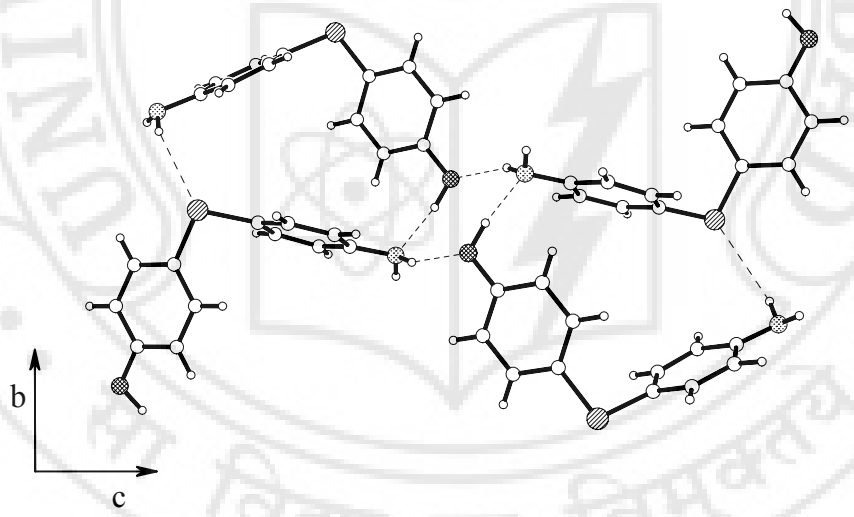

Figure 7. Square motif in 4-(4-aminophenylsulfamyl)phenol (**1a**). Note the windmill type arrangement.

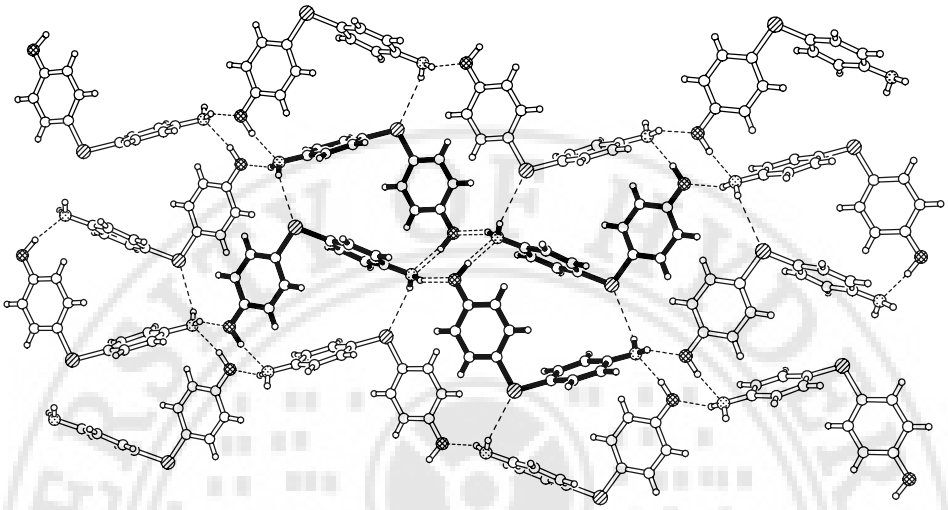

Figure 8. A sheet consisting of molecule type **A** is shown. **B** molecules form similar sheets, and sheets of type **A** and type **B** molecules stack, alternately. Tetrameric loop synthon with the windmill ensemble is highlighted.

3.4.2 4-(4-Aminophenyldisulfamyl)phenol, 2c

Aminol **2c** adopts a very different crystal packing to that of **2**, **2a**, and **2b**. If substitution involves more than one group on the surface of isometric molecules the identity in crystal packing generally disappears. This could be expected given the pronounced change in molecular geometry caused by the smaller torsion angle about C–S–S–C bond (Figures 1 and 9) which is 83.3(1)° in **2c** compared with a C–C–C–C or C–S–C–C torsion angle of approximately 0°in **2**, **2a**, and **2b**. So **2c** is U–shaped while **2**, **2a**, and **2b** are linear. In the square motif structure of **1** it has been seen that the molecules arrange in pairs to form dimers which then stack end-to-end about the square motif to form chains. The same type of dimer is found in compound **2c** but instead of aligning end-to-end the dimers align side by side in offset rows. This arrangement allows the N(H)O hydrogen bridges to form infinite chains, rather than square motifs (Figure 10). However, the bulk arrangement of the molecules in the

crystal is reminiscent of the packing of **1** (Figure 10 compare with Figure 6 in Chapter 2). In this way compound **2c** contains elements of both the square motif structure of **1** and the infinite chain structure of **3**. It can be considered as a bridge between the two structures in which some of the structural elements of compound **1** have been broken down and reformed into those found in **3** but the structure is not completely identical to either structure. There is an N–H···π interaction, however, unlike in **1** and **3**, and this interaction does not take the idealized geometry with the closest approach of the hydrogen to the ring being to the ring centroid. Instead, the hydrogen atom interacts with an individual C=C bond of the ring (a type V interaction as defined by Malone [1.31e]), this indicates that the N–H···π bridge is losing out (in terms of geometry) in the formation of this intermediate structure. The herringbone interaction is still observed with an angle between the phenyl—aniline ring plane of 75°.

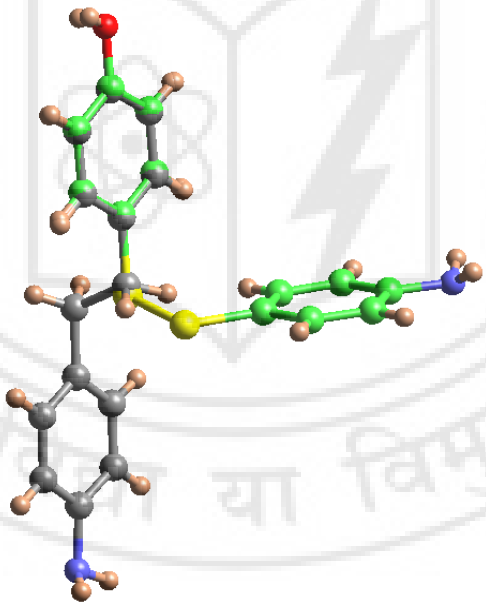

Figure 9. Overlay diagram of compound **2c** on **2**. The phenolic rings are superimposed. Notice that the molecular geometry of **2c** is bent.

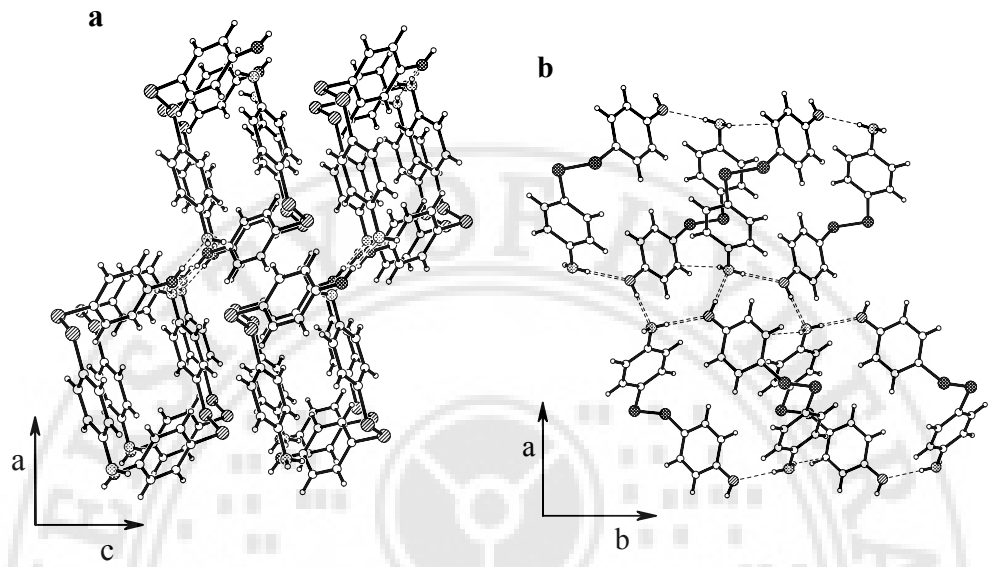

Figure 10. Crystal structure of 4-(4-aminophenyldisulfamyl)phenol **2c** (a) *ac* plane. (b) *ab* plane showing helical infinite chain of hydrogen bridges.

3.5 General discussion of aminophenols in the study

Two significant points emerge from the study of these sulfur substituted compounds. First, the relationship between the square motif structure of **1** and the infinite chain structure of **3** can be understood by the study of aminol **2c**. All the compounds studied in this section can be included in either the variable or fixed series already identified (see also Chapter 2). **2c** is considered as a bridging structure between **1** and **3**, and as such lies between them in the series. In the same way, **3a** lies between **3** and **5**.

1 → **2c** → **3** → **3a** → **5** → → β-As : Variable series

0 = **2** = **2a** = **2b** = **4** = β-As : Fixed series

Secondly, the way the infinite chains pack in the *bc* plane clearly illustrates the differences between the infinite chain structures and the β-As sheet structures, while at the same time demonstrating the direct relationship between the structural

synthons formed, and the unit cell dimensions. The separation of the sheets can be understood to be directly related to the width of the molecule in the direction of the *b* axis and this in turn depends on the geometry of the molecule. All the β-As sheet structure discussed so far have a 'linear' geometry characterized by a C–O vector to C–N vector angle of approximately 180° whereas all the non–β-As sheet structures have exhibited a more bent geometry (Table 2). Lattice energy calculations confirm that β-As sheet structures are more stable [2.8]. NIPMAT plots and simulated powder spectra for **2**, **2a** and **2b** show the near identity of crystal packing [3.8].

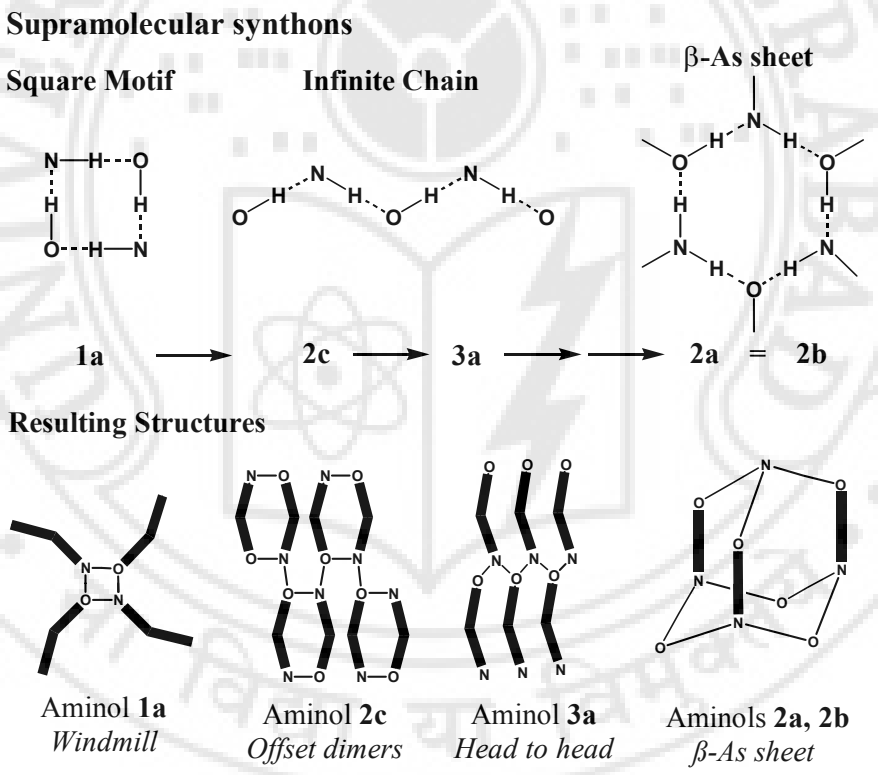

Scheme 2. β-As sheet, infinite chain, and square motif synthons. N—O represents the N(H)O hydrogen bridge i.e. either an O–H···N or an N–H···O interaction. Thick lines represent the hydrocarbon fragment of the molecule.

Overall, good isostructurality is observed between **2** and its S-analogues, while **3a** is similar to **5**. There is an interplay of geometrical and chemical effects. In **1** and **1a**, where isostructurality is not observed, it is chemical effects that cause the change in structure with the N–H···π interaction being replaced by an N–H···S interaction. Similarly the differences between **2** and **2c** can be attributed to the change in torsion angle resulting from the exchange of a CH_2–CH_2 for a S–S group. In the other isostructural cases the geometrical factors are either consistent with or outweigh the chemical effects.

3.6 Conclusions

Scheme 2 outlines the structural features and robust synthons in this family of compounds. The structures of these supraminols further confirm that the infinite chain is the key synthon in the family. The way in which the fixed and the variable series relate to each other is also clearly understood:

1a ← 1 → 2c → 3 → 3a → 5→ → 0 = 2 = 2a = 2b = 4 = β-As

Variable → Fixed

It is significant to note that the synthons discussed here are all constructed from a N(H)O synthons and that nowhere in these structures do O–H···O or N–H···N hydrogen bridges occur.

2a and **2b** are isostructural, **2c** contains elements of both the square motif (**1)** and the infinite chain (**3)** and as such is considered as bridging these two structural patterns while **3a** is similar to **5**.

In all the supraminols discussed in this chapter the N-atoms of the aniline functionality are distinctly pyramidal (Table 2). Is this the driving force for the formation of both β-As sheet and other unsaturated either N–H···π or N–H···S containing structure types? Or is it a consequence of the hydrogen bonding?

This study shows that even for compounds with complex crystal structures, the packing may be reasonably anticipated provided a sufficient number of examples is available. These observations are rationalised in terms of geometrical and chemical effects of the molecular functionality.

3.7 Experimental section

4-(4-Aminophenylsulfamyl)phenol, 1a

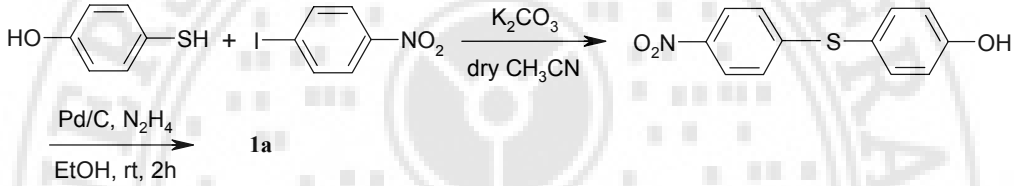

To a solution of 4-hydroxythiophenol (151 mg, 1.2 mmol) and anhy. K_2CO_3 in dry CH_3CN (20 mL), 4-nitroiodobenzene (300 mg, 1.2 mmol) was added under N_2 atmosphere and refluxed for 12 h. The workup yielded 208 mg (70%) of 4-hydroxy-4'-nitrodiphenylsulfide [3.9a]. To this nitrothioether (250 mg, 1.01 mmol) in 10 mL of EtOH, $N_2H_4.H_2O$ (0.26 mL, 5.4 mmol) and Pd/C were added and stirred for 2 h at room temperature [3.9b]. The reaction mixture was filtered off and evaporated to yield 153 mg (70%) of **1a** with mp 147-148 °C. IR (cm^{-1}): 3371, 3308. ^{1}H NMR (DMSO-d_6): δ 5.30 (s, 2H), 6.52 (d, J 8, 2H), 6.70 (d, J 8, 2H), 7.10 (m, 4H), 9.45 (s, H).

4-(4-Aminobenzylsulfamyl)phenol, 2a

As in **1a** the thiolation reaction of 4-hydroxythiophenol with 4-nitrobenzyl bromide gave 62% of 4-nitrobenzyl-4'-hydroxyphenylthioether. To a solution of the nitrothioether (250 mg, 0.957 mmol) in dry EtOAc, $SnCl_2.2H_2O$ (1.07 g, 4.78 mmol) was added and refluxed for 1.5 h. The mixture was cooled, neutralised with $NaHCO_3$,

and worked up to give 152 mg (69%) of **2a** [3.9c] with mp 211-212 °C. IR (cm^{-1}): 3360, 3287. ^1H NMR (DMSO-d_6): δ 4.0 (s, 2H), 5.0 (s, 2H), 6.52 (d, J 8, 2H), 6.70 (d, J 8, 2H), 6.94 (d, J 8, 2H), 7.1(d, 2H), 9.42 (s, 1H).

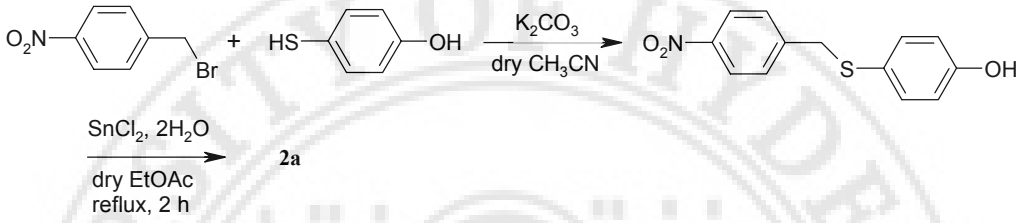

4-(4-Aminophenylsulfamylmethyl)phenol, 2b

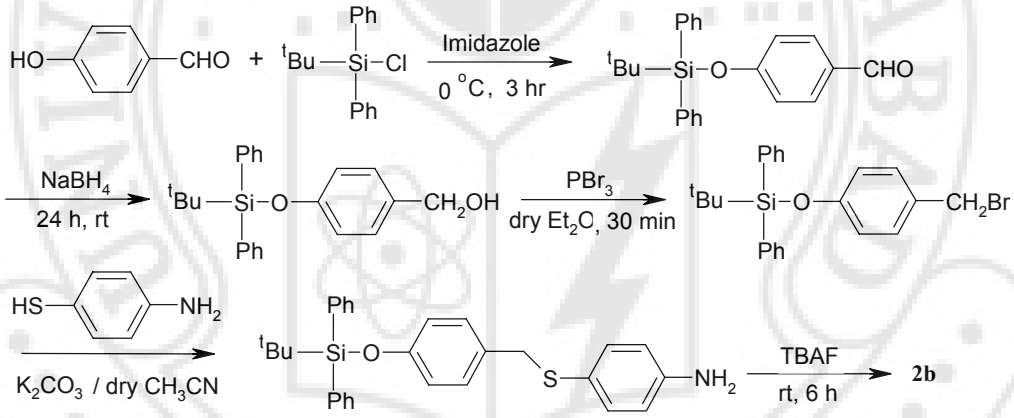

4-Hydroxybenzaldehyde (800 mg, 6.55 mmol) was subjected to phenolic protection using *t*-butylchlorodiphenylsilane (5.40 g, 19.65 mmol) and imidazole (668 mg, 9.82 mmol) in dry DMF in N_2 atmosphere at 0°C for 3 h, followed by workup and purification to obtain 1.89 g (80%) of the silylated compound [3.9d]. Then the silyl protected benzaldehyde (1 g, 2.77 mmol) was reduced using $NaBH_4$ (157 mg, 4.16 mmol) to yield 623 mg (62%) of the corresponding alcohol. This benzyl alcohol 500 mg, (1.37 mmol) was converted to the silyl protected benzyl bromide with PBr_3

0.64 mL (0.685 mmol) in dry Et_2O (20 mL) and was stirred at 0 °C for 1 h. The reaction mixture was subjected to workup and immediately added dropwise to a refluxing solution of 4-hydroxythiophenol (172 mg, 1.37 mmol) and anhy. K_2CO_3 in dry CH_3CN. The resultant mixture was refluxed for 12 h to yield 712 mg (55%) of silyl protected aminophenol. Then the compound (500 mg, 1.06 mmol) was deprotected using TBAF (0.306 mL, 1.06 mmol) [3.9e] in THF to produce100 mg (60%) of **2b** with mp 205-207 °C. IR (cm^{-1}): 3369, 3295, ^{1}H NMR (DMSO-d_6): δ3.85 (s, 2H), 5.24 (s, 2H), 6.47 (d, J 8, 2H), 6.70 (d, J 8, 2H), 7.00 (m, 4H), 9.30 (s, 1H).

4-(4-Aminophenyldisulfamyl)phenol, 2c

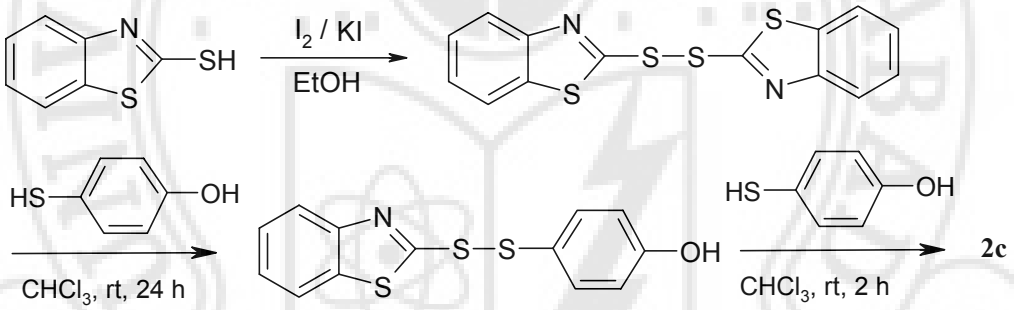

2,2'-Dithiobis(benzothiazole) (BTS–SBT) was prepared by the standard procedure of dimerization of 2-mercaptobenzothiazole in I_2 and EtOH. To a solution of 4-hydroxythiophenol (152 mg, 1.21 mmol) (P–HBSH) in 20 mL of $CHCl_3$, a stirred suspension of 2,2'-diithiobis(benzothiazol) disulfide (800 mg, 1.20 152 mmol) in 100 mL of $CHCl_3$ was added. Stirring was continued at room temperature for 24 h to give 275 mg (50%) of unsymmetrical 2-benzothiazolyl 4-hydroxyphenyl disulfide (P–HBS–SBT). Using the preceding procedure, the reaction of P–HBS–SBT (200 mg, 0.438 mmol) with 66 mg (0.530 mmol) of 4-aminothiophenol yielded, after work up, 79 mg (60%), mp 113-115 °C of **2c** [3.9f]. IR (cm^{-1}): 3370, 3305, 750, ^{1}H NMR

(DMSO-d_6): δ 5.35 (s, 2H), 6.48 (d, J 8, 2H), 6.75 (d, J 8, 2H), 7.05 (d, J 8, 2H), 7.20 (d, J 8, 2H), 9.40 (s, 1H).

4-[2-(4-Aminophenylsulfamyl)ethyl]phenol, 3a

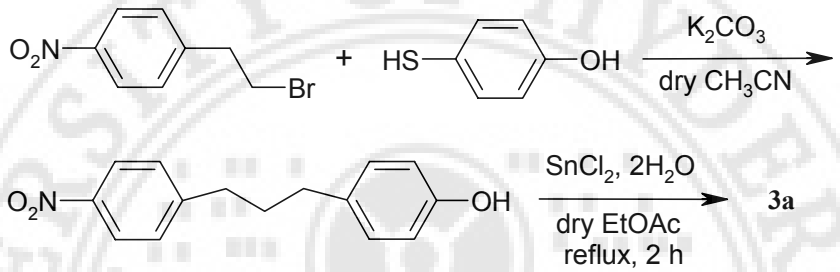

Treatment of 4-nitrophenylethyl bromide with 4-hydroxythiophenol as in the case of **1a** yielded (55%) 4-nitrophenylethyl-4'-hydroxyphenylsulphide. This was reduced with $SnCl_2.2H_2O$ as in **2a** to get **3a** in 65% yield with mp 116-118 °C. IR (cm^{-1}): 3370, 3305, ^{1}H NMR (DMSO-d_6): δ 2.54 (t, 2H), 3.34 (t, 2H), 6.15 (d, J 8, 2H), 6.72 (d, J 8, 2H), 6.88 (d, J 8, 2H), 7.15 (d, J 8, 2H), 9.50 (s, 1H).

Crystallization

Diffraction quality single crystals were achieved by recrystallizing aminols **1a** and **2c** from CH_3OH, **2a** and **3a** using 1:1 EtOH/benzene and **2b** with dioxane.

X-ray diffraction

The X-ray data were collected at the University of Durham, U.K. by Dr. C.K. Broder and Mr. P.S. Smith under the supervision of Prof. J.A.K. Howard. The X-ray data were performed on a Bruker SMART CCD 1K area detector (**2b**, **2c** and **3a**) or the Bruker SMART-6000 diffractometer (**1a**) using Mo K_α radiation (λ = 0.71073 Å). Reflections for **2a** were collected on a Rigaku AFC6S diffractometer using Cu K_α

radiation (λ = 1.54178 Å). The structure solutions and refinements were accomplished using the SHELXS-97 and SHELXL-97 programs built-in with the Siemens SHELXTL-98 (Version 5.1) package [2.12]. In all cases the hydrogen atoms were located in difference Fourier maps and refined isotropically. All the relevant geometrical analysis was carried out with PLATON 2002 [2.13] on Silicon Graphics Octane2 workstation (Table 2). For more crystallographic details see also appendix.

Cambridge Structural Database study

A CSD search on C–S–C

The search was carried out using the Cambridge Structural Database (Version 5.23, April 2002) for error free Ar–S–Ar organic acyclic structures, non-ionic, non polymeric structures with R < 0.10. Disordered, 'no co-ordinates present' structures were excluded from the search. Of the 589 entries in the subset, 21 hits with corresponding Ar–C–Ar were found. Of these only 8 pairs were found that are isostructural.

Table 4. CSD refcodes of organic (Ar–S–Ar/Ar–C–Ar) structural pairs.

Isostructural	Non-isostructural
Ar–S–Ar/Ar–C–Ar pair	
DAPHSD, CEHCOH	BIRFEN, ZZZEMS01/02/03
HPTBZC, GUHKUP	BODPEP, SUBRAC05
LMETON02, LNLEUC10	CUZZAY, CUZYEB
MDTHAC, PIMELA04	DABMOI, DABKUM
MDTPRA, AZELAC03	GALCEB, GALCAX
TGLYCL/01, GLURAC03/04	LIQWAJ, BITVUV
ZAGKAT, ZAGJUM	LIQWIR, PENTAN01
ZZZPZE01, PIMELA	NTPXMB10, CBYMBZ
	PHMESF, BOKCEJ
	VUKPOG, JEMTIE
	WANWOX, WANXOY
	WANWEN, WANWUD
	WANWIR, WANXEO

A CSD search on benzene-thiophene exchange

A search of the CSD (Version 5.23, April 2002) for error free thiophene only organic, non-ionic, non polymeric structures with R < 0.10 was performed. 'No co-ordinates present' structures were excluded from the search. Of the 8 entries in the subset, 2 hits with the corresponding benzene structure were found and they are isostructural (VEVJUB, FACROQ; WOZVEX, WOZWAT).

A CSD search on Ar–S–S–Ar torsion angle

A search of the CSD (Version 5.23, April 2002) for error free C–S–S–C organic, aromatic, acyclic, non-ionic, non polymeric structures with R<0.10. Disordered, 'no co-ordinates present' structures were excluded from the search. The torsion angles of approximately 90° are average for Ar–S–S–Ar systems. Disulfide compounds are comparatively rare, with only a total of 51 hits in the database.

CHAPTER FOUR

MOLECULAR COMPLEXES OF SOME DIANILINES AND DIPHENOLS

4.1 Introduction

Two-component ordered crystals are usually termed molecular complexes by organic chemists, molecular compounds by inorganic chemists, while metallurgists prefer the term intermetallic compounds [4.1]. A molecular complex can be further stated to be a crystalline material that consists of chemically distinct and electrically neutral molecular species held together by non-covalent interactions. Therefore it is possible to distinguish molecular complexes from solid solutions or inclusion compounds [4.2]. The formation of a molecular complex is favoured when the intermolecular interactions between molecules of different components is stronger than those in the homomeric crystal. The formation of an energetically favourable crystal also depends on entropic and ethalpic factors. According to Kitaigorodskii all these two-component systems fall into the broad category of *mixed crystals* [4.1].

Mixed binary crystals consist of two molecules in differing shape and size [4.3]. The mixture of the two components can give a single-phase system. Molecules can be mixed in a liquid state (melt) or in a solid state (solid solution). Accordingly, molecular complexes are of significance in crystal engineering [1.2]. Desiraju noted that the formation of a molecular complex **A•B** is an indication that interactions of the type **A**···**B** are more significant than interactions of the type **A**···**A** or **B**···**B** [4.4]. Thus the studies of the binary crystals of organic substances are important for understanding the nature of intermolecular interactions.

4.2 1:1 Diamine–diol complexes

Molecules are structured aggregates of atoms joined by covalent bonds while crystals are aggregates of molecules interacting noncovalently. Strong hydrogen

bonding interactions contribute to structural predictability in crystal engineering [4.5]. Specificity of recognition between amino and hydroxy functionalities to give supraminol structures have been studied extensively [4.6]. The Hanessian and Ermer groups have shown that hierarchic crystal structures with a saturation of O–H···N and N–H···O hydrogen bridges are obtained in several cases [1.25, 1.24]. Desiraju *et al.* have shown that deviations from hierarchy [4.7] are also not uncommon with N–H···π bridges [1.29] making their appearance in many cases.

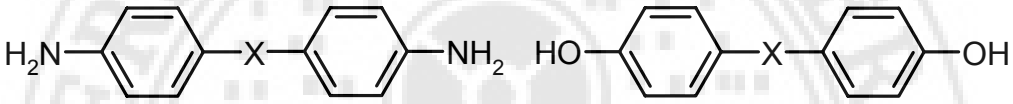

7, **X=CH$_2$** **9**, **X=CH$_2$**

8, **X=S** **10**, **X=S**

I = (**7**)•(**9**) **II** = (**7**)•(**10**)

III = (**8**)•(**9**) **IV** = (**8**)•(**10**)·

Scheme 1

With reference to the supraminols, the formation of 1:1 amine–alcohol (or phenol) molecular complexes is favoured because the resulting N(H)O hydrogen bridges are better than the O–H···O and N–H···N bridges in the crystal structures of the respective individual components. Ermer and Eling isolated the 1:1 complex between *p*-phenylenediamine and hydroquinone and between aromatic based extensions of these compounds [1.24]. Hanessian *et al.* have reported many examples of helical diamine–diol complexes [1.25]. Independently Loehlin [1.40], Toda [1.38–1.39], Roelens [1.34] and their co-workers have also observed the formation of 1:1 amine–alcohol molecular complexes. In all these cases, saturation of N(H)O hydrogen bridge forming ability is observed. The hydrogen bridge directed molecular complexation of diamines and diphenols in a wide variety of compounds allows the

formulation of general rules about the hydrogen bridge driven molecular recognition within these molecules. With this background it is a worthwhile approach to examine whether the single compound can be utilized in the investigation of the hydrogen bridge preferences of a molecular complex.

Table 1. Pertinent structural parameters in molecular complexes **I-IV**.

compound	**I**	**II**	**III**	**IV**
Synthon	square motif	square motif	infinite chain	cyclohexane chair
C–O, C–O; C–N, C–N angle [°][a]	121 ; 105	117 ; 107	114 ; 104	120 ; 111
C_k* [%][b]	0.67	0.66	0.70	0.66
pyramidal factor[c]	0.285, 0.298	0.267, 0.291	0.306, 0.330	0.295, 0.330
latt. energies [kcal mol^{-1}][d]:				
van der Waals	–33.6265	–36.6518	–36.9673	–36.1518
electrostatic	–20.9314	–24.5305	–23.0903	–29.3588
hydrogen bridge	–12.7683	–13.5359	–10.9266	–18.2951
total energy	–67.3262	–74.7182	–70.9842	–65.9497

a) The angle between the C–O, C–O and C–N, C–N vectors in the molecular complexes have been calculated using *RPluto*. This gives a measure of the linearity of the molecule. b) C_k*, packing fraction calculated with *PLATON*. c) The perpendicular distance from the basal plane to the apex of the pyramid. d) Lattice energies calculated using *Cerius*^{2} from Accelrys [2.8].

In this work, the 1:1 molecular complexes **I-IV** formed by all combinations of diamines **7** and **8** with diols **9** and **10** have been examined. The prototype structures for these molecular complexes are aminophenols **1**, 4-(4-aminobenzyl)-phenol, and **1a**, 4-(4-aminophenylsulfamyl)phenol. The structures **1** and **1a** are based on that of 3-aminophenol [1.29]. Optimisation of herringbone interactions is the primary structural effect and this leads to the formation of weak N–H···π, N–H···S and C–H···O bridges [1.21] rather than to a saturation of N(H)O bridges. Both **1** and **1a** have a square motif N(H)O synthon and replacement of the $–CH_2–$ group in **1** by

an isosteric S-atom in **1a** causes, however, an exchange of an N–H···π by an N–H···S bridge. Complexes **I-IV** have been undertaken to further assess the structural consistency and structural interference in supraminol systems.

Table 2. Intermolecular interactions for the molecular complexes in this study.

Aminol	H-bridge	*d* (Å)[a]	*D* (Å)	*θ* (deg)
I	O–H···N	1.81	2.7760(18)	168.75(7)
	O–H···N	1.85	2.8010(18)	160.78(7)
	N–H···O	2.19	3.120(2)	152.64(7)
	N–H···O	2.29	3.1938(19)	148.07(7)
	N–H···π	2.62	3.397	134.0
	N–H···π	2.84	3.638	135.9
	C–H···O	2.36	3.294(2)	143.09(7)
	C–H···π	2.59	3.641	161.1
	C–H···π	2.70	3.712	154.7
	C–H···π	2.71	3.730	156.3
	C–H···π	2.82	3.881	166.0
	C–H···π	2.88	3.862	150.1
II	O–H···N	1.78	2.760(3)	174.37(14)
	O–H···N	1.85	2.798(3)	160.94(14)
	N–H···O	2.12	3.078(3)	157.88(13)
	N–H···O	2.25	3.167(3)	150.12(14)
	N–H···π	2.55	3.340	135.1
	N–H···π	2.96	3.739	134.2
	C–H···O	2.46	3.372(3)	141.09(16)
	C–H···S	3.04	3.789(3)	126.76(14)
	C–H···π	2.69	3.690	153.0
	C–H···π	2.73	3.736	155.0
	C–H···π	2.74	3.745	155.0
III	O–H···N	1.86	2.8234(16)	164.49(6)
	O–H···N	1.86	2.8381(17)	175.24(8)
	N–H···O	2.09	3.0958(18)	174.41(8)
	N–H···O	2.09	3.0565(17)	160.02(8)
	C–H···S	2.78	3.6976(15)	141.56(7)
	C–H···π	2.79	3.823	157.6
	C–H···π	2.82	3.868	160.8
IV	O–H···N	1.70	2.6775(18)	170.52(8)
	O–H···O	1.83	2.8122(16)	174.29(8)

N–H···O	2.06	3.0423(19)	162.86(9)
N–H···O	2.18	3.1369(18)	156.42(9)
N–H···N	2.04	3.042(2)	171.14(9)
N–H···S	2.77	3.7060(15)	154.24(8)
C–H···S	2.81	3.7982(16)	151.19(8)
C–H···S	2.90	3.9282(18)	157.84(10)
C–H···S	2.94	4.0245(16)	172.27(8)
C–H···O	2.76	3.637(2)	137.52(9)

[a] O–H, N–H and C–H distances are neutron normalized to 0.983, 1.009 and 1.083 Å.

4.3 Complex I. 1:1 4-(4-aminobenzyl)aniline (7) • 4-(4-hydroxybenzyl)phenol (9)

The structure of complex **I** is closely related to the structure of aminol **1** and in both cases the structure is made up of square motif N(H)O synthons that are linked together to form chains. The minor differences between **I** and aminol **1** lie in the internal geometry of the chains and the way in which they pack together. In **I**, the square motifs are constituted with functionalities from two diamine and two diphenol molecules (Figure 1). The planes of adjacent square motifs in a chain are ~55 degrees to each other whereas in **1** they are parallel.

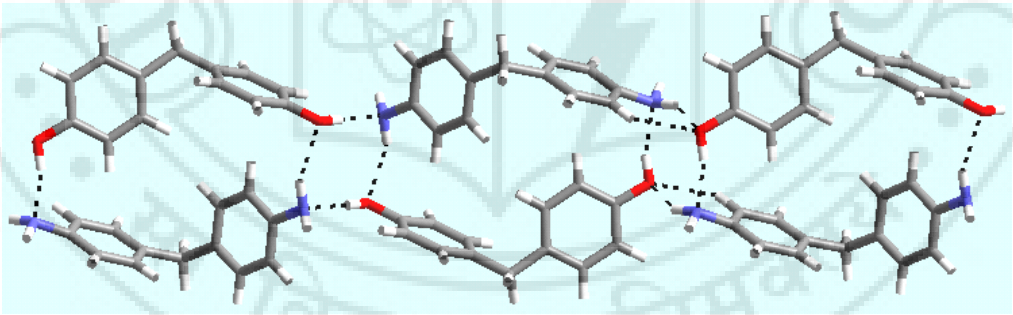

Figure 1. Complex **I** showing the square motifs of hydrogen bridges forming chains. Notice also the C–H···O interactions.

The aniline hydrogens that are not involved in a tetramer loop interact with the phenol rings of an adjacent chain to form N–H···π interactions. C–H···π

interactions are formed at the other face of the same phenol ring (Figure 2) [1.31]. The crystal structure is further stabilized by C–H···O interactions. Geometrical parameters for hydrogen bridges are given in Table 2.

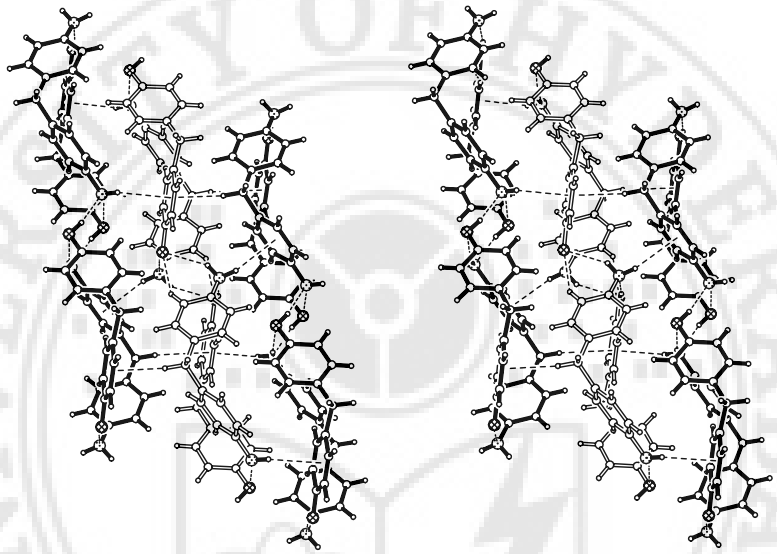

Figure 2. Complex **I**. Close packing of chains. Notice the N–H…π interactions.

4.4 Complex II. 4-(4-aminobenzyl)aniline (7) • 4-(4-hydroxyphenylsulfanyl)-phenol (10)

The substitution of the $–CH_2–$ group in the diphenol component of **I** by an S-atom in to give complex **2** has very little effect on the crystal structure. This is a good example of shape and size factors being important in crystal packing and has been noted previously [4.7]. The cell dimensions of **I** and **II** are nearly identical and **II** also consists of square synthon linked chains connected with N–H···π interactions. A comparison of the unit cell dimensions gives an isostructurality parameter (Π) of 0.0082 [3.7], where zero indicates an exact match. Compare the overall crystal

packing of **II** shown in figure 4 with that of **I** in figure 2. NIPMAT plots and simulated powder spectra for **I** and **II** shows the near identity of crystal packing. One might infer that mixed crystal formation is taking place and the interchangeability of the linker CH_2/S between aniline and phenol rings leads to isomorphous structures.

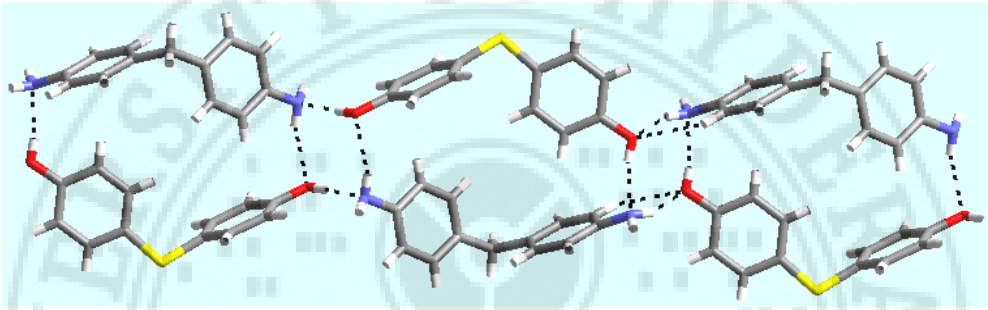

Figure 3. Square motif in complex **II**. Compare this with Figure 1.

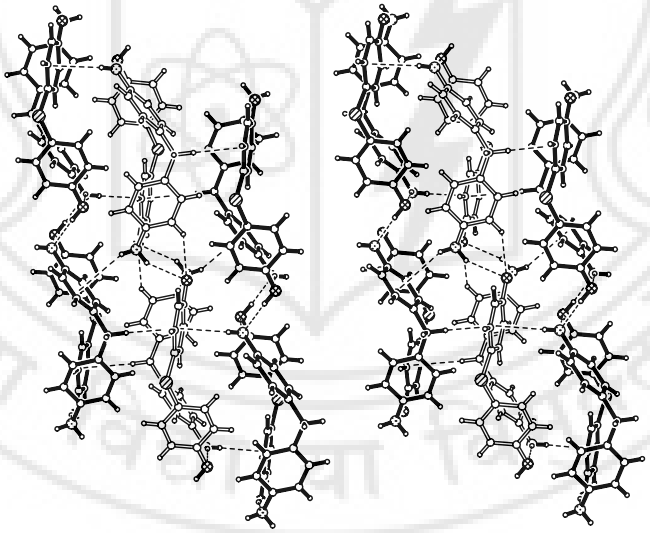

Figure 4. Complex **II**. Close packing of chains. Notice the N–H…π interactions.

4.5 Complex III. 4-(4-aminophenylsulfanyl)aniline (8) • 4-(4-hydroxybenzyl)-phenol (9)

The CH_2/S exchange does not take place in the crystal structure of complex **III**. Replacement of the $–CH_2–$ group in the dianiline component of complex **I** by an S-atom changes the packing. The major synthon in complex **III** is a one dimensional infinite chain of N(H)O bridges [1.20] (Figure 5). Cross-linking of these chains is shown schematically in figure 6. In simple aminols that have the N(H)O linear chain the additional N–H group forms an N–H···π interaction. However, in **III** this interaction loses out and the N–H group is free. Instead, the electronegative S-atom can more likely to activate an adjacent phenyl H-atom to the extent of promoting a C–H···S dimer synthon (Figure 7).

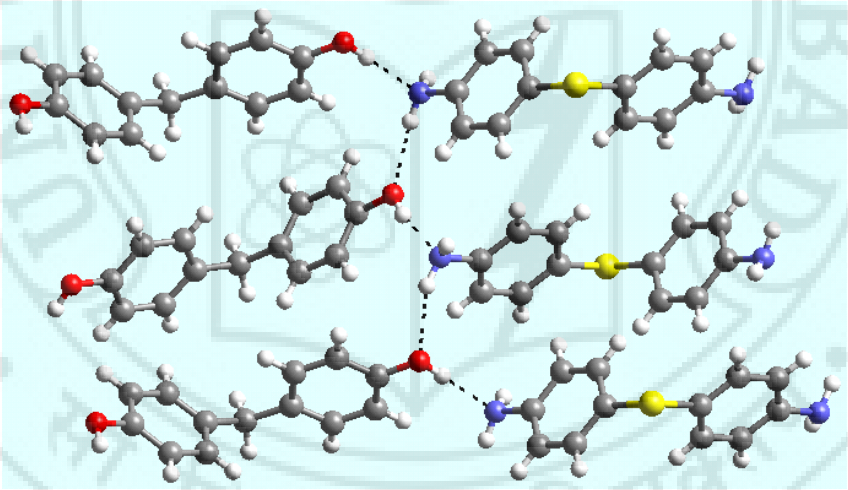

Figure 5. Infinite N(H)O chain in complex **III**.

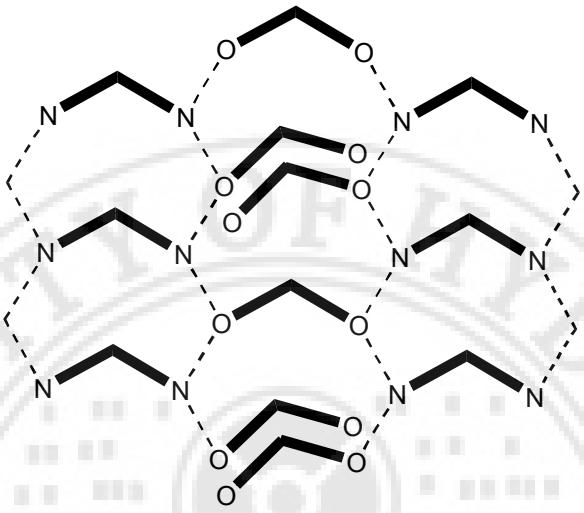

Figure 6. Schematic of crosslinking of molecules in complex **III**. N(H)O hydrogen bridges are shown as dotted lines.

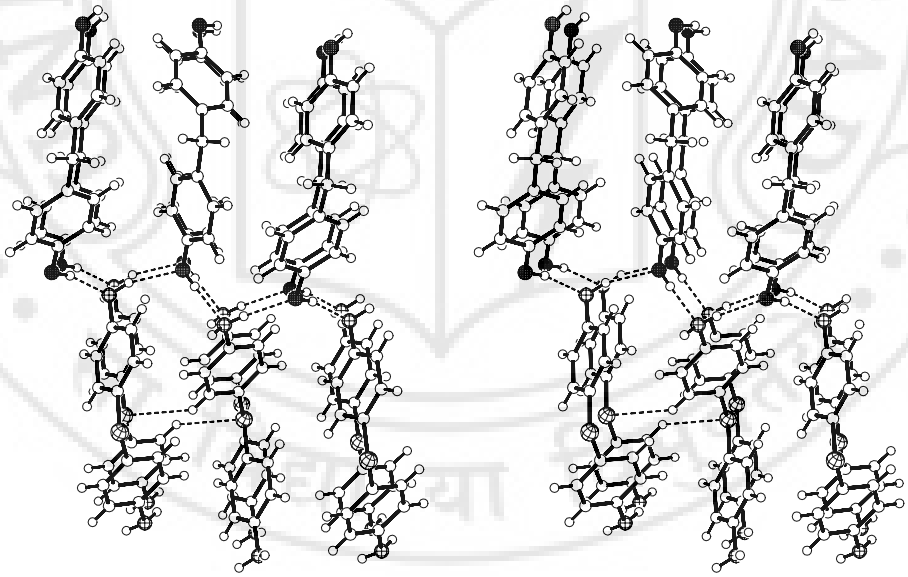

Figure 7. Stereoview of the packing in complex **III**. Note the C–H···S dimer synthon.

4.6 Complex IV. 4-(4-hydroxyphenylsulfanyl)phenol (8) • 4-(4-aminophenyl-sulfanyl)aniline (10)

At first glance crystal structure of complex **IV** (orthorhombic $P2_12_12_1$) appears to be similar to that of aminol **1a**. The "windmill" type arrangement of molecules is seen (Figure 8) [4.7]. However, the N(H)O networking is not built with tetramer loop synthon as in **1a** but rather there is a new arrangement that could be termed as a supramolecular cyclohexane chair. In addition to the N(H)O bridges there are also O–H···O and N–H···N interactions. This is very unusual in a supraminol and has never been observed previously in this group of compounds. The aniline N-atom completes its tetrahedral coordination with an N–H···S bridge.

It is interesting to note that in **IV** the N(H)O synthon is more likely a primary structure stabilizing factor as the O–H···N is stronger than the O–H···O interaction (Table 2). A CSD search [1.19] was carried out for measuring the relative strengths of phenolic O–H···N(aniline) and phenolic O–H···O(phenolic) interactions (experimental section). The study shows that phenolic O–H···O(phenolic) is in general stronger than the phenolic O–H···N(aniline). In **IV**, the O–H···O(phenolic) is found to be weaker than O–H···N(aniline). Therefore N(H)O hydrogen bridges are the primary structure stabilizing interactions.

4.7 General discussion of complexes I-IV

The propensity towards formation of 1:1 phenol-aniline complexes is noted in this group of compounds and confirms earlier trends. The formation of N(H)O bridges is a dominant feature in all these molecular complexes. It is noteworthy that in the crystallization experiments, none of the uncomplexed substances **7-10** were recovered if 1:1 stoichiometries of the dianiline and diphenol components were taken. This shows the specificity of aniline–phenol recognition. The three major supramolecular synthons observed are given in Scheme 2. The square motif and

infinite chain have been observed before. The supramolecular cyclohexane chair is seen for the first time here.

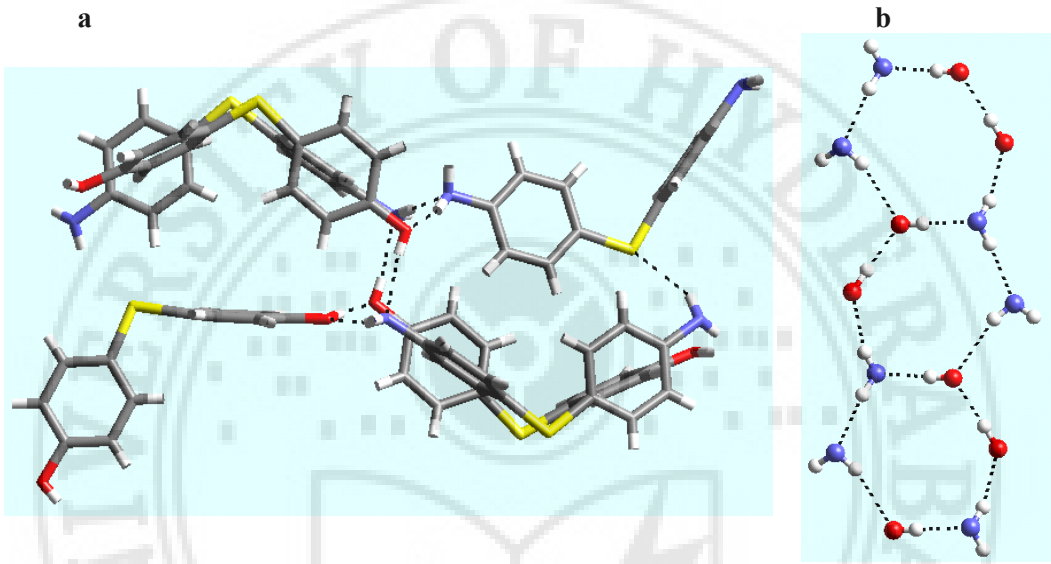

Figure 8. (a) Complex **IV** to show supramolecular cyclohexane chair and N–H···S bridge. (b) Detail of chair. Note N(H)O, O–H···O and N–H···N interactions.

Complexes **I** and **II** are isostructural and are closely related to aminol **1a** but complex **III** is distinct. This suggests in some subtle way that the role of the dianiline component is more significant than that of the diphenol in the supraminol recognition bearing out Kitaigorodskii's comment mentioned earlier [4.1]. The very different structure of complex **IV** shows that the system has been disturbed to a sufficient extent by S-atom replacement in both diamine and diphenol components. Complex **IV** is not related to aminol **1a** in the way that complex **I** is related to aminol **1**. The pyramidality factor shows that the N atoms are distinctly pyramidal in all the four complexes (Table 1).

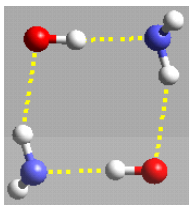

1 and 2

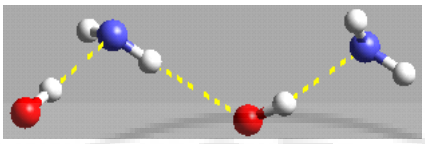

3

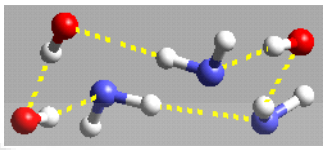

4

Scheme 2. Square motif, infinite chain and cyclohexane chair synthons. Note the O–H···O and N–H···N bridges in the cyclohexane chair (**IV**).

4.8 Conclusions

This series highlights the advantages of molecular complexation in crystal engineering and also highlights some of the difficulties of crystal structure prediction. The subtleties of a crystal structure are clearly seen in the large changes in overall structure despite the presence of the same (square motif) synthon, and in the way that exchanging $–CH_2–$ groups by S-atoms may have little (complex **II**), moderate (complex **III**) or major (complex **IV**) structural effects. To conclude, crystal engineering with complementary multifunctional multicomponent systems requires a detailed understanding of the factors that control supramolecular organization. However, the device of molecular complexation affords entry into this difficult problem.

4.9 Experimental section

General methods

All compounds were commercially available except for diphenol **9**, 4-(4-hydroxybenzyl)phenol. Diphenol **9** was prepared from dianiline **7** by diazotization followed by hydrolysis. Stoichiometric amounts of the components were ground well, dissolved in the appropriate solvents and recrystallized. All the melting points were determined on a Mettler Toledo DSC 822e instrument.

Complex I. Diamine **7** (24 mg, 0.125 mmol) and diphenol **9** (25 mg, 0.125 mmol) were dissolved in 1:1 hot MeOH–benzene. Colourless block-like crystals were formed after three days; mp 135.5 °C.

Complex II. Diamine **7** (24 mg, 0.125 mmol) and diphenol **10** (27 mg, 0.125 mmol) were dissolved in hot EtOH. Block-like colourless crystals were obtained after slow evaporation of the solvent; mp 132.5 °C.

Complex III. Diamine **8** (27 mg, 0.125 mmol) and diphenol **9** (25 mg, 0.125 mmol) were dissolved in 1:1 hot MeOH–xylene. Colourless cube-like crystals were obtained after a few days upon slow evaporation; mp 109.9 °C.

Complex IV. Diamine **8** (27 mg, 0.125 mmol) and diphenol **10** (27 mg, 0.125 mmol) were dissolved in hot ethanol. Light yellow prism shaped crystals were obtained after one week upon slow evaporation of the solvent; mp 121.8 °C.

X-ray crystallography

The X-ray data were collected at the University of Durham, U.K. by Dr. C.K. Broder and Mr. R. Mondal under the supervision of Prof. J.A.K. Howard. The X-ray reflections were collected on a Bruker SMART–1000 diffractometer (**I**, **II**) or the Bruker SMART–6000 diffractometer (**III**, **IV**) using Mo K_α radiation (λ = 0.71073 Å). The structure solution and refinements were carried out using SHELXTL (Version 5.1) programs [2.12]. In all cases, the hydroxy and amine H-atoms were located in difference Fourier maps and refined isotropically. The other H-atoms were either fixed in geometrically sensible positions (**II**) or located in difference Fourier maps and refined isotropically (**I**, **III**, **IV**). All interatomic distance and related calculations were carried out with PLATON2002 [2.13]. For further crystallographic data, see appendix.

A CSD search on phenolic O–H···N (anilino) and phenolic O–H···O (phenolic)

A search of the CSD (Version 5.24, November 2002) for error free Ar–OH organic, aromatic, non-ionic, non polymeric structures with R < 0.1. Disordered, 'no co-ordinates present' structures were excluded from the search. Of the 3811 entries in the subset, 25 and 346 hits with the corresponding phenolic O–H···N (anilino) and phenolic O–H···O (phenolic) respectively were found. The distance and angle for both the interactions was created in the range: 1.2–2.2 Å, 130–180°. The highest population of O–H···O distance is 1.76–1.83 Å. O–H···N occurrences are relatively less but the highest population distance is found to be 1.82 Å.

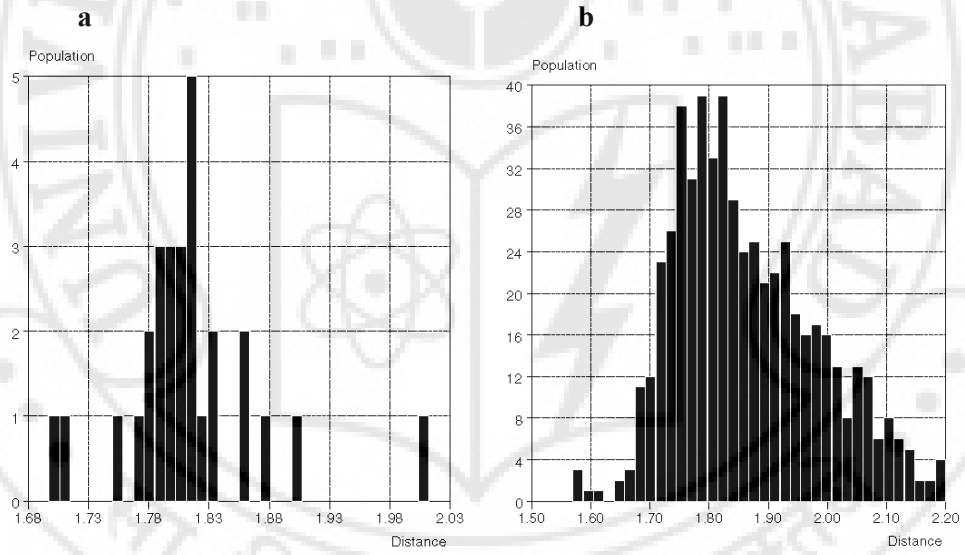

Figure 8. Histogram of (a) O–H···N and (b) O–H···O interactions.

CHAPTER FIVE

FROM MOLECULAR TO CRYSTAL STRUCTURE

5.1 Introduction

Crystals are composed of molecules but in the outlook of crystal engineering strategies the practical problem is that crystal structures cannot be easily anticipated from molecular structures [5.1]. This is a difficult task for two reasons. As discussed in previous chapters the first relates to the complementary nature of both geometrical and chemical recognition, or in other words because a functional group approach to crystal structure prediction is generally inapplicable [5.2]. In supramolecular chemistry, hydrocarbon residues are also considered as functional groups. The second difficulty concerns the weak long-range interactions [5.3] which can direct the course of crystallization or close packing. So, similar molecules can have dissimilar crystal structures and dissimilar molecules can have similar structures. Both these problems are not persistent in hydrocarbon crystals. However, in heteroatom containing structures the recognition events are complex.

The patterns and trends observed so far provide a good understanding of the structural features possible for a family of supraminols and the geometrical and chemical reasons why one structural synthon [1.17] is preferred over another. In this chapter five compounds **2d**, **1b**, **6a, 6b** and **6c** have been synthesized. These are basically related to crystal structures **1** through **5, 1a, 2a, 2b, 2c** and **3a** seen previously (Scheme 1). Each compound explores a different aspect of the structural principles discussed above. These structures offer a chance for crystal engineering and, where the design strategy fails, provide further insight into the structural chemistry of these compounds. The understanding of network architectures is an advantageous exercise in crystal engineering. Inorganic solids provide a wealth of information about various network architectures [5.4]. The exercise of generating

organic network structures by analyzing examples of inorganic solids can improve design strategies [5.5].

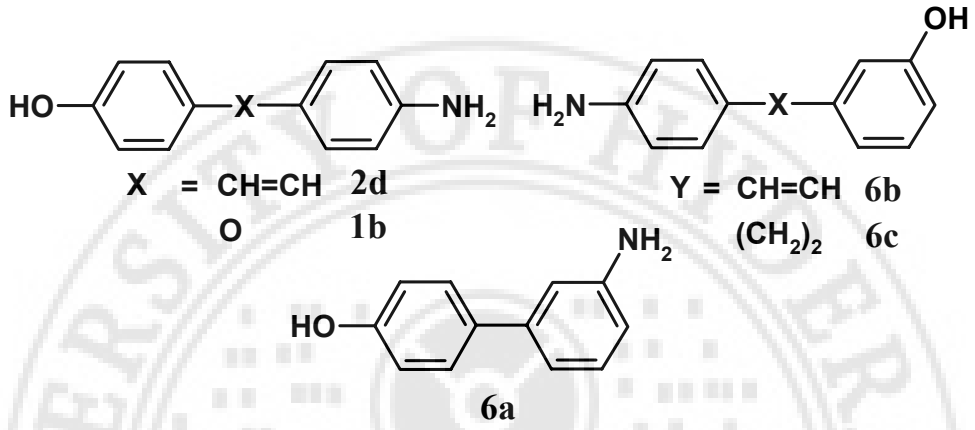

6a

Scheme 1

5.2 Saturated hydrogen bridge patterns

Hydroxy and primary amines are complementary H-bonding partners in that a single donor–double acceptor (oxygen) perfectly matches the coordination properties of a double donor–single acceptor (nitrogen). Ermer *et al*. [1.24] showed that N–H···O and O–H···N complementarity [1.20] in amine alcohols leads to super arsenic sheet (β-As) or super-black phosphorus (black-P) types. The hydrogen bridge capabilities of N–H and O–H groups are fully saturated in these networks by N–H···O and O–H···N hydrogen bridges. Hanessian and coworkers [1.25] observed a 1-dimensional N(H)O ladder with tetramer loops. Desiraju, Howard *et al*. [1.29] showed that the influence of unfavourable molecular geometry leads to lower dimensional unsaturated hydrogen bridge patterns (tetramer loop, infinite chain), wherein free N–H groups forms N–H···π hydrogen bridges. Loehlin *et al.* [1.40] classified SHB architectures into two types. They are the hexagonal chickenwire and ladder patterns shown in the scheme 2.

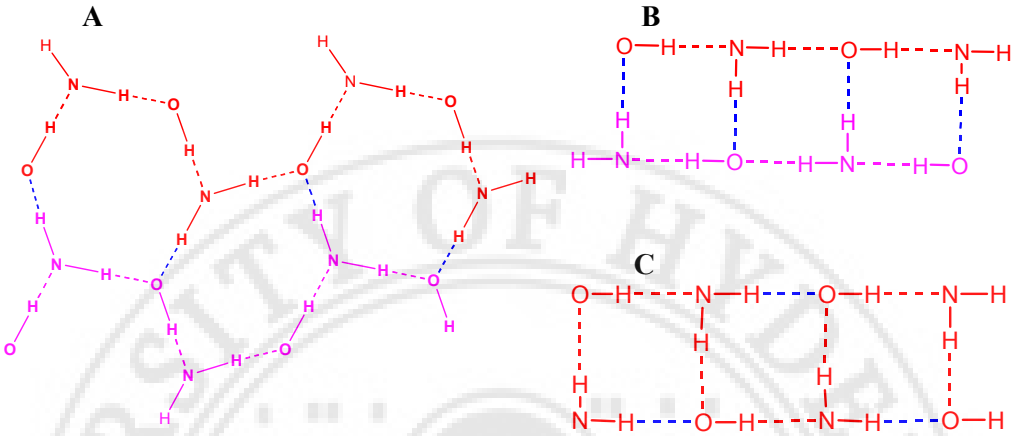

Scheme 2. Supramolecular patterns with saturated N(H)O interactions: (**A**) Parallel infinite chains with sawtooth geometry connected to form β-As or black-P sheets. (**B**) and (**C**) SHB ladders.

A comprehensive CSD survey (Version 5.24, November 2003 release and including the structures reported in this thesis) [1.19] for SHB motifs in supraminols reveals that there are a total of 26 SHB architectures with N(H)O bridges. Of these, 20 structures belong to the β-As sheet type, one to the black-P category and five to the SHB ladder arrangement **B**. There are also 2 other entries in the CSD pertaining to the saturated ladder type **C** structures but the overall interactions in those supraminols are unsaturated with *free* N–H groups being present. Relevant refcodes are given in the experimental section.

5.3 Effect of molecular shape to produce the β-As sheet

4-[(E)-2-(4-Aminophenyl)-1-ethenyl]phenol, **2d**, and aminol **2** are very similar and the saturated ethane bond of the linker is exchanged for an unsaturated ethene bond. This is but a small chemical change in supramolecular terms and it is not expected that the structure would deviate from the β-As sheet. Indeed this was found

to be the case. Equivalent synthons lead to virtually identical crystal structures. The unit cell dimensions of **2d** are comparable to those of compounds **2**, **2a**, **2b**, and **4**, with the isostructurality parameter (Π) for **2** compared with **2d** of 0.027 (Figure 1) [3.7].

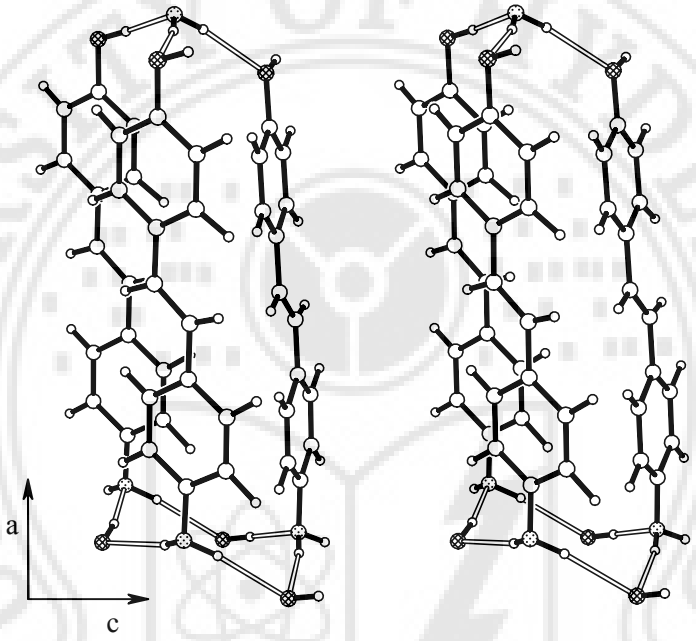

Figure 1. Stereoview of diamond structure in 4-[(E)-2-(4-aminophenyl)-1-ethenyl]phenol **2d**.

5.4 Substitution: shape versus electronic factors

4-(4-Aminophenoxy)phenol, **1b**, is the O-analog of aminols **1** and **1a**, and as such it might be expected to form a square motif structure. However, while an S-atom can often be exchanged for a CH_2 group to form an isostructural crystal, the same cannot be said for exchange by an O-atom. A CSD search [1.19] was carried out for oxygen substituted and comparable unsubstituted compound. A total of 4 pairs were found of which one is isostructural. The C–C–C angle tends to be 109°, in S-

substituted compounds the C–S–C angle is approximately 100°, whereas the C–O–C angle is ideally 120° (Figure 2). An angle of 120° would suggest that an infinite chain structure is also a logical prediction for the structural type (experimental section). When the structure of **1b** was determined it was immediately apparent from the unit cell dimensions that the structural motif was neither that of a square motif nor that of an infinite chain but the β-As sheet structure (Figure 3). This is a super diamond network. A closer study revealed the reasons for such an unlikely result.

Table 1. Structural parameters for the supraminols **2d**, **1b**, **6a**, **6b** and **6c**.

compound	**2d**	**1b**	**6a**	**6b**	**6c**
structure	β-As	β-As	infinite chain	tube	tube
mp [°C]	272–275	155–157	180–182	202	143
C–O, C–N angle [°][a]	173.8	141.6	121.4	122.4	124.1 123.2
herringbone angle [°][b]	67 and 70	62 and 69	89.4	52	61 and 67
C_k* [%][c]	0.723	0.716	0.703	0.721	0.709
pyramidal factor[d]	0.300	0.337	0.300	0.327	0.339 0.334
latt. energies [kcal mol^{-1}][e]:					
van der Waals	–23.5826	–18.7798	–16.5686	–15.1612	–13.8491
electrostatic	–16.0236	–16.7818	–14.2359	–10.1065	–9.6844
hydrogen bridge	–8.2482	–7.4019	–6.7081	–5.4784	–5.0034
total energy	–47.8544	–42.9635	–37.5126	–30.7461	–28.5369

a) The angle between the C–O and C–N vectors have been calculated using *RPluto*. b) The angle between two adjacent aromatic ring planes have been calculated using *RPluto*. c) C_k*, packing co-efficient calculated with *PLATON*. d) The perpendicular distance from the basal plane to the apex of the pyramid. e) Lattice energies calculated using *Cerius*^{2} from Accelrys.

Firstly, the geometry of the molecule shows that it has had to distort to obtain as large a C–O : C–N vector angle as possible; while the angle at the oxygen atom (C–O–C) is 120° as expected (for CSD search, see experimental section), the C–O,

C–N vector angle is 141° (Table 1), which is much larger than the corresponding angle seen in any of the infinite chains or square motif structures. To achieve this large C–O, C–N vector angle the whole molecule is considerably bent (Figure 4). The O-atom is shifted about 0.2Å out of the plane of each of the phenyl rings. The NH_2 and OH groups are also bent out of the plane of their respective phenyl rings but to a lesser extent (0.1 and 0.06Å respectively).

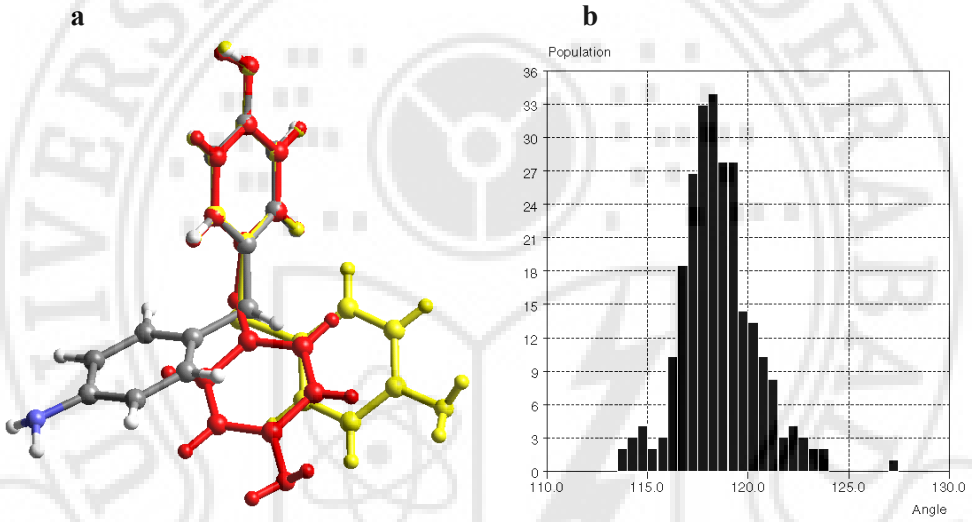

Figure 2. (a) Overlay diagram of aminol **1b** on aminols **1** and **1a**. Note the conformational flexibilities of **1b**, **1** and **1a**. (b) Histogram of C–O–C angle.

Secondly, the volume of the O-atom is much less than that of the $–CH_2–$ group or the S-atom (11Å^3 compared to 19.1Å^3 and 22.8Å^3 respectively) and this allows the molecules to fit closer together. Further, while the molecules can pack better than would be possible for the S or CH_2 substituted structures, they cannot pack as closely as the more linear molecules that form β-As sheet structures. This gives rise to an elongation of the two N–H···O hydrogen bridges (and therefore the *b* axis)

to 2.3Å and 2.4Å, compared with an average value of 2.2Å and 2.3Å for the other β-As sheet structures.

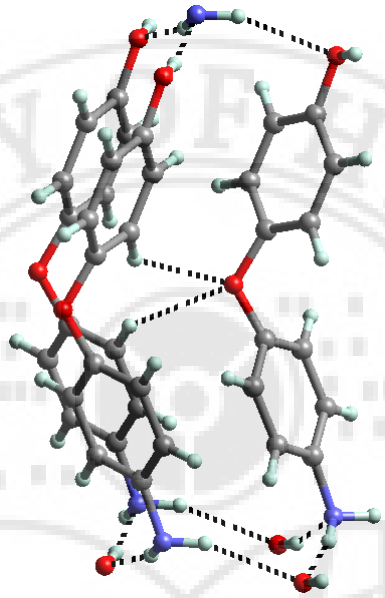

Figure 3. β-As sheet structure of 4-(4-aminophenoxy)phenol **1b**.

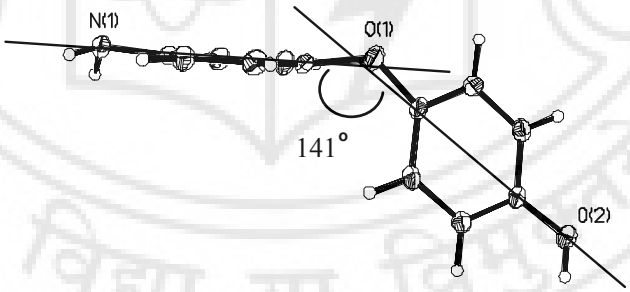

Figure 4. The flexing of **1b** to achieve a large C–O, C–N vector angle. Note that phenolic end of the molecule is also bent to a similar degree.

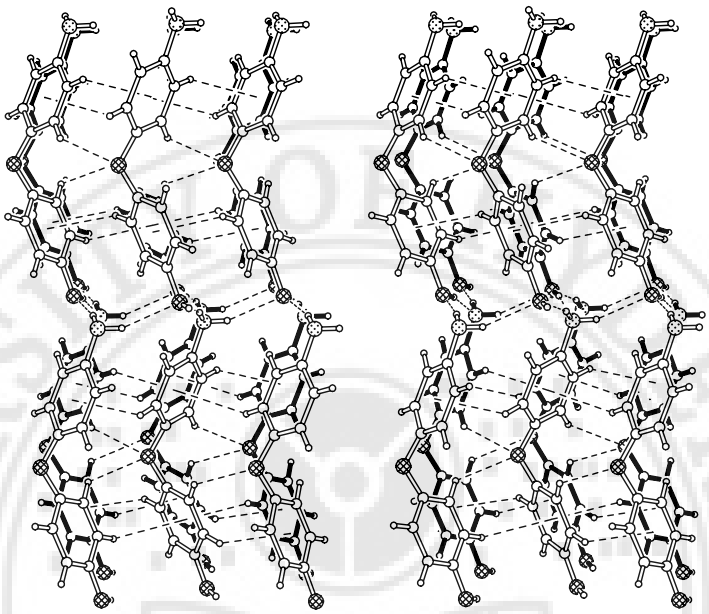

Figure 5. Stereoview of the overall crystal packing in **1b**. Notice the bifurcated C–H···O and also C–H···π interactions.

Finally, the greater electronegativity of the O-atom relative to –S– and $–CH_2–$ increases the donor ability of the adjacent phenyl hydrogen atoms (for Mulliken charges see Scheme 3 and experimental section). This promotes the formation of bifurcated C–H···O hydrogen bridges [1.21a]. This is an additional factor in pulling adjacent molecules close together and rather than being a consequence of the structure it is more likely to be playing an important role in aligning the molecules so as to achieve the β-As structure (Figures 3 and 5). This illustrates the role of chemical influences. For example, if molecules of aminol **1** were aligned in the same way there would be repulsion between the methylene H- and aromatic H-atoms. The structure is further stabilized by herringbone interactions (Figure 5 and Table 1).

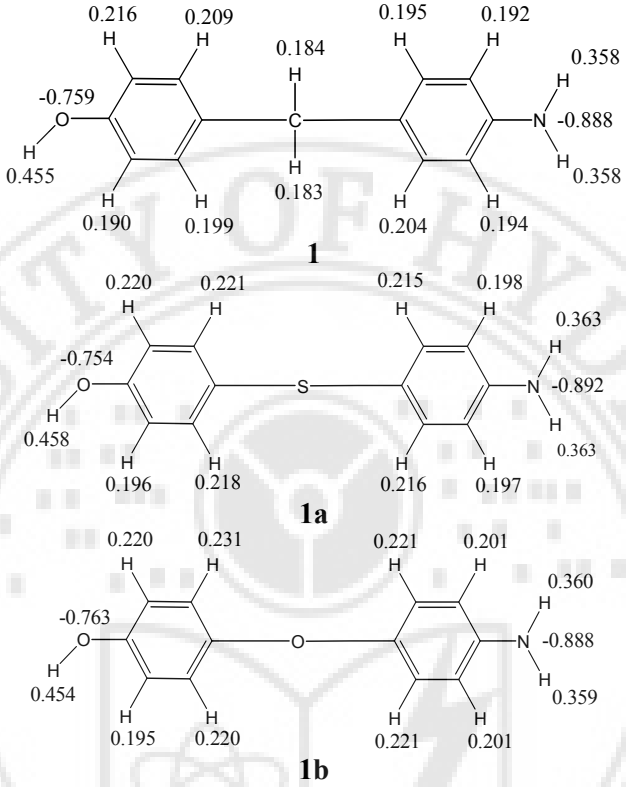

Scheme 3. Note that in **1b**, the phenyl hydrogens adjacent to linker O-atom are activated.

When chemical factors within the odd series are considered the structures can be seen to tend towards the β-As sheet as the electronegativity increases. By replacement of $-CH_2-$ by an S-atom *i.e.*, a slight increase in electronegativity, compound **1a** takes a square motif with additional C–H···S hydrogen bridges that change the motif to a windmill arrangement. This suggests that **1b** (with a greater increase in electronegativity) could take either a structure similar to **1a** or an infinite chain type structure. But interestingly, **1b** exceeded the predictions in achieving the target structure *i.e.*, a β-As sheet structure in even within the n = odd series. It is a

matter of speculation whether extensions of the series **1** to **5** with n = 7, 9 would adopt the β-As sheet structure.

Table 2. Pertinent hydrogen bridges for the compounds in this study.

Aminol	H-bridge	d (Å)[a]	D (Å)	θ (deg)
2d	O–H···N	1.84	2.819(4)	170.1
	N–H···O	2.12	3.125(4)	170.6
	N–H···O	2.26	3.253(4)	165.9
1b	O–H···N	1.84	2.8008(19)	163.8
	N–H···O	2.26	3.1991(16)	153.3
	N–H···O	2.34	3.3271(19)	164.7
	C–H···π	2.68	3.565	138.5
	C–H···π	2.71	3.612	139.5
	C–H···π	2.74	3.631	139.0
	C–H···π	2.77	3.654	138.5
6a	O–H···N	1.73	2.701(2)	166.0
	N–H···O	2.05	3.017(2)	160.6
	N–H···π	2.51	3.359	141.8
	C–H···O	2.43	3.230(2)	129.9
	C–H···π	2.52	3.494	149.1
	C–H···π	2.80	3.736	144.5
6b	O–H···N	1.78	2.7547(19)	167.5
	N–H···O	2.08	3.0194(19)	152.3
	N–H···O	2.16	3.0944(18)	151.9
6c	O–H···N	1.75	2.725(2)	167.5
	O–H···N	1.82	2.804(2)	173.4
	N–H···O	2.01	2.970(2)	157.6
	N–H···O	2.15	3.088(2)	154.8
	N–H···O	2.18	3.113(3)	152.9
	N–H···O	2.28	3.123(3)	139.7

[a] O–H, N–H and C–H distances are neutron normalized to 0.983, 1.009 and 1.083 Å.

5.5 Effect of molecular shape to give the infinite chain

Kitaigorodskii's close-packing principle [1.15] states that mutual recognition between molecular shapes is the key element in understanding the packing of

molecular crystals. Given that 4-(3-aminophenyl)phenol, **6a**, has nearly the same shape as **3**, especially with respect to the all-important –OH and $-NH_2$ groups, it is predicted that the crystal structure would contain the infinite chain motif. This prediction was borne out in practice.

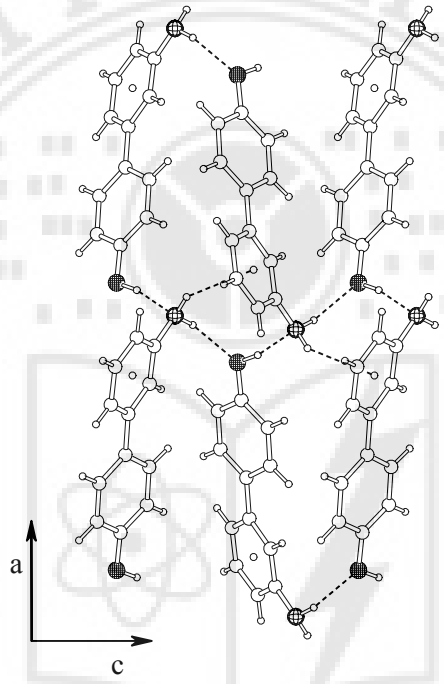

Figure 6. The Infinite chain motif in 4-(3-aminophenyl) phenol **6a**.

Aminol **6a** has a molecular geometry comparable with that of 3AP and **3**. The angle between the C–O and C–N vectors is 121° compared to 121° for 3AP and 124° for **3**. The value of Π for **6a** in relation to **3** is 0.15. The crystal packing motif is identical and it is only the molecular length that varies. This is reflected in the change in length of *a*-axis (Figure 6). The N–H···π bridge is slightly weaker than that seen for **3** (Table 2) [4.7]. It is apparent that controlled variation of the substituent groups

present on an organic molecule may allow subsequent crystallization into particular and desired packing arrangements.

The infinite chain in **6a** takes the form of a zigzag chain of N(H)O hydrogen bridges. This is projected on to both the *ac* and *bc* planes of the crystal lattice (Figure 7). The infinite chain of aminol **6a** is comparable to that of 3AP and aminol **3**.

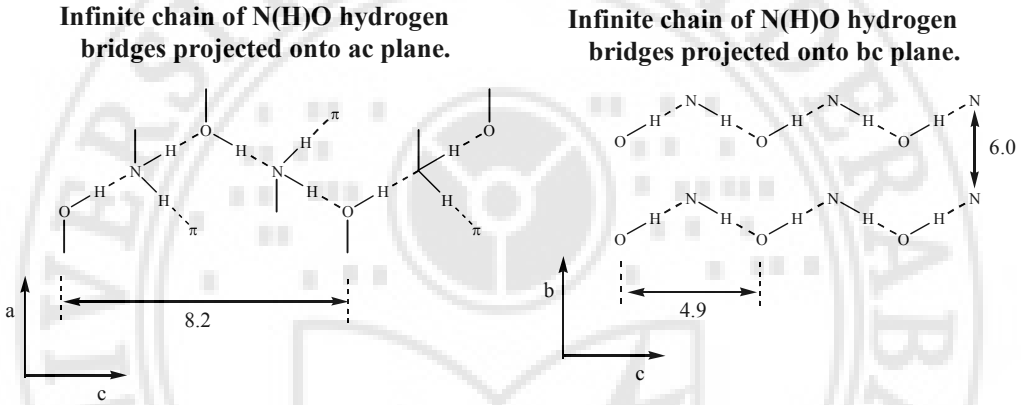

Figure 7. Schematic of the N(H)O infinite chain in **6a**.

5.6 A novel saturated hydrogen bridge (SHB) pattern in supraminols

In the exploration of supraminols, a very interesting and novel SHB architecture which has not been reported previously was found. Aminols 3-[(E)-2-(4-aminophenyl)-1-ethenyl]phenol, **6b**, and 3-(4-aminophenethyl)phenol, **6c**, were predicted to form the infinite chain $\cdots(N\text{–}H\cdots O\text{–}H\cdots)_n$ structure seen in 3AP and elsewhere [1.29] as the C–O, C–N vector angle is nearly 120° (Table 1). However, the structures of **6b** and **6c** are very different (Figure 8) from those seen in other aminols. In **6b** the angle between phenyl planes is 52.8°, and in **6c** it is 62.3° and 66°, compared to 12.3° for **6a**. The molecules of **6b** form centrosymmetric O–H···N dimers (1.78Å, 167.5°), which are further connected through N–H···O bridges (2.08Å, 152.3°) at the amine and hydroxy sites leading to a sheet structure *via* infinite N(H)O

networking. These sheets further stack along the *a*-axis so that adjacent N(H)O infinite chains are cross-linked with N–H···O bridges (2.16Å, 151.9°) to give a SHB tube organization.

It would be expected that **6b** and **6c** would be isostructural, and it has been previously noted that the exchange of an ethylene bridge for an ethane bridge is not predicted to have an effect on the molecular packing. In fact, **6b** crystallizes in the space group *Pccn*, while **6c** solves in the related but lower symmetry space group $Pna2_1$ (Z'=2) [5.6]. The structure of **6c** is pseudosymmetric to that of **6b**. However, the unit cell dimensions are similar, with an isostructurality parameter Π of 0.0069 and the molecular arrangements within the crystals are nearly identical.

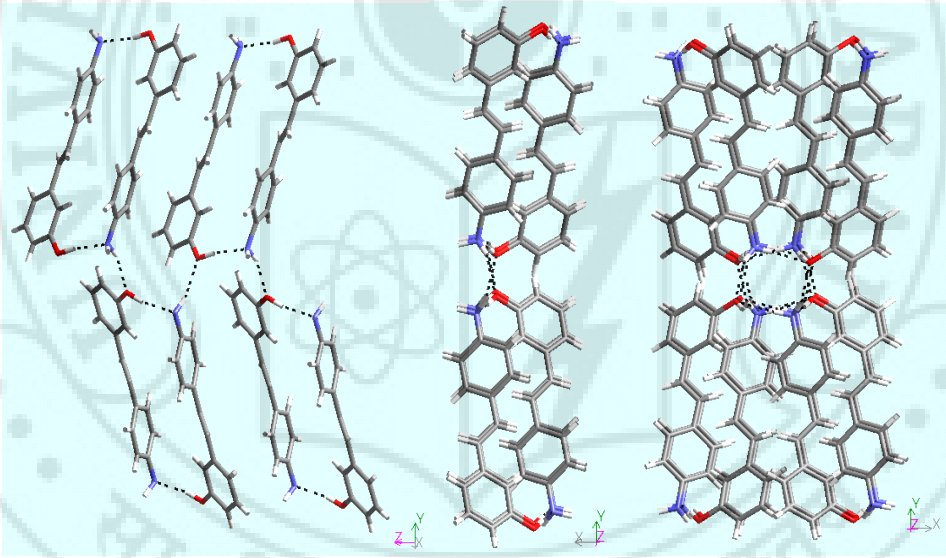

a **b** **c**

Figure 8. 3-[(E)-2-(4-aminophenyl)-1-ethenyl]phenol **6b**, (a) showing the infinite chain, (b) stacking viewed down *c*-axis, and (c) these adjacent infinite chains cross-link through N–H···O to form SHB tube. Note that the crystal structure of 3-(4-aminophenethyl)phenol, **6c** is identical.

Notably, these structures can be considered as a narrow ribbon section of the β-As sheet that has been rolled up to form a tube. In the β-As sheet two infinite

chains with sawtooth geometry are connected to form either O–H···N or N–H···O hydrogen bridges (Scheme 2). Here, the tube is completed with a saturation of the N(H)O interactions. However, this analogy to the β-As sheet is only partly valid because in the β-As sheet the molecules lie above and below the sheet. In the tube structures of aminols **6b** and **6c** molecules must radiate from only one surface (the outside) of the tube but in terms of hydrogen bond valence the system is N(H)O saturated like the β-As sheet.

Considering the column from end on it can be seen that the cross-linked chains are effectively generate twisted square motifs that stack to form the tube (Figure 9). These square motifs are constructed from N–H···O hydrogen bridges only (rather than N–H···O–H···N), with the hydroxy hydrogen atoms linking each square motif to the one below. In Hanessian's structures the same interactions are found but one OH group links to a square motif below, while the other links to one above, to form a helical ladder structure. In this way structures of **6b** and **6c** can be considered as containing elements of all three major synthons in this family (square motif, infinite chain and β-As sheet) [4.7].

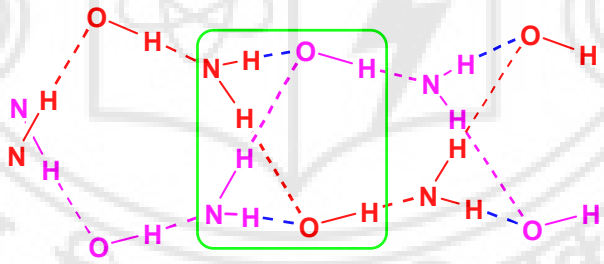

Figure 9. Schematic of two infinite chains (offset dimers colour coded as red and pink) running in a zig-zag manner viewed down the *a*-axis. These two infinite chains are cross-linked *via* N–H···O interactions (blue) to form 1D SHB tube. Notice that the two OH groups in the square motif (green) project towards the same side.

5.6.1 Topological similarities of organic and inorganic crystal structures

The analogy between inorganic and organic crystal structures facilitates the understanding of complex organic supramolecular systems [5.5]. The hydrogen bridge pattern in **6b** and **6c** is topologically the same as that of the anion network in the rare zeolite variant narsarsukite $Na_4(TiO)_2(Si_8O_{20})$ [5.7]. This rare network topology is not even mentioned in Wells' compilation [5.4]. Figure 10 shows the SHB tube structure in aminols **6b** and **6c** (**D**), the topology of Si-atoms in narsarsukite (**E**) and the SiO_4 tetrahedra-based structure of the zeolite (**F**). Peacor and Buerger [5.7a] reported the crystal structure of narsarsukite in 1962 and stated that it is based on a new arrangement of Si-tetrahedra. The structure can be described as being made up of tubes having composition Si_4O_{10} parallel to the *c*-axis and bonded by Ti-octahedra. The Na-atoms occupy voids running between the tubes and chains and have an irregular co-ordination of O-atoms. The most important feature of the network is a multiple chain of linked silicon tetrahedra parallel to the *c* axis of a type unknown except in narsarsukite. It can also be analyzed as a sequence of rings of 4 tetrahedra, linked together to form a tube. It is also useful to note that the tube can be formed by rolling up a hexagonal sheet of composition Si_4O_{10} of the type that occurs in the phyllosilicates. Similarly, the tube of N(H)O interactions in aminols **6b** and **6c** is formed in exactly the same way by 'rolling up a hexagonal sheet' of composition N(H)O of the type that occurs in the β-As supraminols.

The formation of topologically identical and rare networks in compounds that belong to entirely differing domains shows the universality of close-packing [5.8]. While the network arrangement in a crystal may be rationalized in terms of the constituent interactions, entirely different interaction types may lead to the same network. In other words, the network structure of a crystal is a higher-level property and the description of any crystal structure as a network is more likely to bring out similarities and differences between it and other crystal structures.

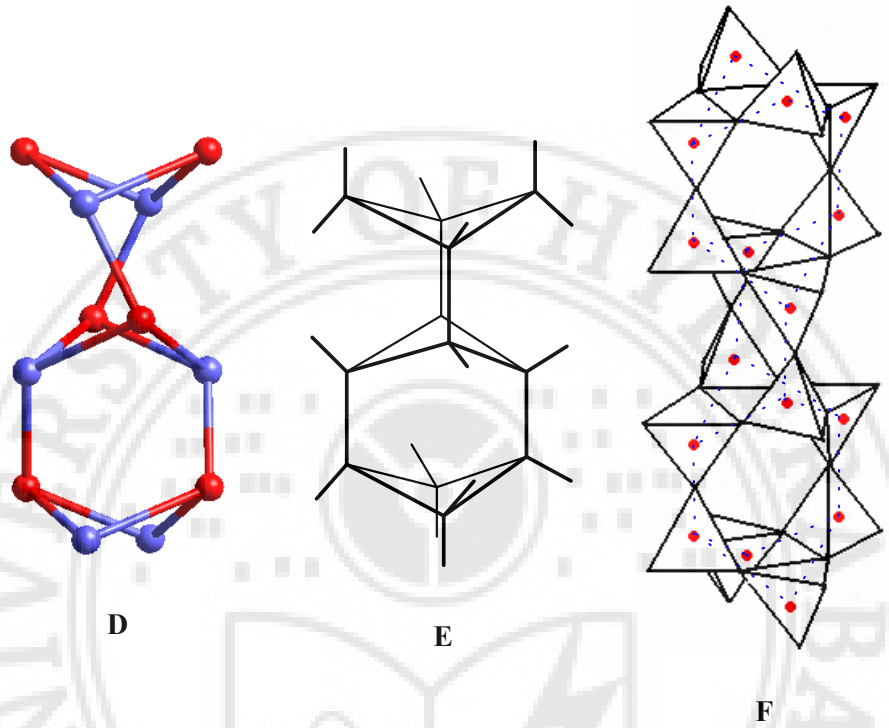

Figure 10. (**D**) SHB tube in **6b** and **6c**. (**E**) Anion network in narsarsukite. The nodes are Si-atoms. **(F)** Anion network showing also SiO_4 tetrahedra.

5.7 Conclusions

Scheme 4 summarises the structural features in this family of compounds. A partial success has been achieved in the prediction of structural motifs of these aminols. The structures of two of the five compounds studied with crystal engineering considerations in mind (**2d**, **6a**) could be anticipated reasonably well. That the structure of **1b** could not be predicted is not particularly disappointing and the observed structure actually provides more useful information. Aminol **1b** illustrates the geometric limits to which the β-As sheet structure can be pushed and a stable structure still obtained, and demonstrates that molecular linearity is *not* a prerequisite

for β-As sheet adoption. The lattice energy calculations (Table 1) [2.8] indicate that **1b** is slightly less stable than the other β-As sheet structures, but more stable than the square motif and infinite chain structures. In all the supraminols discussed in this study the N atoms of the anilino functionality are distinctly pyramidal (Table 1) [2.10]. NIPMAT plots and simulated powder spectra for **2** and **2d**; 3AP, **3** and **6a**; **6b** and **6c** show the near identity of crystal packing [3.8].

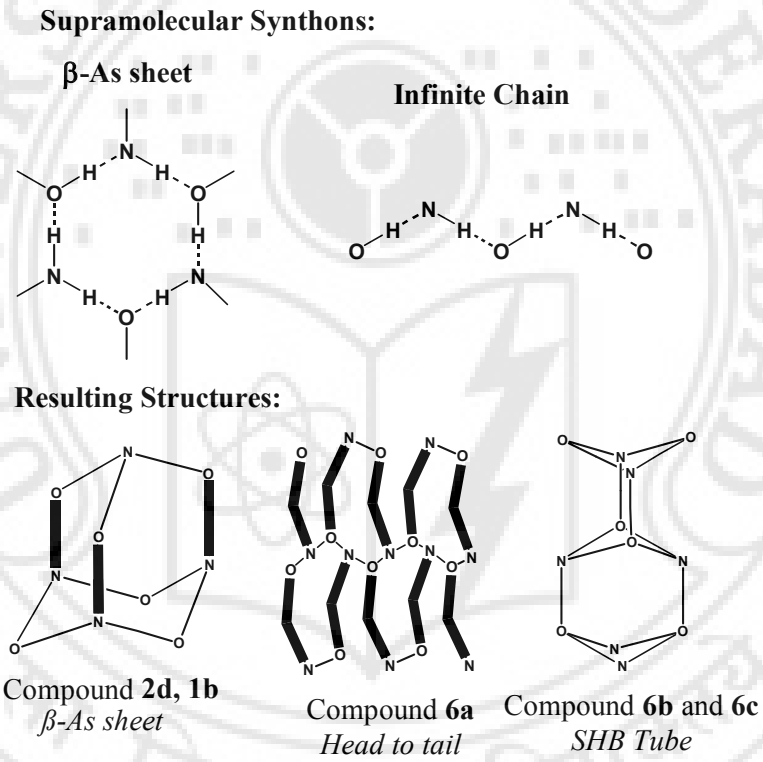

Scheme 4. β-As sheet and infinite chain synthons. N—O represents the N(H)O hydrogen bridge. Thick lines represent the hydrocarbon fragment of the molecule.

In compounds **6b** and **6c**, the modularity of this structural system fails. It is interesting to note that while the structure is at first glance very different to the other structures discussed in the supraminols it can be described using all three of the

synthons simultaneously, synthons that individually describe the structures of all the other compounds in this thesis. This demonstrates that it is the supramolecular synthons, the kinetically favoured fragments, that are the real kernel of a crystal structure [1.17]. Also, the structure is not unprecedented it is closely related to the topology of narsarsukite, and as such, may lead eventually to a comprehensive structural model that will explain not like the types of extended aminophenols discussed elsewhere, but all (simple) compounds and co-crystals that contain both amino and hydroxy moieties in equal proportions.

It is noteworthy that a good level of understanding has now been obtained of these supraminol systems. The infinite chain is the key synthon in this family.
From this work the following can be examined:
1) From a study of the 4-amino-3-hydroxy- analogues of **6a** it would be interesting to verify whether these compounds crystallize with the infinite chain motif.
2) The crystal structure of **1b** can be further studied by incorporating the sterically bulky groups to examine the β-As sheet.

The correspondences between molecular and crystal structure now having been understood in this group of compounds, it can be concluded that aminophenols are amenable to the principles of crystal engineering.

5.8 Experimental section

Synthetic procedures

General methods. All other melting points were recorded on a Fisher-Johns melting point apparatus and are uncorrected. ^{1}H NMR (200 MHz) was recorded in DMSO-d_6 on a Bruker-AC-200 spectrometer. All reactions were carried out using standard techniques and general literature procedures. The synthesis of the aminophenols in this study are given, whenever there is a considerable variation from the literature procedures.

4-[(E)-2-(4-Aminophenyl)-1-ethenyl]phenol, 2d

To 4-nitrophenylacetic acid (1.81 g, 10 mmol), piperidine (850 mg, 10 mmol) was added dropwise, then 4-hydroxybenzaldehyde (1.22 g, 10 mmol) and the mixture heated at 100 °C under vacuo for 1h, then for an additional 2 h at 150 °C. This mixture was taken in 30% NaOH solution and heated on a water bath, then neutralised with conc. HCl, to give a yellow precipitate (90%) of 4,4'-hydroxynitrostilbene [5.9a]. This was reduced with $SnCl_2.2H_2O$, as in **2a** (c.f. Chapter 3), to produce **2d** in 17% yield, mp 270 °C. IR (cm^{-1}): 3356, 3292, 3015. ^1H NMR: δ 5.18 (s, 2H), 6.52 (d, J 8, 2H), 6.75 (d, J 8, 2H), 6.81 (s, 2H), 7.2 (d, J 8, 2H), 7.32 (d, J 8, 2H), 9.40 (s, 1H).

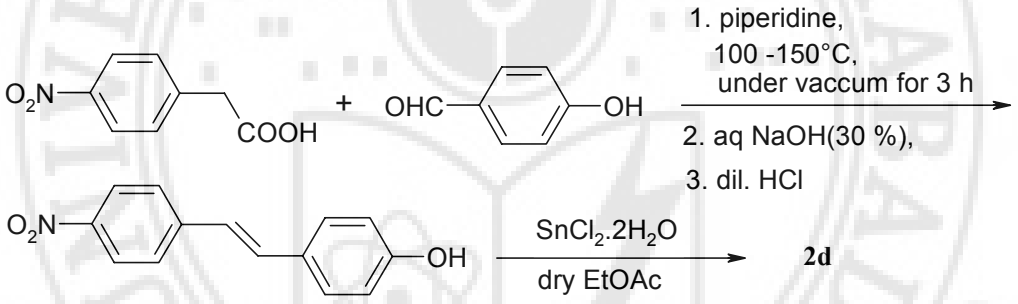

4-(4-Aminophenoxy)phenol, 1b

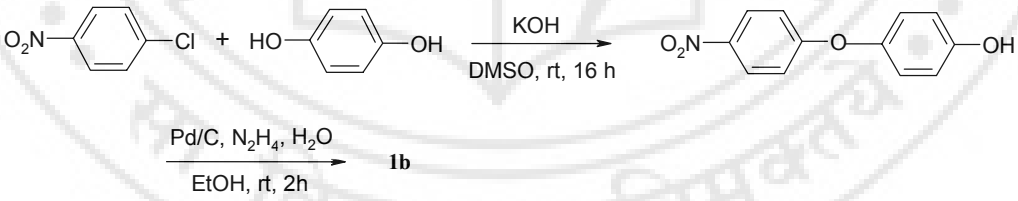

To a degassed solution of hydroquinone (270 mg, 2.5 mmol) in DMSO, KOH (56 mg, 10 mmol), 4-chloronitrobenzene (392 mg, 2.5 mmol) was added, and refluxed for 16 h [5.9b]. Workup yielded 400 mg (70%) of 4,4'-hydroxynitrodiphenylether. To this compound (250 mg, 1.08 mmol) 10 mL of EtOH,

$N_2H_4.H_2O$ (0.26 ml, 5.4 mmol), Pd/C were added and stirred at room temperature for 1 h. The reaction mixture was filtered off and evaporated to yield 152 mg (70%) of **1b**, mp 157 °C. IR (cm^{-1}): 3368, 3304, 1874. ^{1}H NMR: δ 4.85 (s, 2H), 6.5 (d, J8, 2H), 6.7 (m, 6H), 9.00 (s, 1H).

4-(3-Aminophenyl)phenol, 6a

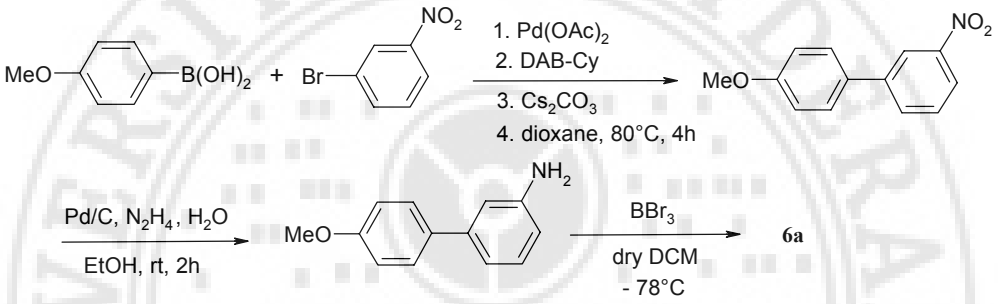

A solution of 4-methoxyboronic acid (200 mg, 1.31 mmol), 3-nitrobromobenzene (246 mg, 1.22 mmol), $Pd(OAc)_2$ (3% mol), DAB-Cy (3% mol) and Cs_2CO_3 (2 equiv) in dioxane (3 mL) was refluxed for 4 h under inert conditions as in the modified Suzuki-Miyaura cross-coupling [5.9c]. Workup afforded 241 mg (80%) of 4-methoxy-3'-nitrobiphenyl. To this compound (250 mg, 1.09 mmol) were added 10 mL of EtOH and $N_2H_4.H_2O$ (0.35 mL, 8.89 mmol) and stirred for 2 h at room temperature as for **1b**. The reaction mixture was filtered off and evaporated to yield 152 mg (70%) of 4,3'-methoxyaminobiphenyl. Methoxy deprotection as in **2** (c.f. Chapter 2) gave 50 mg (40%) of **6a**, mp 183 °C. IR (cm^{-1}): 3398, 3317, 3202. ^{1}H NMR: δ 5.1 (s, 2H), 6.49 (d, J 8, 1H), 6.66 (d, J 8, 1H), 6.72 (s, 1H), 6.78 (d, J 8, 2H), 7.03 (t, J 8, 1H), 7.34 (d, J 8, 2H), 9.43 (s, 1H).

3-[(E)-2-(4-Aminophenyl)-1-ethenyl]phenol, 6b

Aminol **6b** was prepared as described in **2d** but with 3-hydroxybenzaldehyde to yield (62.2%) of 3,4'-hydroxynitrostilbene. This was reduced with $SnCl_2.2H_2O$ as

in **2a** (c.f. Chapter 3) to afford **6b** in 26.5% yield, mp 202 °C. IR (cm^{-1}): 3356, 3290, 3020. ^1H NMR: δ 5.28 (s, 2H), 6.53 (d, J 8, 2H), 6.57 (d, J 8, 1H), 6.75 (d, J 8, 1H), 6.92 (m, 3H), 7.1 (t, J 8, 1H), 7.26 (d, J 9, 2H), 9.38 (s, 1H).

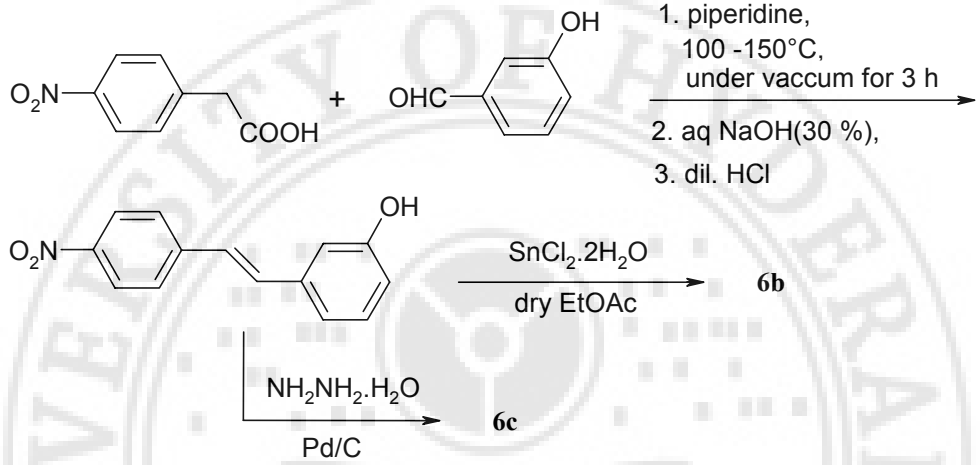

3-(4-Aminophenethyl)phenol, 6c

To a solution of 3,4'-hydroxynitrostilbene (241 mg, 1 mmol) in EtOH (10 mL), Pd/C and $N_2H_4.H_2O$ (0.7 mL, 14 mmol) were added and the mixture refluxed for 3 h, filtered and evaporated, as in **2** (c.f. Chapter 2), to yield 50 mg (23.5%) of **6c**, mp 143 °C. IR (cm^{-1}): 3373, 3292, 2926. ^1H NMR: δ 2.66 (s, 4H), 4.80 (s, 2H), 6.44 (d, J 8, 2H), 6.55 (m, 3H), 6.83 (d, J 8, 2H), 7.00 (t, J 9, 1H), 9.18 (s, 1H).

Crystallization

Diffraction quality single crystals were achieved by recrystallizing the aminols **2d** and **1b** from EtOH, **6a** with 1:1 EtOAc/CH_3CN and for **6b** and **6c**, 1:1 EtOAc/CH_3NO_2 was used.

X-ray crystallography

The X-ray data were collected at the University of Durham, U.K. by Dr. C.K. Broder and Mr. P.S. Smith under the supervision of Prof. J.A.K. Howard. The X-ray diffraction were carried out on a Bruker SMART–6000 diffractometer (**2d**, **6a, 6b** and **6c**) or the Bruker SMART–1000 diffractometer (**1b**) using Mo K_α radiation (λ = 0.71073 Å). The structure solution and refinements were carried out using SHELXTL (Version 5.1) programs [2.12]. In all cases the hydroxy and amine hydrogen atoms were located in difference Fourier maps and refined isotropically. The other hydrogen atoms were either fixed in geometrically sensible positions (compounds **1b**, **7a** and **7b**), or located in difference Fourier maps (compounds **2d** and **6a**) and refined isotropically. All the intermolecular interactions and related calculations were carried out with PLATON 2002 [2.13] on Silicon Graphics Octane2 workstation (Table 2). The relevant crystallographic information is given in the appendix.

Database analysis

Refcodes for SHB patterns

(a) β-As sheet: AMPHOL01, HIBFUT, NISMAD, PITYAS, PITYEW, PITYIA, PITYOG, PITZAT, SARDAQ, SARDIY, SARDOE, SARJUQ, ZAPFAX, ZAPFEB and also 6 β-As structures reported in this thesis (for compounds **2**, **4**, **2a**, **2b**, **2d** and **1b**)

(b) Black phosphorus (black-P) sheet: JAKKEL

(c) SHB ladder: GUCQUQ, GUCREB, GUCRIF, HYDETH, ZAVXAV.

(d) SHB ladder in unsaturated supraminols include: PIWXOI, PIWXUO.

A CSD search on C–O–C and C–C–C

A search of the CSD (Version 5.23, April 2002) for error free Ar–O–Ar organic, aromatic, acyclic, non-ionic, non polymeric structures with R<0.075.

Disordered, 'no co-ordinates present' structures were excluded from the search. Of the 418 entries in the subset, 4 hits with corresponding C–O–C were found. Of these only one pair (CAKGOK, GUHKUP) was found that is isostructural, while non-isostructural pairs include NPXMBZ10, CBYMBZ; CUCVER, CEHCOH; XILQOY, XILRAL.

CSD search on C–O–C angle

A search of the CSD (Version 5.23, November 2002) for error free C–O–C organic, aromatic, acyclic, non-ionic, non polymeric structures with $R < 0.10$ was performed. No disorder, 3-D co-ordinates and have chemical/crystallographic connectivities which match, were accepted. The average Ar–O–Ar angle was found to be 118–120°. Diaryl ether compounds are relatively less, with only a total of 168 entries in the CSD.

Restricted Hartree Fock (RHF) computation of charge

The Mulliken charge of aminols **1b**, **1** and **1a** were calculated in Restricted Hartree Fock (RHF) with 6-31G* basis set using Spartan program [5.10]. It is evident that the electronegative O-acceptor (more basic—linker between the phenyl rings) and the activated phenyl C–H donors (more acidic—ones adjacent to the linker) promote the formation of bifurcated C–H···O hydrogen bridges.

REFERENCES AND NOTES

CHAPTER ONE

[1.1] (a) G.M.J. Schmidt, *Pure Appl. Chem*., **1971**, *27*, 647. (b) *Organic Solid State Chemistry*, Ed., G.R. Desiraju, *Studies in Organic Chemistry* 32, Elsevier, Amsterdam, **1987**.

[1.2] G.R. Desiraju, *Crystal Engineering. The Design of Organic Solids*; Elsevier: Amsterdam, **1989**.

[1.3] Selected references on crystal engineering of organic molecular solids include: (a) *The Crystal as a Supramolecular Entity*. Perspectives in Supramolecular Chemistry, Vol. 2; G.R. Desiraju, Ed.; Wiley, Chichester, **1996**. (b) *Comprehensive Supramolecular Chemistry*; J.L. Atwood, J.E.D. Davies, D.D. MacNicol and F. Vögtle, Eds.; Pergamon: Oxford, Vols. 6, 7, 9, 10, **1996**. (c) C.B. Aakeröy, *Acta Crystallogr*., **1997**, *B53*, 569. (d) *Design of Organic Solids*; E. Weber, Ed.; *Topics in Current Chemistry*; Springer: Berlin, Vol. 198, **1998**. (e) *Crystal Engineering: From Molecules and Crystals To Materials*; D. Braga and A.G. Orpen, Eds.; NATO ASI Series Kluwer: Dordrecht, Netherlands, **1999**. (f) *Crystal Engineering: The Design and Application of Functional Solids*; K.R. Seddon and M.J. Zaworotko, Eds.; NATO ASI Series Kluwer: Dordecht, Netherlands, **1999**. (g) J.W. Steed and J.L. Atwood, *Supramolecular Chemistry*, Wiley, Chichester, **2000**, *11*, pp. 389–463. (h) G.R. Desiraju, *Curr. Sci.,* **2001***, 81,* 1038. (i) C.V.K. Sharma, *Cryst. Growth Des.,* **2002**, *2*, 465. (j) M.D. Hollingsworth, *Science*, **2002**, *295*, 2410. (k) *Crystal Design. Structure and Function.* Perspectives in Supramolecular Chemistry*,* Vol. 7; G.R. Desiraju, Ed.; Wiley, Chichester, **2003**. (l) B. Kahr, *Cryst. Growth Des.,* **2004**, *4*, 3.

[1.4] (a) J.-M. Lehn, *Angew. Chem., Int. Ed.*, **1990**, *29*, 1304. (b) J.-M. Lehn, *Supramolecular Chemistry: Concepts and Perspectives*, VCH, Weinheim, **1995**. (c) D.N. Reinhoudt and M. Crego-Calama, *Science*, **2002**, *295*, 2403.

[1.5] G.R. Desiraju, *Nature (London)*, **2001**, *412*, 397.

[1.6] That observed crystal structures cannot be predicted so easily is revealed in the difficulties encountered in crystal structure prediction. See (a) A. Gavezzotti, *Acc. Chem. Res.,* **1994**, *27*, 309. (b) T. Beyer, T. Lewis and S.L. Price, *CrystEngComm*, **2001**, *3*, 178. (c) G.R. Desiraju, *Nature Materials,* **2002**, *1*, 77. (d) J.D. Dunitz, *Chem. Commun.,* **2003**, 545.

[1.7] L. Pauling and M. Delbrück, *Science*, **1940**, *92*, 77.

[1.8] (a) K.C. Nicolaou, D. Vourloumis, N. Wissinger and P.S. Baran, *Angew. Chem. Int. Ed.*, **2000**, *39*, 44. (b) K.C. Nicolaou and E.J. Sorenson, *Classics in Total Synthesis*, Wiley-VCH, Weinheim, **1996**.

[1.9] J.D. Dunitz, *Pure Appl. Chem*., **1991**, *63*, 177.

[1.10] (a) D. Braga, F. Grepioni and G.R. Desiraju, *Chem. Rev*., **1998**, *98*, 1375. (b) D. Braga and F. Grepioni, *Acc. Chem. Res*., **2000**, *33*, 601.

[1.11] (a) T.L. Threllfall, *Analyst*, **1995**, *120*, 2435. (b) J.A.R.P. Sarma and G.R. Desiraju, *Crystal Engineering*: *The Design and Application of Functional Solids*; Eds., M.J. Zaworotko and K.R. Seddon, Kluwer: Dordrecht, **1999**, 325. (c) J. Bernstein, R.J. Davey and J.-O. Henck, *Angew. Chem*., *Int. Ed*., **1999**, *38*, 3440. (d) V.S.S. Kumar, S.S. Kuduva and G.R. Desiraju, *J. Chem. Soc., Perkin Trans. 2*, **1999**, 1069. (e) J. Bernstein, *Polymorphism in Molecular Crystals*, Clarendon Press, Oxford, **2002**. (f) V.S.S. Kumar, A. Addlagatta, A. Nangia, W.T. Robinson, C.K. Broder, R. Mondal, I.R. Evans, J.A.K. Howard and F.H. Allen, *Angew. Chem*., *Int. Ed*., **2002**, *41*, 3848. (g) R.K.R. Jetti, R. Boese, J.A.R.P. Sarma, L.S. Reddy and G. R. Desiraju, *Angew Chem. Int. Ed.,* **2003**, *42*, 1963. (h) R.J. Davey, *Chem.*

Commun., **2003**, 1463. (i) L. Yu, *J. Am. Chem. Soc*., **2003**, *125*, 6380. (j) P.K. Thallapally, R.K.R. Jetti, A. Katz, H.L. Carrell, K. Singh, K. Lahiri, S. Kotha, R. Boese and G.R. Desiraju, *Angew. Chem., Int. Ed*., **2004**, *43*, 1149.

[1.12] (a) J. Zyss and J.-F. Nicoud, *Curr. Opin. Solid State Mater. Sci*., **1996**, *1*, 533. (b) C.F.V. Nostrum and R.J.M. Notle, *Chem. Commun*., **1996**, 2385. (c) O. Kahn, *Curr. Opin. Solid State Mater. Sci*., **1996**, *1*, 547. (d) N. Bowden, A. Rerfort, J. Carbeck and G.M. Whitesides, *Science*, **1997**, *276*, 233. (e) T.J. Barton, L.M. Bull, W.G. Klemperer, D.A. Loy, B. McEnaney, M. Misono, P.A. Monson, G. Pez, G.W. Scherer, J.C. Vartuli and O.M. Yaghi, *Chem. Mater*., **1999**, *11*, 2633. (f) P.J. Langley and J. Hulliger, *Chem. Soc. Rev*., **1999**, *28*, 279. (g) M.J. Zaworotko, *Angew. Chem*., *Int. Ed*., **2000**, *39*, 220. (h) K.T. Holman, A.M. Pivovar, J.A. Swift and M.D. Ward, *Acc. Chem. Res*., **2001**, *34*, 107.

[1.13] (a) G. Klebe, *J. Mol. Biol*., **1994**, *237*, 212. (b) S. Sarkhel and G.R. Desiraju, *Proteins*, **2003**, *3*, 675.

[1.14] J.M. Robertson, *Proc. R. Soc. London*, **1951**, *A207*, 101.

[1.15] A.I. Kitaigorodskii, *Molecular Crystals and Molecules*; Academic, New York, **1973**.

[1.16] G.R. Desiraju and A. Gavezzotti, *J. Chem. Soc., Chem. Commun*., **1989**, 621.

[1.17] (a) G.R. Desiraju, *Angew. Chem., Int. Ed. Engl.,* **1995**, *34*, 2311. (b) A. Nangia and G.R. Desiraju, *Topics in Current Chemistry*, **1998**, *198*, 57.

[1.18] (a) G.M. Whitesides, E.E. Simanek, J.P. Mathias, C.T. Seto, D.N. Chin, M. Mammen and D.M. Gordon, *Acc. Chem. Res*., **1995**, *28*, 37. (b) M.C.T. Fyfe and J.F. Stoddart, *Acc. Chem. Res*., **1997**, *30*, 393.

[1.19] (a) F.H. Allen and O. Kennard, *Chem. Des. Automat. News,* **1993**, *8*, 31. (b) F.H. Allen, W.D.S. Motherwell, P.R. Raithby, G.P. Shields and R. Taylor,

New J. Chem., **1999**, *23*, 25. (c) F.H. Allen, *Acta Crystallogr.*, **2002**, *B58*, 380. (d) A. Nangia, *CrystEngComm*, **2002**, *4*, 93.

[1.20] (a) G.A. Jeffrey, *An Introduction to Hydrogen Bonding*, Oxford University Press, Oxford, **1997**. (b) G.A. Jeffrey and W. Saenger, *Hydrogen Bonding in Biological Structures*, Springer, Berlin, **1991**. (c) L. Pauling, *The Nature of the Chemical Bond*, 3rd Ed., Cornell University Press, Ithaca, NY, **1960**.

[1.21] (a) G.R. Desiraju and T. Steiner, *The Weak Hydrogen Bond in Structural Chemistry and Biology*, Oxford University Press, Oxford, **1999**. (b) T. Steiner, *Angew. Chem., Int. Ed.*, **2002**, *41*, 48. (c) V.R. Vangala, G.R. Desiraju, R.K.R. Jetti, D. Bläser and R. Boese, *Acta Crystallogr.*, **2002**, *C58*, 635.

[1.22] (a) O. Navon, J. Bernstein and V. Khodorkovsky, *Angew. Chem., Int. Ed.*, **1997**, *36*, 601. (b) J.M.A. Robinson, D. Philp, K.D.M. Harris and B.M. Kariuki, *New J. Chem.*, **2000**, *24*, 799. (c) Q. Chu, Z. Wang, Q. Huang, C. Yan and S. Zhu, *J. Am. Chem. Soc.*, **2001**, *123*, 11069. (d) R.B. Walsh, C.W. Padgett, P. Metrangolo, G. Resnati, T.W. Hanks and W.T. Pennington, *Cryst. Growth Des.*, **2001**, *1*, 165. (e) E. Bosch and C.L. Branes, *Cryst. Growth Des.*, **2002**, *2*, 299. (f) A. Crihfield, J. Hartwell, D. Phelps, R.B. Walsh, J.L. Harris, J.F. Payne, W.T. Pennington and T.W. Hanks, *Cryst. Growth Des.*, **2003**, *3*, 313.

[1.23] (a) M.L. Huggins, *J. Org. Chem.*, **1936**, *1*, 405. (b) G.R. Desiraju, *Acc. Chem. Res.*, **2002**, *35*, 565.

[1.24] O. Ermer and A. Eling, *J. Chem. Soc., Perkin Trans. 2,* **1994**, 925.

[1.25] (a) S. Hanessian, A. Gomtsyan, M. Simard and S. Roelens, *J. Am. Chem. Soc.,* **1994**, *116*, 4495. (b) S. Hanessian, M. Simard and S. Roelens, *J. Am. Chem. Soc.,* **1995**, *117*, 7630. (c) S. Hanessian, R. Saladino, R. Margarita and M. Simard, *Chem. Eur. J.,* **1999**, *5*, 2169. (d) A. Nangia, *Curr. Sci.*,

2000, 374. (e) S. Hanessian and R. Saladino, in *Crystal Design. Structure and Function*. Perspectives in Supramolecular Chemistry, G.R. Desiraju, Ed.; Wiley, New York, **2003**, *7*, 77.

[1.26] C.J. Brown, *Acta Crystallogr*., **1951**, *4*, 100.

[1.27] (a) R. Liminga and I. Olovsson, *Acta Crystallogr.,* **1951**, *4*, 100. (b) R. Liminga, *Acta Chem. Scand.,* **1967**, *21*, 1206.

[1.28] (a) A. Gavezzotti, *Chem. Phys. Lett.,* **1988**, *161*, 67. (b) P.M. Zorkii and O.N. Zorkaya, *J. Struct. Chem.*, **1995**, *36*, 704. (c) V.R. Vangala, A. Nangia and V.M. Lynch, *Chem. Commun*., **2002**, 1304. (d) E.A. Meyer, R.K. Castellano, and F. Diederich, *Angew. Chem., Int. Ed.,* **2003**, *42*, 1210.

[1.29] F.H. Allen, V.J. Hoy, J.A.K. Howard, V.R. Thalladi, G.R. Desiraju, C.C. Wilson and G.J. McIntyre, *J. Am. Chem. Soc.,* **1997**, *119*, 3477.

[1.30] Previous X-ray crystal structure determinations of 2AP and 3AP include: (a) J.D. Korp, I. Bernal, L. Aven and J.L. Mills, *J. Cryst. Mol. Struct*., **1981**, *11*, 117. (b) C. de Rango, S. Brunie, G. Tsoucaris, J.P. Declercq and G. Germain, *Cryst. Struct. Commun.*, **1974**, *3*, 485.

[1.31] (a) H.S. Rzepa, M.L. Webb, A.M.Z. Slawin and D.J. Williams, *J. Chem. Soc*., *Chem. Commun*., **1991**, 765. (b) L.R. Hanton, C.A. Hunter and D.H. Purvis, *J. Chem. Soc., Chem. Commun.*, **1992**, 1134. (c) M.A. Viswamitra, R. Radhakrishnan, J. Bandekar and G.R. Desiraju, *J. Am. Chem. Soc.,* **1993**, *115*, 4868. (d) T. Steiner, E.B. Starikov, A.M. Amado and J.J.C. Teixeira-Dias, *J. Chem. Soc*., *Perkin. Trans. 2*, **1995**, 1321. (e) J.F. Malone, C.M. Murray, M.H. Charlton, R. Docherty and A.J. Lavery, *J. Chem. Soc*., *Faraday Trans*., **1997**, *93*, 3429. (f) M. Nishio, M. Hirota and Y. Umezawa, *The CH/π Interaction*, Wiley-VCH, New York, **1998**. (g) Z. Ciunik and G.R. Desiraju, *Chem. Commun*., **2001**, 703. (h) A.D. Bond, *Chem Commun*., **2002**, 1664.

[1.32] S. Kashino, M. Tomita and M. Haisa, *Acta Crystallogr.*, **1988**, *C44*, 730.

[1.33] The crystal structure of 4-chloro-2-aminophenol has been determined to a low accuracy (S. Ashfaquzzaman and A.K. Pant, *Acta Crystallogr.*, **1979**, *B35*, 1394) and therefore is not discussed in any further detail.

[1.34] Selected references that describe the structural chemistry of supraminols include: (a) S. Roelens, P. Dapporto and P. Paoli, *Can. J. Chem.,* **2000**, *78*, 723. (b) B. O'Leary, T.R. Splading, G. Ferguson and C. Glidewell, *Acta Crystallogr.,* **2000**, *B56*, 273. (c) P. Dapporto, P. Paoli and S. Roelens, *J. Org. Chem.,* **2001**, *66*, 4930. (d) J. Lewinski, J. Zachara, T. Kopec, B.K. Starawiesky, J. Lipkowski, I. Justyniak and E. Kolodziejczyk, *Eur. J. Inorg. Chem.,* **2001**, *5*, 1123.

[1.35] D. Mootz, D. Brodalla and M. Wiebcke, *Acta Crystallogr.*, **1989**, *C45*, 754.

[1.36] E.A. Meyers and W.N. Lipscomb, *Acta Crystallogr*., **1955**, *C8*, 583.

[1.37] J. Donohue, *Acta Crystallogr*., **1958**, *C11*, 512.

[1.38] (a) F. Toda, S. Hyoda, K. Okada and K. Hirotsu. *J. Chem. Soc. Chem. Commun*., **1995**, 1531.

[1.39] (a) F. Toda, K. Tanaka, T. Hyoda and T.C.W. Mak, *Chem. Lett*., **1988**, 107. (b) I. Goldberg, Z. Stein, A. Kai and F. Toda, *Chem. Lett*., **1987**, 1617.

[1.40] (a) J.H. Loehlin, M.C. Etter, C. Gendreau and E. Cervasio, *Chem. Mater.,* **1994**, *6*, 1218. (b) J.H. Loehlin, K.J. Franz, L. Gist and R.H. Moore, *Acta Crystallogr.,* **1998**, *B54*, 695.

CHAPTER TWO

[2.1] G.R. Desiraju, *Science*, **1997**, *278*, 404.

[2.2] (a) C.B. Aakeröy, A.M. Beatty and B.A. Helfrich, *J. Am. Chem. Soc.,* **2002**, *124*, 14425. (b) P. Vishweshwar, A. Nangia and V.M. Lynch, *Cryst. Growth Des*., **2003**, *3*, 783.

[2.3] (a) N.N.L. Madhavi, C. Bilton, J.A.K. Howard, F.H. Allen, A. Nangia and G.R. Desiraju, *New J. Chem*., **2000**, *24*, 1. (b) G.R. Desiraju, *Nature*, **2001**, *412*, 397.

[2.4] A. Baeyer, *Ber. Chem. Ges.,* **1877**, *10*, 1286.

[2.5] (a) R. Boese, H.C. Weiss and D. Bläser, *Angew. Chem., Int. Ed..,* **1999**, *38*, 988. (b) V.R. Thalladi, M. Nüsse and R. Boese, *J. Am. Chem. Soc.,* **2000**, *122*, 9227. (c) V.R. Thalladi and R. Boese, *New J. Chem.,* **2000**, *24*, 579. (d) V.R. Thalladi, R. Boese and H.C. Weiss, *J. Am. Chem. Soc.,* **2000**, *122*, 1186. (e) V.R. Thalladi, R. Boese and H.C. Weiss, *Angew. Chem., Int. Ed.*, **2000**, *39*, 918. (f) A.D. Bond, *Chem. Commun*., **2003**, 250. (g) P. Vishweshwar, A. Nangia and V.M. Lynch, *Cryst. Growth Des.,* **2003**, 3, 783. (h) A.D. Bond, *New J. Chem*., **2004**, 104.

[2.6] A very similar series that shows this sort of structural modulation are provided by the 2,3-dicyano-5,6-dichloro-1,4-dialkoxybenzenes studied by D.S. Reddy, Y.E. Ovchinnikov, O.V. Shishkin, Y.T. Struchkov and G.R. Desiraju, *J. Am. Chem. Soc.,* **1996**, *118*, 4085.

[2.7] (a) S.S. Kuduva, J.A.R.P. Sarma, A.K. Katz, H.L. Carrell and G.R. Desiraju, *J. Phys. Org. Chem*., **2000**, *13*, 719. (b) M.I. Cabaco, Y. Danten, M. Besnard, M.C. Bellissent-Funel, Y. Guissani and B. Guillot, *Mol. Phys.,* **1997**, *90*, 817. (d) A.R. Katritzky, R. Jain, A. Lomaka, R. Petrukhin, U. Maran and M. Karelson, *Cryst. Growth Des.,* **2002**, *1*, 261.

[2.8] *Cerius*^{2}*,* Accelrys Ltd., 334 Cambridge Science Park, Cambridge CB4 0WN, U. K. www.accelrys.com.

[2.9] For a full description on the polymorph prediction sequence used by the program see: R.J. Gdanitz, in *Theoretical Aspects and Computer Modeling of the Solid State* (Ed.: A. Gavezzotti), Wiley: Chichester, **1997**, p. 185.

[2.10] *RPLUTO*, A program for crystal structure visualization, Cambridge Crystallographic Data Centre, Cambridge, 2002 (http://www.ccdc.cam.ac.uk).

[2.11] References concerning the synthesis of aminophenols in this study include: (a) *Chem. Abstr.*, **1939**, *33*, 6879p. (b) R. Ketcham, D. Jambotkar and L. Martinelli, *J. Chem. Soc.,* **1962**, *27*, 4666. (c) N.R. Ayyangar, A.G. Lugade, P.V. Nikrad and V.K. Sharma, *Synthesis*, **1981**, 640. (d) E.H. Vickery, L.F. Pahler and E.J. Eisenbraun, *J. Org. Chem.*, **1979**, *44*, 4444. (e) A.I. Vogel, *A text book of practical organic chemistry*, 5th ed., ELBS, Essex : Longman, **1989**, p1034. (f) N.A. Cortex and R.F. Heck, *J. Org. Chem.,* **1978**, *43*, 3985. (g) G.W. Gribble, W.J. Kelly, and S.E. Emery, *Synthesis,* **1978**, 763. (h) A.I. Vogel, *A text book of practical organic chemistry*, 5th ed., ELBS, Essex : Longman, **1989**, p1033. (i) T. Kolasa, D.E. Gunn, P. Bhatia, A. Basha, R.A. Craig, A.O. Stewart, J.B. Bouska, R.R. Harris, K.I. Hulkower, P.E. Malo, R.L. Bell, G.W. Carter and C.D.L. Brooks, *J. Med. Chem.*, **2000**, *43*, 3322. (j) A.I. Vogel, *A text book of practical organic chemistry*, 5th ed., ELBS, Essex : Longman, **1989**, 476.

[2.12] SHELXTL version 5.1: Bruker AXS: Madison,WI, **2001**.

[2.13] A.L. Spek, (**2002**) *PLATON*, *A multipurpose crystallographic tool*, Utrecht University, Utrecht, The Netherlands.

[2.14] (a) F.H. Allen, J.A.K. Howard, V.J. Hoy, G.R. Desiraju, D.S. Reddy and C.C. Wilson, *J. Am. Chem. Soc.,* **1996**, *118*, 4081. (b) C.C. Wilson, *J. Mol. Struct.,* **1997**, *405*, 207. (c) C.C. Wilson, *J. Appl. Cryst.,* **1997**, *30*, 184.

CHAPTER THREE

[3.1] (a) L. Fábián and A. Kálmán, *Acta Crystallogr.*, **1999**, *B55*, 1099. (b) A. Kálmán, L. Fábián, G. Argáy, G. Bernáth and Z. Gyarmati, *J. Am. Chem. Soc*., **2003**, *125*, 34.

[3.2] (a) P.K. Thallapally, K. Chakraborty, H.L. Carrell, S. Kotha and G.R. Desiraju, *Tetrahedron*, **2000**, *56*, 6721. (b) A.J. Elgavi, B.S. Green and G.M.J. Schmidt, *J. Am. Chem. Soc*., **1973**, *95*, 2058. (c) G.J. Sloan and A.R. McGhie, *Techniques of Chemistry*, Wiley, New York, **1988**, 29.

[3.3] (a) A. Kálmán, G. Argáy, L. Fábián, G. Bernath and F. Fulop, *Acta Crystallogr.,* **2001**, *B57*, 539. (b) M. Muthuraman, Y. Le Fur, M.B. Beucher, R. Masse, J.-F. Nicoud, S. George, A. Nangia and G.R. Desiraju, *J. Solid State Chem*., **2000**, *152,* 221. (c) A. Kálmán, L. Fábián and G. Argáy, *Chem. Commun*., **2000**, 2255. (d) G.R. Desiraju and J.A.R.P. Sarma, *Proc. Ind. Acad. Sci., (Chem. Sci.),* **1986**, *96*, 599. (e) N.N.L. Madhavi, A.M. Katz, H.L. Carrell, A. Nangia and G.R. Desiraju, *Chem. Commun*., **1997**, 1953.

[3.4] A. Kálman and L. Párkányi, *Adv. Mol. Struct. Res*., **1997**, *3*, 189.

[3.5] (a) U. Rychlewska and B. Warzajtis, *Acta Crystallogr*., **2002**, *B58*, 265. (b) E. Bosch and C.L. Barnes, *Cryst. Growth Des*., **2002**, *2*, 299. (c) R.K.R. Jetti, A. Nangia, F. Xue and T.C.W. Mak, *Chem. Commun*., **2001**, 919. (d) A. Dey, R.K.R. Jetti, R. Boese and G.R. Desiraju, *CrystEngComm*, **2003**, *5*, 248.

[3.6] A. Kálman, L. Párkányi and G. Argáy, *Acta Crystallogr*., **1993**, *B49*. 1039.

[3.7] P.-O. Lowdin, *J. Chem. Phys*., **1950**, *18*, 365.

[3.8] G. R. Desiraju, *Acc. Chem. Res*., **1996**, *29*, 441.

[3.9] References pertaining to the synthesis of aminols discussed in this chapter include: (a) A.I. Vogel, *A text book of practical organic chemistry*, 5th ed.,

ELBS, Essex : Longman, **1989**, p 986. (b) B.M. Adger and R.G. Young, *Tetrahedron Lett*., **1984**, *25*, 5219. (c) F.D. Bellamy and K. Ou, *Tetrahedron Lett*., **1984**, *25*, 839. (d) R.C. Ronald, J.M. Lansinger, T.S. Lillie and C.J. Wheeler, *J. Org. Chem.,* **1982**, *47*, 2451. (e) B.H. Lipshutz and J.J. Pegram, *Tetrahedron Lett*., **1980**, *21*, 3343. (f) E. Brzezinska and A.L. Ternay, *J. Org. Chem*., **1994**, *59*, 8239.

CHAPTER FOUR

[4.1] A.I. Kitaigorodskii, *Mixed Crystals*; Springer, New York, **1984**.

[4.2] G.R. Desiraju, *CrystEngComm*, **2003**, *5*, 466.

[4.3] (a) C.R. Theocharis, G.R. Desiraju and W. Jones, *J. Am. Chem. Soc*., **1984**, *106*, 3606. (b) J.A.R.P. Sarma and G.R. Desiraju, *J. Chem. Soc., Perkin Trans. 2*, **1987**, 1187.

[4.4] (a) J.A.R.P Sarma and G.R. Desiraju, *J. Chem. Soc*., *Perkin Trans. 2*, **1985**, 1905. (b) G.R. Desiraju, *Proc. Indian Acad. Sci. (Chem. Sci.)*, **1984**, *93*, 407.

[4.5] (a) A. Nangia and G.R. Desiraju, *Design of Organic Solids*; E. Weber, Ed.; *Topics in Current Chemistry*; Springer: Berlin, **1998**; Vol. 198, pp 57-95. (b) V.S.S. Kumar, A. Nangia, A.K. Katz and H.L. Carrell, *Cryst. Growth Des*., **2002**, *2*, 313. (c) N. Shan, A.D. Bond and W. Jones, *Cryst. Eng*., **2002**, *5*, 9. (d) D.B. Varshney, G.S. Papaefstathiou and L.R. MacGillivray, *Chem. Commun*., **2002**, 1964. (e) B.R. Bhogala and A. Nangia, *Cryst. Growth Des*., **2003**, *3*, 547. (f) J.F. Remenar, S.L. Morissette, M.L. Peterson, Bč. Moulton, J.M. MacPhee, H.R. Guzmán and Ö. Almarsson, *J. Am. Chem. Soc*., **2003**, *125*, 8456. (g) R.D.B. Walsh, M.W. Bradner, S. Fleischman, L.A. Morales, B. Moulton, N. Rodriguez-Hornedo and M.J. Zaworotko, *Chem. Commun*., **2003**, 186. (h) R. Boese, M.T. Kirchner, W.E.

Billups and L.R. Norman, *Angew. Chem*., *Int. Ed*., **2003**, *42*, 1961. (i) X. Gao, T. Friščić and L.R. MacGillivray, *Angew. Chem. Int. Ed.,* **2004**, *43*, 232.

[4.6] References include: [1.3c,d], [1.17], [1.21], [1.24], [1.25], [1.26], [1.29], [1.32], [1.33], [1.34–1.40] and [2.1].

[4.7] V.R. Vangala, B.R. Bhogala, A. Dey, G.R. Desiraju, C.K. Broder, P.S. Smith, R. Mondal, J.A.K. Howard and C.C. Wilson, *J. Am. Chem. Soc*., **2003**, *125*, 14495.

CHAPTER FIVE

[5.1] (a) G.R. Desiraju and A. Gavezzotti, *Acta Crystallogr*., **1989**, *B45*, 473. (b) A. Gavezzotti and G.R. Desiraju, *Acta Crystallogr*., **1988**, *B44*, 427. (c) G.R. Desiraju and A. Gavezzotti, *J. Chem. Soc., Chem. Commun.*, **1989**, 621. (d) G.R. Desiraju, in *Implications of Molecular and Materials Structure for New Technologies*, Eds., J.A.K. Howard, F.H. Allen and G.P. Shields, Kluwer, Dordrecht, **1999**, pp 321-339. (e) J.A.R.P. Sarma and G.R. Desiraju, *Cryst. Growth Des*., **2002**, *2*, 93.

[5.2] (a) D. Das, R.K.R. Jetti, R. Boese and G.R. Desiraju, *Cryst. Growth Des*., **2003**, *3*, 675. (b) S.S. Kuduva, D.C. Craig, A. Nangia and G.R. Desiraju, *J. Am. Chem. Soc*., **1999**, *121*, 1936.

[5.3] D.E. Williams, *Acta Crystallogr*., **1974**, *A30*, 71.

[5.4] A.F. Wells, *Structural Inorganic Chemsitry*, 5th ed.; Oxford University Press: Oxford, **1984**.

[5.5] (a) O. Ermer, *J. Am. Chem. Soc*., **1988**, *110*, 3747. (b) D.S. Reddy, D.C. Craig and G.R. Desiraju, *J. Chem. Soc., Chem. Commun.,* **1995**, 339.

[5.6] (a) S. Aitipamula, G.R. Desiraju, M. Jaskólski, A. Nangia and R. Thaimattam, *CrystEngComm*, **2003**, *5*, 447. (b) J.W. Steed, *CrystEngComm*, **2003**, *5*, 169.

[5.7] (a) D.R. Peacor and M.J. Buerger, *Am. Mineral*., **1962**, *47*, 539. (b) F.R. Ribeiro, A.E. Rodrigues, L.D. Rollmann and C. Naccache, *Zeolites: Science and Technology;* E80, NATO ASI Series: Boston, **1984**.

[5.8] Selected references that describe network structures include: (a) J. Bernstein, R.E. Davis, L. Shimoni and N.-L. Chang, *Angew. Chem., Int. Ed. Engl*., **1995**, *34*, 1555. (b) S.R. Batten and R. Robson, *Angew. Chem., Int, Ed.,* **1998**, *37*, 1460. (c) S. Leininger, B. Olenyuk and P.J. Stang, *Chem. Rev*., **2000**, *100*, 853. (d) B. Moulton and M.J. Zaworotko, *Chem. Rev.,* **2001**, *101*, 1629. (e) M. Eddaoudi, D.B. Moler, H. Li, B. Chen, T.M. Reineke, M. O'keffe and O.M. Yaghi, *Acc. Chem. Res*., **2001**, *34*, 319. (f) S.R. Batten, *CrystEngComm*, **2001**, *18*, 1. (g) K. Biradha, *CrystEngComm,* **2003**, *5*, 374. (h) O.M. Yaghi, M. O'Keeffe, N.W. Ockwig, H.K. Chae, M. Eddaoudi and J. Kim, *Nature (London),* **2003**, *423*, 705. (i) M. Oh, G.B. Carpenter and D.A. Sweigart, *Acc. Chem. Res.,* **2004**, *37*, 1.

[5.9] References with regard to the synthesis of aminophenols described in this chapter include: (a) *Chem. Abstr*., **1959**, *53*, 18908i. (b) R.A.W. Johnstone and M.E. Rose, *Tetrahedron*, **1979**, *35*, 2169. (c) G.A. Grasa, A.C. Hiller and S.P. Nolan, *Org. Lett.,* **2001**, *3*, 1007.

[5.10] *Spartan Pro* 1.0, Wave Function Inc., 18401 von Karman Avenue, Suite 370, Irvine, CA 92612.

APPENDIX I

Table 1. Salient Crystallographic details of the aminols discussed in this thesis.

	Chapter 2			
	1(Neutron)	**1(X-ray)**	**2**	**3**
Empirical formula	$C_{13}H_{13}NO$		$C_{14}H_{15}NO$	$C_{15}H_{17}NO$
Formula wt.	199.25		213.27	227.30
Crystal system	Monoclinic		Monoclinic	Orthorhombic
Space group	$P2_1/n$ (no. 14)		Pc (no. 7)	$Pca2_1$ (no. 29)
T [K]	12(2)	100(2)	100(2)	100(2)
a [Å]	5.9180(12)	5.9820(3)	13.682(3)	23.9370(7)
b [Å]	19.213(4)	19.3670(9)	5.2619(11)	6.2160(2)
c [Å]	9.6510(19)	9.7390(4)	8.1916(2)	8.3970(3)
α [deg]	90	90	90	90
β [deg]	101.25(3)	100.860(2)	107.28(3)	90
γ [deg]	90	90	90	90
Z	4		2	4
V [Å^3]	1076.3(4)	1108.09(9)	563.1(2)	1249.41(7)
D_{calc} [mg/m^3]	1.230	1.194	1.258	1.208
F (000)	21.27	424	228	488
θ /° range	1.56–24.72	2.10–27.48	1.56–30.32	1.70–28.27
Index ranges	$0 \le h \le 17$	$-7 \le h \le 7$	$-18 \le h \le 15$	$-31 \le h \le 31$
	$0 \le k \le 51$	$-25 \le k \le 25$	$-7 \le k \le 7$	$-5 \le k \le 8$
	$-29 \le l \le 24$	$-12 \le l \le 12$	$-10 \le l \le 11$	$-11 \le l \le 10$
N-total	6172	12178	6709	8492
N-independent	2406	2535	2509	3069
N-observed	2396	2010	2321	2615
Parameters	253	188	205	223
R_1	0.0791	0.0449	0.0405	0.0389
wR_2	0.2230	0.1049	0.1087	0.0856
GOF	1.081	1.030	1.034	1.016

Table 1. *Continued…*

Chapter 2		*Chapter 3*		
4	**5**	**1a**	**2a**	**2b**
$C_{16}H_{19}NO$	$C_{17}H_{21}NO$	$C_{12}H_{11}NOS$	$C_{13}H_{13}NOS$	$C_{13}H_{13}NOS$
241.32	255.35	217.28	231.30	231.30
Monoclinic	Monoclinic	Monoclinic	Monoclinic	Monoclinic
Pc	*Pc*	$P2_1/n$	*Pc*	*Pc*
(no. 7)	(no. 7)	(no. 14)	(no. 7)	(no. 7)
105(2)	100(2)	120(2)	100(2)	120(2)
15.7888(16)	14.9554(9)	9.8597(3)	13.844(3)	13.7422(12)
5.2088(6)	11.2370(8)	10.0879(3)	5.1626(10)	5.1725(4)
8.3399(8)	8.6841(6)	21.8081(7)	8.2485(16)	8.3055(7)
90	90	90	90	90
100.912(5)	90.893(3)	102.809(1)	107.22(3)	105.548(4)
90	90	90	90	90
2	4	8	2	2
673.48(12)	1459.2(2)	2115.13(11)	563.07(21)	568.76(8)
1.190	1.162	1.365	1.364	1.351
260	552	912	244	244
2.63–27.54	2.27–27.55	1.92–26.90	3.34–74.96	1.54–27.51
$-20 \le h \le 19$	$-19 \le h \le 19$	$-12 \le h \le 12$	$-17 \le h \le 17$	$-17 \le h \le 14$
$-6 \le k \le 5$	$-11 \le k \le 4$	$-12 \le k \le 12$	$-6 \le k \le 6$	$-6 \le k \le 6$
$-10 \le l \le 10$	$-11 \le l \le 11$	$-27 \le l \le 27$	$-6 \le l \le 10$	$-8 \le l \le 10$
4048	9991	20994	3842	3913
2816	5476	4561	1935	1847
2235	4996	3382	1807	1549
240	367	295	158	157
0.0418	0.0355	0.0464	0.0435	0.0402
0.0921	0.0885	0.1242	0.1170	0.0841
1.030	1.033	1.034	1.095	1.021

Table 1. *Continued…*

Chapter 3		*Chapter 4*		
2c	**3a**	**7**	**8**	**9**
$C_{12}H_{11}NOS_2$	$C_{14}H_{15}NOS$	$C_{13}H_{14}N_2 \cdot C_{13}H_{12}O_2$	$C_{13}H_{14}N_2 \cdot C_{12}H_{10}O_2S$	$C_{12}H_{12}N_2S \cdot C_{13}H_{12}O_2$
249.34	245.33	398.50	416.54	416.52
Monoclinic	Monoclinic	Monoclinic	Monoclinic	Monoclinic
$P2_1/c$	Pc	$P2_1/n$	$P2_1/n$	$P2_1/n$
(no. 14)	(no. 7)	(no. 14)	(no. 14)	(no. 14)
100(2)	100(2)	120(2)	100(2)	120(2)
10.4321(12)	12.6341(9)	11.401(4)	11.2547(11)	5.2528(1)
8.1179(11)	5.8636(4)	9.943(3)	10.1129(9)	42.3571(6)
14.791(2)	8.5671(5)	19.681(6)	19.9982(17)	9.4214(1)
90	90	90	90	90
109.633(6)	90.351(3)	103.500(10)	103.654(5)	94.8010(10)
90	90	90	90	90
4	2	4	4	4
1179.8(3)	634.65(7)	2169.4(12)	2211.8(4)	2088.84(5)
1.404	1.284	1.221	1.251	1.324
520	260	848	880	880
2.07–28.32	1.61–30.08	1.9–29.0	1.9–27.5	1.9–27.5
$-12 \le h \le 13$	$-17 \le h \le 17$	$-15 \le h \le 15$	$-14 \le h \le 14$	$-6 \le h \le 6$
$-7 \le k \le 10$	$-6 \le k \le 7$	$-13 \le k \le 13$	$-13 \le k \le 13$	$-54 \le k \le 55$
$-19 \le l \le 19$	$-11 \le l \le 11$	$-26 \le l \le 26$	$-25 \le l \le 25$	$-12 \le l \le 12$
8343	4751	24503	15070	20890
2926	3138	5700	5052	4793
2568	3045	4521	2881	4032
157	166	375	295	367
0.0348	0.0322	0.0437	0.0571	0.0368
0.0836	0.0822	0.1095	0.1162	0.0923
1.078	1.055	1.03	0.99	1.03

Table 1. *Continued…*

Chapter 4	*Chapter 5*			
10	**2d**	**1b**	**6a**	**6b**
$C_{12}H_{12}N_2S \cdot C_{12}H_{10}O_2S$	$C_{14}H_{13}NO$	$C_{12}H_{11}NO_2$	$C_{12}H_{11}NO$	$C_{14}H_{13}NO$
434.56	211.25	201.22	185.22	211.25
Orthorhombic	Monoclinic	Monoclinic	Orthorhombic	Orthorhombic
$P2_12_12_1$	*Pc*	*Cc*	$Pca2_1$	*Pccn*
(no. 19)	(no. 7)	(no. 9)	(no. 29)	(no. 56)
120(2)	120(2)	120(2)	120(2)	120(2)
9.9090(4)	12.951(8)	22.4911(11)	19.2352(8)	11.4815(5)
10.2700(4)	5.226(3)	5.4647(2)	6.0039(3)	26.0534(16)
22.0100(8)	8.046(3)	8.0466(4)	8.1627(4)	7.1885(4)
90	90	90	90	90
90	98.12(3)	95.674(2)	90	90
90	90	90	90	90
4	2	4	4	8
2239.86(15)	539.2(5)	984.14(8)	942.68(8)	2150.3(2)
1.289	1.301	1.358	1.305	1.305
912	224	424	392	896
1.90–20.0	1.59–27.00	1.82–27.49	2.12–27.11	1.56–26.99
$-13 \le h \le 13$	$-8 \le h \le 16$	$-29 \le h \le 29$	$-24 \le h \le 24$	$-14 \le h \le 9$
$-14 \le k \le 14$	$-5 \le k \le 6$	$-7 \le k \le 7$	$-7 \le k \le 7$	$-33 \le k \le 27$
$-30 \le l \le 30$	$-10 \le l \le 8$	$-10 \le l \le 10$	$-10 \le k \le 10$	$-9 \le l \le 8$
46859	3112	5187	9004	11281
6408	1601	2069	2083	2354
5751	1205	2042	1688	1474
360	197	180	139	197
0.0369	0.0392	0.0329	0.0378	0.0416
0.0936	0.0996	0.0863	0.0930	0.0838
1.04	1.045	1.047	1.033	0.906

Table 1. *Continued…*

Chapter 5
6c
$C_{14}H_{15}N_1O_1$
213.27
Orthorhombic
Pna2_1
(no. 33)
120(2)
7.6679(2)
26.1975(6)
11.1698(2)
90
90
90
8
2243.79(9)
1.263
912
1.55–27.00
$-9 \le h \le 9$
$-33 \le k \le 33$
$-14 \le l \le 14$
24522
4897
3673
409
0.0398
0.0796
0.929

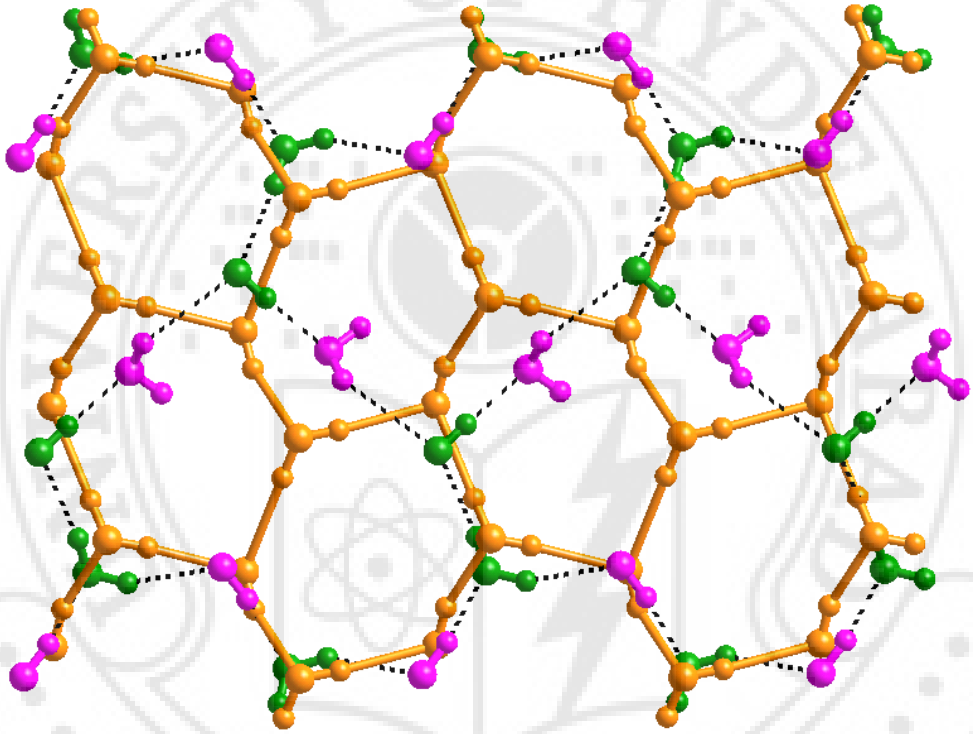

Figure showing how the cross-linked infinite chains in 4-[4-(4-aminophenyl)pentyl]phenol relate to the β-As sheet in 4-[4-(4-aminophenyl)butyl]phenol (overlaid in orange). Symmetry independent molecules A (green) and B (magenta) are colour coded.